



**National Library
of Canada**

**Bibliothèque nationale
du Canada**

Canadian Theses Service

Service des thèses canadiennes

Ottawa, Canada
K1A 0N4

NCTICE

The quality of this microform is heavily dependent upon the quality of the original thesis submitted for microfilming. Every effort has been made to ensure the highest quality of reproduction possible.

If pages are missing, contact the university which granted the degree.

Some pages may have indistinct print especially if the original pages were typed with a poor typewriter ribbon or if the university sent us an inferior photocopy.

Reproduction in full or in part of this microform is governed by the Canadian Copyright Act, R.S.C. 1970, c. C-30, and subsequent amendments.

AVIS

La qualité de cette microforme dépend grandement de la qualité de la thèse soumise au microfilmage. Nous avons tout fait pour assurer une qualité supérieure de reproduction.

S'il manque des pages, veuillez communiquer avec l'université qui a conféré le grade.

La qualité d'impression de certaines pages peut laisser à désirer, surtout si les pages originales ont été dactylographiées à l'aide d'un ruban usé ou si l'université nous a fait parvenir une photocopie de qualité inférieure.

La reproduction, même partielle, de cette microforme est soumise à la Loi canadienne sur le droit d'auteur, SRC 1970, c. C-30, et ses amendements subséquents.



National Library
of Canada

Bibliothèque nationale
du Canada

Canadian Theses Service Service des thèses canadiennes

Ottawa, Canada
K1A 0N4

The author has granted an irrevocable non-exclusive licence allowing the National Library of Canada to reproduce, loan, distribute or sell copies of his/her thesis by any means and in any form or format, making this thesis available to interested persons.

The author retains ownership of the copyright in his/her thesis. Neither the thesis nor substantial extracts from it may be printed or otherwise reproduced without his/her permission.

L'auteur a accordé une licence irrévocable et non exclusive permettant à la Bibliothèque nationale du Canada de reproduire, prêter, distribuer ou vendre des copies de sa thèse de quelque manière et sous quelque forme que ce soit pour mettre des exemplaires de cette thèse à la disposition des personnes intéressées.

L'auteur conserve la propriété du droit d'auteur qui protège sa thèse. Ni la thèse ni des extraits substantiels de celle-ci ne doivent être imprimés ou autrement reproduits sans son autorisation.

ISBN 0-315-55452-5

Canada

THE UNIVERSITY OF ALBERTA

THE HEPATIC TRANSPORT AND METABOLISM OF LIDOCAINE

BY



BRADLEY A. SAVILLE

A THESIS

SUBMITTED TO THE FACULTY OF GRADUATE STUDIES AND RESEARCH
IN PARTIAL FULFILLMENT OF THE REQUIREMENTS FOR THE DEGREE
OF DOCTOR OF PHILOSOPHY

DEPARTMENT OF CHEMICAL ENGINEERING

EDMONTON, ALBERTA

FALL, 1989



University of Alberta
Edmonton

Faculty of Pharmacy and Pharmaceutical Sciences

Canada T6G 2N8

3118 Dentistry/Pharmacy Centre, Telephone (403) 492-3362

August 24, 1989

Faculty of Graduate Studies
2-8 University Hall
CAMPUS

Re: Acceptance of Mr. Bradley Saville's thesis

The undersigned agree that Mr. Saville may use, in his thesis, material co-authored by himself and Drs. Yun K. Tam and Murray R. Gray.

Sincerely,

Murray R. Gray, Ph.D.
Associate Professor

Yun K. Tam, Ph.D.
Associate Professor

THE UNIVERSITY OF ALBERTA

RELEASE FORM

NAME OF AUTHOR: BRADLEY A. SAVILLE

TITLE OF THESIS: THE HEPATIC TRANSPORT AND METABOLISM OF LIDOCAINE

DEGREE: DOCTOR OF PHILOSOPHY

YEAR THIS DEGREE GRANTED: 1989

Permission is hereby granted to THE UNIVERSITY OF ALBERTA LIBRARY to reproduce single copies of this thesis and to lend or sell such copies for private, scholarly, or scientific research purposes only.

The author reserves other publication rights, and neither the thesis nor extensive abstracts from it may be printed or otherwise reproduced without the author's written permission.


(Student's signature)

2317 360 Ridelle Avenue
Toronto, Ontario
M6E 1K1

(Student's permanent address)

Date:

Aug 18/89

THE UNIVERSITY OF ALBERTA

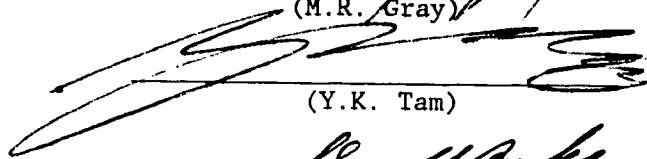
FACULTY OF GRADUATE STUDIES AND RESEARCH

The undersigned certify that they have read, and
recommend to the Faculty of Graduate Studies and Research
for acceptance, a thesis entitled

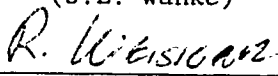
The Hepatic Transport and Metabolism of Lidocaine

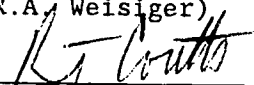
submitted by Bradley A. Saville in partial fulfillment of
the requirements for the degree of Doctor of Philosophy

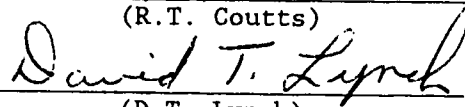

(M.R. Gray)

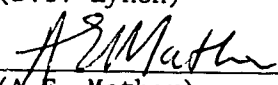

(Y.K. Tam)


(S.E. Wanke)


(R.A. Weisiger)


(R.T. Coutts)


(D.T. Lynch)


(A.E. Mather)

Date:

Aug 17/89

Dedication

This thesis is dedicated to the following people:

To Sandra, for your love, support and encouragement.

To Mom, Dad, Glenn, and Bruce, for your love, and for always being there when needed.

To my Grandmother, an excellent role model and guide - Thanks, I shall always remember you.

ABSTRACT

The physical structure of the liver suggests that net changes in effluent drug concentration are a consequence of a series of steps: uptake of substrate into liver cells, reactions within the cells, and release of substrate and product from the cells. Lidocaine, an efficiently eliminated anti-arrhythmic agent, was administered to the isolated rat liver to investigate these metabolic processes.

To investigate steady-state metabolism and slow changes in enzyme activity, lidocaine was continuously infused into the liver until steady state was reached. Irreversible binding of the substrate to liver components and the overall flow rate of perfusate in the liver had a minimal effect upon drug and metabolite levels. One isozyme of cytochrome P-450 which mediated lidocaine deethylation showed characteristics consistent with substrate-induced enzyme inactivation; the apparent rate of inactivation was $7.0 \mu\text{mol}/(\text{ml} \cdot \text{min})$.

Subsequent step changes in the inlet concentration were used to obtain information on rates of cellular uptake and release, and to assess the extent of mixing within the organ. A heterogeneous model combining mass transfer and enzyme reactions was required to simulate the effluent levels of lidocaine and its metabolites. For lidocaine, the rates of uptake and release were 1200 s^{-1} and 46 s^{-1} , respectively. The rate of intracellular reaction was 0.49 s^{-1} . Effluent levels of lidocaine, therefore, were primarily influenced by linear mass transport into and out of the liver cells and enzymatic conversion into various species. The rate of

lidocaine uptake was fast, but still 50 times less than the rate of galactose uptake, suggesting passive transport between the cells and the vasculature. Although the rates of mass transfer differed for each species, the ratio of the rate of uptake to the rate of release was the same. The results suggested that all three species had an affinity for the cellular region of the liver; tissue concentrations were approximately 5 times greater than vascular concentrations, and the tissue could act as a large reservoir for the compounds. Due to the large capacity of the organ for uptake of lidocaine and its metabolites, effluent concentrations were insensitive to mixing phenomena occurring in the liver vasculature.

ACKNOWLEDGEMENTS

I would like to thank Soheir Tawfik and Hugh Semple for their invaluable assistance in handling the surgical procedures necessary to complete the experiments. I would also like to thank NSERC and the Alberta Heart Foundation, for providing funds to complete this research, and The University of Alberta, for the Dissertation Fellowship which expedited completion of this work.

TABLE OF CONTENTS

Chapter		page
	LIST OF TABLES	xi
	LIST OF FIGURES	xii
	NOMENCLATURE	xv
	GLOSSARY	xx
1	LIVER PHYSIOLOGY AND HEPATIC MODELS	1
	Liver physiology and function	1
	Liver models	8
	Existing models for hepatic elimination	9
	Heterogeneous models	19
	References	31
2	MATERIALS AND METHODS	36
	References	39
3	LIDOCAINE METABOLISM: GENERAL CHARACTERISTICS AND STEADY STATE MODELLING	40
	Material balance data	41
	Kinetics of steady state elimination	44
	References	51

Chapter		page
4	INVESTIGATION OF TIME-DEPENDENT LIDOCAINE METABOLISM:	
	EFFECTS OF ENZYME INACTIVATION	54
	Introduction	54
	Theory	56
	Results and discussion	62
	Conclusions	74
	References	75
5	IMPLICATIONS OF ENZYME INACTIVATION	78
	Methods	80
	Results	81
	Discussion	85
	References	87
6	SHORT-TERM EFFECTS UPON LIDOCAINE METABOLISM:	
	INFLUENCE OF PERFUSATE FLOW AND LIDOCAINE BINDING	89
	Investigation of flow effects	90
	Binding effects	95
	Methods	96
	Results and discussion	97
	Conclusions	99
	References	100

Chapter	page
7	SHORT-TERM EFFECTS UPON LIDOCAINE METABOLISM:
	APPLICATION OF A HETEROGENEOUS MODEL 101
	Development of a heterogeneous model 102
	Theory 103
	Methods 109
	Methods for Parameter Estimation 112
	Results and discussion 113
	Model Verification 124
	Conclusions 128
	References 130
8	SUMMARY AND RECOMMENDATIONS 133
	References 138
	APPENDIX A: HPLC DATA 139
	APPENDIX B: DETAILED RATE EXPRESSIONS FOR LIDOCAINE METABOLISM 141
	APPENDIX C: STATISTICAL DERIVATIONS 142
	APPENDIX D: DERIVATION OF EXPRESSION FOR REGENERATION OF HEPATIC ENZYMES 144

List of Tables

Table	page
3.1 <i>Identification of chromatographic peaks of lidocaine and its metabolites</i>	44
3.2 <i>Kinetic parameters for steady state lidocaine elimination</i>	46
4.1 <i>Time to reach steady state lidocaine concentration</i>	63
4.2 <i>Parameters for inactivation of enzymes during lidocaine elimination</i>	69
4.3 <i>Parameters for other pathways</i>	70
5.1 <i>Interactions of drugs with lidocaine due to inactivation</i>	81
7.1 <i>Average parameters for transport and reaction of lidocaine and its metabolites</i>	117
A.1 <i>Mathematical expressions for HPLC calibration curves</i>	139
A.2 <i>Sensitivity of lidocaine assay</i>	139

List of Figures

Figure	page
1.1 Schematic diagram of liver structure	2
1.2 Representation of the network of blood vessels and sinusoids in the liver (tissue is black).	5
1.3 Fit of the well-mixed model to galactose elimination	11
1.4 Effect of flow rate upon lidocaine elimination	12
1.5 Heterogeneous models for drug elimination in the liver	25
3.1 Pathways for lidocaine metabolism	42
3.2 Chromatogram of effluent sample collected during continuous infusion of lidocaine	43
3.3 Actual vs. predicted effluent concentration of lidocaine	48
3.4 Actual vs. predicted effluent concentration of MEGX	49
4.1. Effects of in vivo pretreatment with (a) lidocaine and (b) saline upon in vitro hepatic metabolism of lidocaine.	55

Figure

page

4.2. <i>In vitro</i> hepatic metabolism of lidocaine (a) following pretreatment and (b) after delaying the initial infusion of lidocaine.	66
4.3. Best fit of the enzyme inactivation model to data from a recirculating system.	72
5.1 Rate of enzyme regeneration following inactivation by lidocaine based on maximal and steady state formation of MEGX.	83
5.2 Effect of enzyme regeneration upon the time to reach steady state concentration of lidocaine.	84
6.1 Effect of perfusate flow rate upon steady state drug and metabolite concentrations	94
7.1 Basic Heterogeneous Model	105
7.2 Concentration of MEGX in liver effluent during washout experiment following MEGX administration	118
7.3 Concentration of 3-OHLID in liver effluent during washout experiment following 3-OHLID administration	119

Figure	page
7.4 Concentrations of lidocaine, MEGX, and 3-OHLID in liver effluent following lidocaine administration	122
7.5 Cross-correlation between rate of reaction and rate of uptake	123
7.6 Best fit of heterogeneous model with enzyme inactivation to composite drug and metabolite concentration data	127
A.1 Chromatogram of liver effluent collected prior to drug administration	140

Nomenclature

A	concentration of albumin for binding process
AUC(t)	area under the lidocaine curve as a function of time
C_i	concentration of species i
eg	C_1 : lidocaine
	C_2 : MEGX
C_{in}	inlet concentration
$C_{i,in}$	inlet concentration of species i
$C_{i,L}$	concentration of species i in liver
$C_{i,O}$	concentration of species i in oxygenator
$C_{i,R}$	concentration of species i in reservoir
C_{Ai}	concentration in the primary compartment of composite unit i
C_{Bi}	concentration in the peripheral compartment of composite unit i
C_{ci}	concentration of free species in cellular compartment i
C_{ij}	concentration in segment i,j
C_{L2}	lidocaine concentration at flow rate Q_2
Cl_{int}	intrinsic clearance
C_{M2}	MEGX concentration at flow rate Q_2
C_{p2j}	precursor concentration in the cellular compartment of unit j
C_{si}	concentration of free species in sinusoid compartment i
C_{sbi}	concentration of bound species in sinusoid compartment i
C_{Ti}	concentration of species i in tissue
C_{Vi}	concentration of material in the extravascular space
D_i	distribution coefficient
D_{pX}	diffusion coefficient in plasma

D_{TX}	coefficient for axial diffusion in tissue
D_{TR}	coefficient for radial diffusion in tissue
E_{1a}	active enzyme fraction for dealkylation
E_d	inactivated enzyme fraction
$E_{1,max}$	maximum amount of dealkylation enzyme
$E_{1,ss}$	steady state amount of dealkylation enzyme
E_t	exit age distribution function
F_A	fraction of total system volume in the primary compartments
F_B	fraction of total system volume in the peripheral compartments
F_C	fraction of total system volume in the plug flow compartments
i	index for radial compartments; index for species identification
j	index for axial compartments; index for reaction identification
k	fraction of the volumetric flow exchanged with the peripheral compartment
k_1	rate constant for lidocaine deethylation
$k_{1,max}$	maximum rate of lidocaine deethylation
k_{1ss}	steady state rate of lidocaine deethylation
k_1'	rate of cellular uptake
k_2	rate of cellular release
k_3	rate of intracellular reaction
k_{12}	rate of uptake into liver cells from the vasculature
k_{21}	rate of release from the liver cells into the vasculature
k_b	rate constant for lidocaine binding
k_d	rate constant for enzyme inactivation

k_d'	pseudo-rate constant for inactivation
k_{dis}	rate of dissociation of bound complex
k_f'	rate constant for product formation
k_f	rate of intracellular formation
k_r	rate of intracellular reaction
k_R	rate of linear reaction for well-mixed model
k_R'	rate of linear reaction for parallel-tube model
k_α	rate constant for formation of enzyme-substrate complex
$k_{-\alpha}$	rate constant of dissociation of enzyme-substrate complex
K_{cr}	partition coefficient between the cellular and the vascular space
K_{cp}	partition coefficient between the extravascular and the vascular space
K_m	Michaelis constant for Michaelis-Menten kinetics
L	length of cylinder or reactor
M	quantity at any time
M_0	initial quantity in the pulse
N	number of composite compartmental units
N_c	number of cellular compartments
N_r	number of radial segments
N_v	number of vascular compartments
N_x	number of axial segments
P	permeability
Q	volumetric flow rate through the organ
Q_s	volumetric flow through a single sinusoid
r_c	radius of capillary

r_i	radius of tissue segment i
R_j	rate of reaction j
S	amount of liver binding sites
S_0	initial amount of liver binding sites
t	time
\bar{t}	mean residence time
u	flow velocity in reactor
V_{1j}	volume of vascular compartment j in the heterogeneous model
V_{2j}	volume of cellular compartment j in the heterogeneous model
V_c	volume of the cellular compartment
V_{cat}	volume of the catheters
V_{ci}	volume of cellular compartment i
V_{ij}	volume of segment i,j
V_{IS}	volume of interstitial space
V_L	volume of liver
V_m	maximal reaction velocity
V_o	volume of oxygenator
V_R	volume of reservoir
V_{si}	volume of sinusoid compartment i
V_v	volume of the vascular compartment
W	liver weight
W_s	flow velocity in the sinusoid
x	distance along the sinusoid
δ	Dirac delta function
γ	ratio of the extravascular volume to the vascular volume
θ_L	dispersion parameter
$\mu_{i,j}$	stoichiometric coefficient for species i and reaction j

ρ	density of liver tissue
σ^2	variance of the exit age distribution curve
θ	ratio of the cellular volume to the vascular volume
τ	average residence time of the system
τ_s	residence time in the sinusoid = L/W_s

GLOSSARY

arteriole:	small terminal twigs of an artery that joins the artery to a capillary or sinusoidal bed
cytoplasm:	the protoplasm of a cell except that of the nucleus
cytosol:	the fluid within the cytoplasm
endoplasmic reticulum:	a network of cellular tissue within the inner granular portion of the cytoplasm of the cell, enclosing the nucleus
endothelial cells:	single layer of thin flattened cells that line internal body cavities
enzyme induction:	process whereby the formation or activity of an enzyme is artificially elevated by administration of a compound
fenestrae:	small openings in a wall; results from broad elastic fibres that fuse to form a perforated sheet
microsome:	a particle obtained by heavy centrifugation of broken cells
parenchymal cells:	the essential and functioning cellular substance of an organ; distinguished from its supportive framework

RTD: residence-time-distribution

sinusoid: a minute endothelium-lined space or passage
for blood in the tissues of an organ

space of Disse: interstitial space between the sinusoid and
the hepatocytes

thoracic artery: any of several branches of the axillary
artery supplying the pectoral muscles, walls
of the thorax, axilla, and adjacent parts

CHAPTER 1: LIVER PHYSIOLOGY AND HEPATIC MODELS

The liver, as the primary organ for detoxification of drugs, incorporates a number of different physiological processes to give the observed range of drug elimination. Net changes in drug concentration are a consequence of a series of steps: uptake of the substrate into liver cells, enzyme reactions within the cells, release of metabolites and unconverted substrate back into the sinusoids, substrate binding to proteins in the blood and liver, and the net flow of the perfusing medium in the vascular network of the liver. An understanding of each of these processes is necessary to fully comprehend the overall process of drug elimination. These physiological processes must be accounted for, either individually or by grouping and approximation, if a model for drug elimination is to be developed.

Liver Physiology and Function

The liver, consisting of 4 lobes, is located in the blood stream between the gastrointestinal tract and spleen, and the thoracic veins leading to the heart. Blood enters the organ through both the portal vein and the hepatic artery, traverses the sinusoids that link the inlet and exit flows, and exits the liver via the hepatic vein (Figure 1.1). The portal vein, hepatic vein, and hepatic artery are all subject to branching; individual branches serve each lobe of the liver (Snell, 1973).

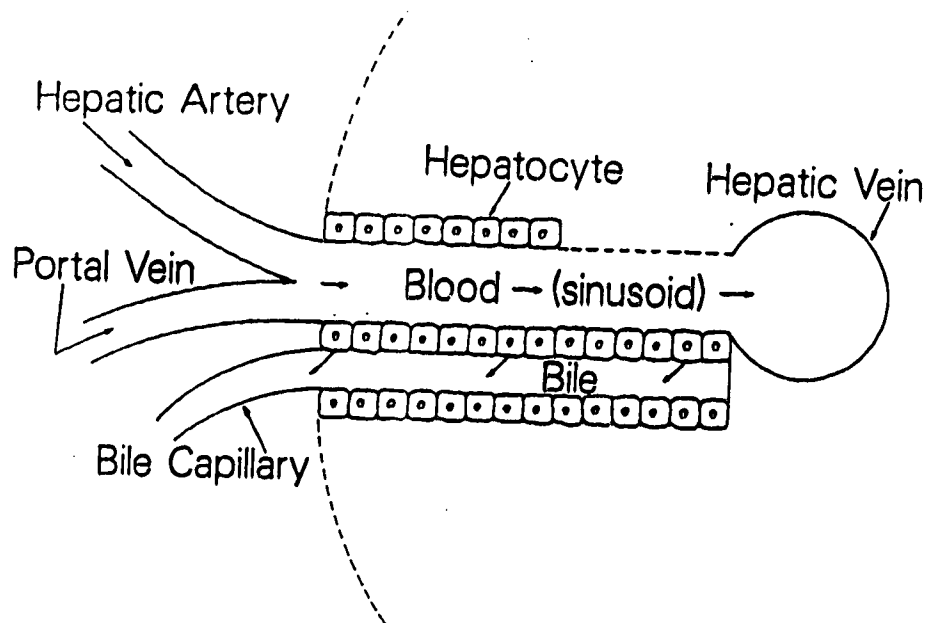


Figure 1.1 Schematic diagram of liver structure

Orally administered substances are absorbed in the gastrointestinal tract, and enter the liver through the portal vein. Drugs administered intravenously circulate through the body, and enter the liver through both the hepatic artery and portal vein. Seventy-five percent of the blood supplied to the liver is via the portal vein; eighty percent of the oxygen is supplied through the hepatic artery (Brauer, 1963). Animals can, however, survive without a blood supply from the hepatic artery, provided the venous blood is oxygenated, and the portal flow exceeds the threshold level of 1.5 ml/(min·g liver) required to prevent collapse of parts of the vascular network (Brauer, 1963). In the normal liver, respiratory action influences total blood flow in the organ. External pressure from the diaphragm affects outflow from the hepatic vein; outflow is stopped during inhalation, and is maximal at the peak of expiration, when the diaphragm is at its highest position. Hence, in live animals, total blood flow is cyclical in nature, subject to periods of full flow and periods when the flow is well below the minimum perfusion rate of 1.5 ml/(min·g liver) (Brauer, 1963).

The vascular network of the organ consists of three regions:

- 1) portal tracts, which are subject to a great deal of branching
- 2) the hepatic vein
- 3) a sinusoidal bed, which serves as the link between the portal tracts and the hepatic vein.

The microvasculature of the liver consists of three forms of sinusoids: direct, branching, and interconnecting sinusoids. Direct sinusoids form a short circuit between the portal and hepatic veins. Branching sinusoids take a long, circuituous route between the inlet

and exit flows, and interconnecting sinusoids link parallel adjacent branching sinusoids like the rungs on a ladder. Koo *et al.* (1975), using electron microscopy, established that direct sinusoids comprised 27% of a typical section of the rat liver; interconnecting and branching sinusoids made up 14 and 59% of the sinusoidal bed, respectively. A polymer cast of the vascular bed of the organ (Figure 1.2) indicates that the liver is a continuous meshwork of highly interconnected blood spaces. The sinusoidal channels are of varying length, and are oriented in a nearly random fashion. It is very unlikely, therefore, that a volume of blood will pass directly from liver inlet to outlet, or follow a simple, predictable path.

Numerous studies on fluid flow in the sinusoids have been conducted. Brauer (1963) emphasized the overall plasticity of the organ, suggesting that each volume of blood has many possible alternate pathways. The path it follows depends only upon the local pressure gradients prevailing at that moment. Reversal of flow within a sinusoid has been observed using *in vivo* microscopy. The concept of flow reversal was supported by Rappaport (1980), who suggested that intermittent opening and closing of the arterioles is common, and is not restricted to the short, interconnecting sinusoids. Further evidence was provided by Lubbers (1968), who indicated that flow in adjacent sinusoids could be countercurrent, and that the characteristic blood flow distribution in the liver changes from moment to moment. Additional studies with vascular tracers showed transient backflow into adjacent sinusoids (Brauer, 1963).

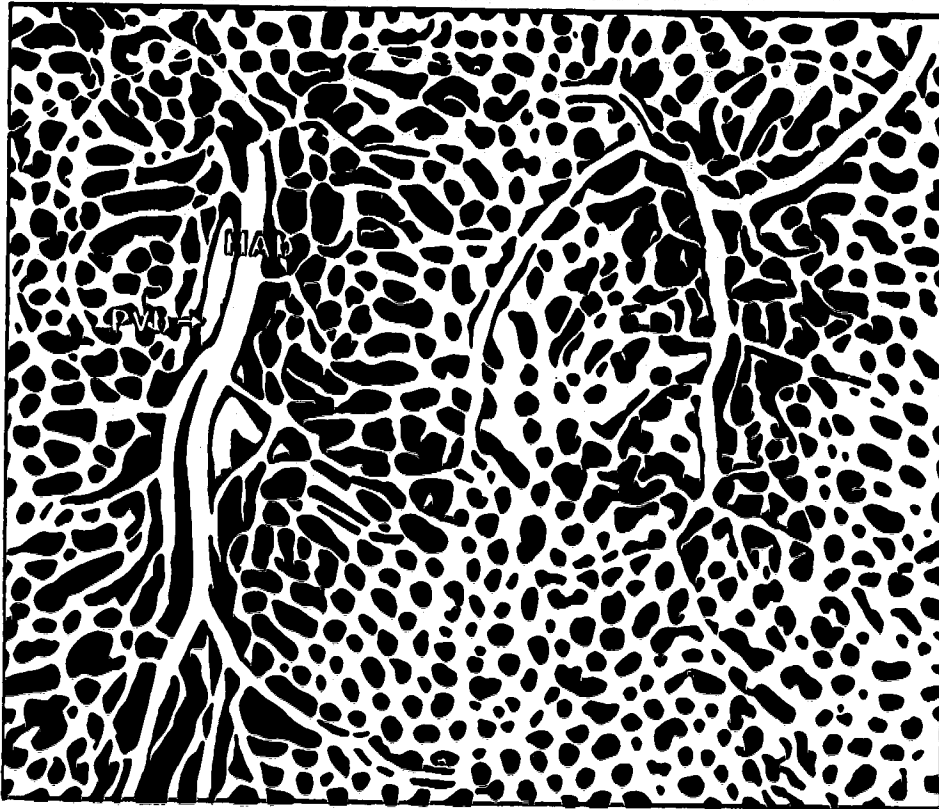


Figure 1.2 Representation of the network of blood vessels and sinusoids in the liver (tissue is black).

PVb is the portal vein; HAb is the hepatic artery. Based on a micrograph of a polymer cast by Motta et al. (1978).

Unquestionably, mixing can occur at various sites within the liver. At each node corresponding to the divergence and convergence of a number of sinusoids, mixing occurs. Furthermore, backmixing within the organ occurs due to flow reversal. The overall picture of the organ suggests extensive mixing, and the time-dependent distribution of blood flow in the organ suggests that different streams will be mixing at different times. The time-dependent flow indicates that a true mathematical description of the physiology of liver blood flow would be extremely complex. Rather, it is apparent that a time and spatially averaged model may be appropriate to describe hepatic blood flow.

The sinusoids of the liver are lined by endothelial cells which contain fenestrae of various sizes. The fenestrae permit dissolved substances to enter the coadjacent endothelial space of Disse, before entering the parenchymal cells of the liver. A monolayer of these parenchymal cells, or hepatocytes, is present for each sinusoid (as in Figure 1.1). Some vascular materials, such as red blood cells, are so large as to prevent their penetration through the fenestrae into the space of Disse. Certain compounds, including albumin, are deemed extravascular compounds. These substances have access to the space of Disse, but cannot permeate into the adjoining hepatocytes. Other materials, such as water and glucose, have full access to the vascular, extravascular, and cellular regions of the liver. Electron microscopic data indicated that the gaps in the endothelial lining of the sinusoids were rather large, leading Brauer (1963) to conclude that the concentration of materials in the space of Disse was very close to the composition of the blood in the sinusoids.

Hence, provided a compound is small enough to gain access to the space of Disse, it seems appropriate to approximate the vascular and interstitial space of the liver as a single unit (as shown in Figure 1.1).

Experiments with vascular and extravascular tracers have established that the volume of the vascular and interstitial region of the liver is approximately 15 percent of the total liver volume (Brauer, 1963; Goresky, 1963). The hepatocytes, which contain the enzymes, occupy about 85 percent of the liver volume. The bile ducts, which occupy less than 1 or 2 percent of the liver volume (Brauer, 1963), are usually lumped with the hepatocytes in heterogeneous models, because the total biliary volume is less than the error in the estimates of the cellular volume of the liver.

Investigation of the mechanisms influencing liver metabolism usually involves the use of tracers. Vascular and extravascular markers provide information on the the relative volumes of the vascular and interstitial spaces of the liver. Administration of a cellular reference allows estimation of the cellular volume, and permits investigation of the transport processes between the cells and the vasculature. The ultimate objective is to examine all facets of liver metabolism, combining transport, volume of distribution, and intracellular reaction. If the metabolism of a reacting species is to be studied, knowledge of its transport characteristics is required. Ideally, a non-reacting analog to the species of interest would be used to examine transport phenomena, and it would be assumed that the transport properties of the drug would be the same as those of the analog. In many instances, however, non-reacting analogs do not

exist, necessitating the use of the species itself as a probe of hepatic transport and reaction. Lidocaine falls into this category. There are no known non-reacting structural analogs of lidocaine, indicating that the drug itself must be used as a reacting tracer. Using appropriate experimental techniques, tracer information can be obtained, and a model for liver metabolism can be developed.

Liver Models

An effective model for liver metabolism should have the following features:

- 1) The model should be physiologically accurate, and would account for the heterogeneous nature of the organ, with a vascular space for fluid flow, and a stationary cellular space. It would also account for the three different regions of the vascular network, and the three forms of sinusoids in the sinusoidal bed. It would describe the time-dependent flow of blood in the organ, including flow reversals, local pressure gradients, and the intermittent operation of some of the sinusoids.
- 2) The model should have a minimum of parameters, and should be easy to use in a predictive fashion. Furthermore, the model should require a minimum of data.
- 3) The model should be applicable to a variety of substrates, and should be capable of predicting the levels of both drugs and metabolites.

Unfortunately, it is virtually impossible to have all three desirable features in a single model. To have complete physiological

accuracy, the model must be mathematically complex with a large number of parameters. Such models are difficult to use in a predictive fashion. To gain mathematical simplicity, approximations of the physiology and mixing characteristics are often made. Nevertheless, by making justifiable and correct approximations, it should be possible to develop a model that is both mathematically simple and broadly applicable.

Existing Models For Hepatic Elimination

The existing models can be categorized according to the approximations made with respect to liver physiology and the degree of mixing within the organ. The simplest models are non-parametric. They have no adjustable parameters to define the role of cellular uptake and intrahepatic mixing, and, therefore, are equivalent to the idealized models used for chemical reactors.

The well-stirred or "venous-equilibrium" model is based upon the assumption of no concentration gradients within the organ. It is assumed that there will be instantaneous equilibration between the vascular and cellular regions of the liver, which permits treating the liver as a homogeneous continuous stirred tank reactor. The mathematical expression for the well-mixed model and rate of reaction R_j is presented in Equation (1.1). The solution of the model in steady state with linear kinetics is presented in Equation (1.2).

$$\frac{dC}{dt} = \frac{Q \cdot (C_{in} - C)}{V_L} - R_j \quad (1.1)$$

$$C = \frac{Q \cdot C_{in}}{(Q + k_R \cdot V_L)} \quad (1.2)$$

The model was successfully applied to the steady-state metabolism of lidocaine by Pang and Rowland (1977), and by Ahmad *et al.* (1983). Mathematically, the model is straightforward and easily applied to the prediction of drug and metabolite levels. However, it cannot describe the metabolism of materials which are limited by transport into the hepatocytes or are subject to incomplete hepatic mixing.

The parallel tube model represents the opposite extreme in mixing behavior, assuming an exponential concentration gradient in a single, unbranched hepatic "tube". It is assumed that the liver is homogeneous, and that flow is unidirectional. The equation follows the form for a plug flow reactor (Equation 1.3). The solution for the effluent concentration with linear kinetics is presented in Equation (1.4).

$$\frac{dC}{dV_L} = - \frac{R_j}{Q} \quad (1.3)$$

$$C = C_{in} \cdot \exp (-k_R' \cdot V_L/Q) \quad (1.4)$$

Bass *et al.* (1976) proposed the use of the parallel-tube model to describe the steady-state metabolism of galactose; however, the data can also be readily described by the well-mixed model (Figure 1.3), using a Michaelis constant of 0.10 mM and a maximum reaction velocity of 0.397 mM/min. Furthermore, Pang and Rowland (1977) demonstrated that the parallel-tube model could not represent the weak dependence of lidocaine metabolism upon flow rate (Figure 1.4).

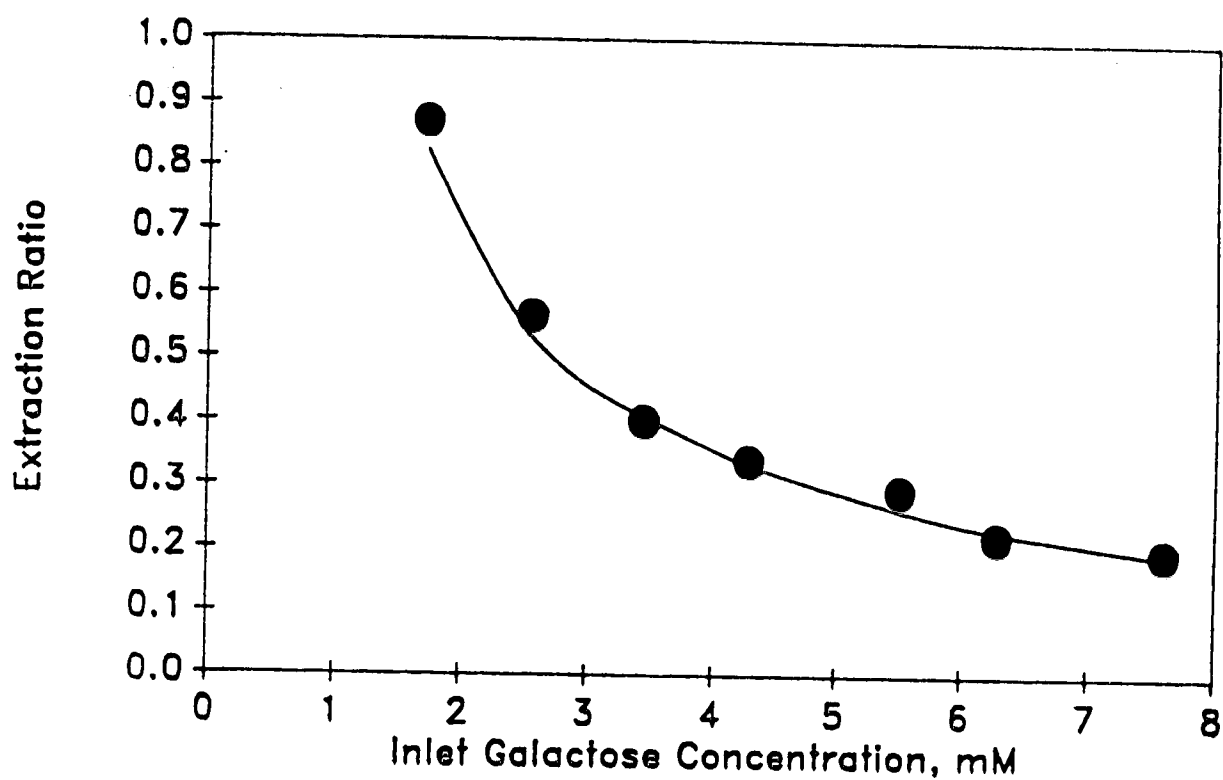


Figure 1.3 *Fit of the well-mixed model to galactose elimination*
Data adapted from Bass *et al.* (1976) originally from Tygstrup and Winkler (1954).

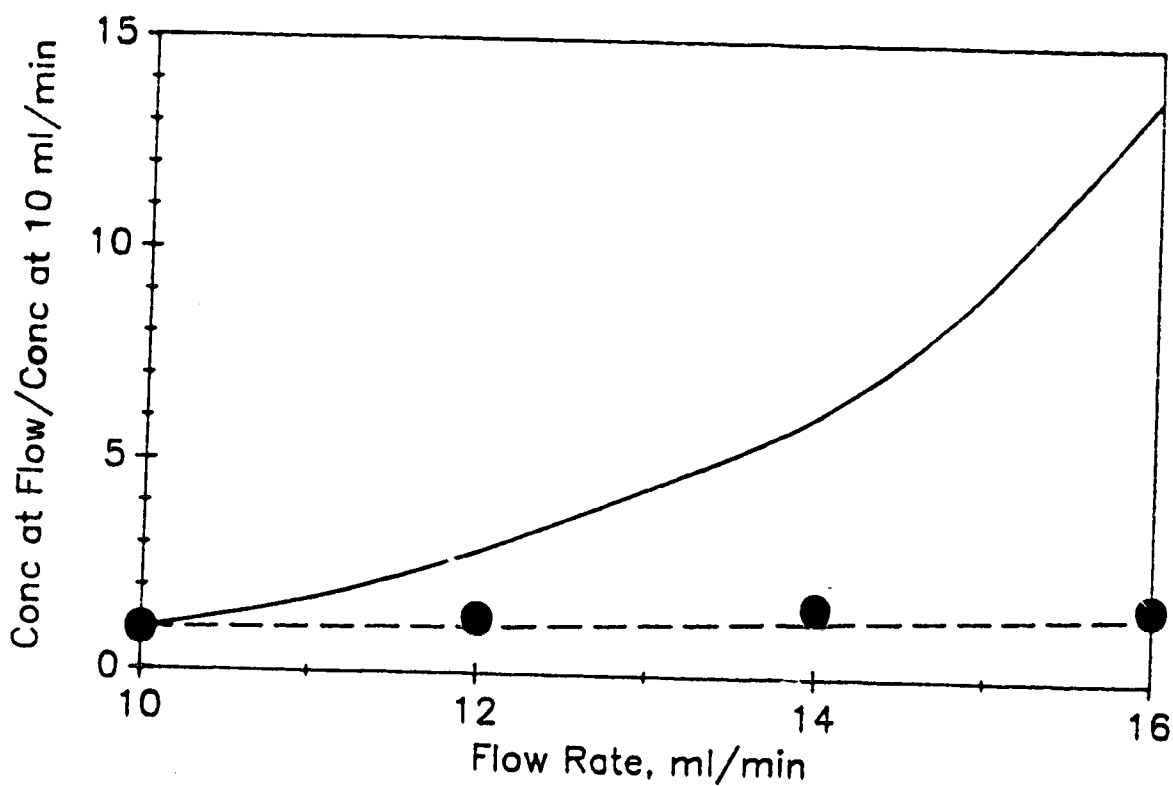


Figure 1.4 Effect of flow rate upon lidocaine elimination

● experimental data; — plug flow model; ----- well-mixed model

Adapted from Pang and Rowland (1977). The vertical axis is the ratio of the effluent concentration at a give flow rate to the concentration at the base rate of 10 ml/min.

Both the well-stirred and the parallel tube models are extreme descriptions of the mixing phenomena occurring within the liver. The physiology of the liver, however, suggests that the actual extent of mixing in the organ should fall between these extremes. Recognizing this, various researchers have proposed mixing models in an effort to accurately describe the mixing phenomena that occur within the liver. One such model is the distributed model, presented by Bass *et al.* (1978) to describe galactose elimination. The model describes the liver as a number of parallel sinusoids of varying length, with plug flow in each sinusoid. To account for the physiological characteristics of the liver, the distributed model assumes a Gaussian distribution of the number and lengths of the sinusoids, giving profiles similar to a residence-time distribution function. In this form, the model is equivalent to a segregated flow model as described in the chemical engineering literature (Dudukovic, 1985; Hill, 1977). Within the model, there is no provision for branching between the sinusoids; rather, all mixing occurs at the outlet of the liver. For non-reacting or linearly-eliminated species, this poses no difficulty. However, for non-linear, saturable elimination, which is typical of enzyme kinetics, the rate of reaction is dependent upon the local concentration. Any mixing that occurs within the organ will dilute the species from a number of sinusoids. The redistribution of the mixed stream into other sinusoids will subsequently affect the local rate of elimination. Hence, application of this model for Michaelis-Menten kinetics can lead to significant errors in the estimates for the maximal reaction velocity (V_{\max}) and the Michaelis constant for saturation (K_m).

It has been suggested that the environment experienced by reactant molecules during their passage through the liver may be important. However, the importance of local mixing processes diminishes for fluids of low viscosity or if interactions with flowing cells and proteins in the medium are negligible. The viscosity of blood is low, and therefore, an assumption of maximum mixing on a microscopic scale is reasonable. Such an assumption permits simplification of mixing processes within the organ, and permits application of a mixing model developed from residence time distribution data.

Two single-parameter homogeneous models of hepatic mixing have been proposed: the axial dispersion model (Roberts and Rowland, 1985), and the series-compartment model (Gray and Tam, 1987). Both are based upon well-established models for chemical reactors. The axial dispersion model assumes that the liver is a packed bed in which different degrees of axial mixing can occur. In theory, a full range of mixing phenomena can be simulated, simply by adjusting the mixing parameter. The dispersion model, however, suffers from a number of drawbacks. The model is complex, necessitating the solution of a partial differential equation with two boundary conditions (Equation 1.5).

$$\theta_L \frac{\partial^2 C}{\partial X^2} - u \frac{\partial C}{\partial X} - k_R C = \frac{\partial C}{\partial t} \quad (1.5)$$

There are four possible sets of boundary conditions for the axial dispersion model, based on the characteristics of the system at the points of tracer injection and collection. At these points, the reactor is described as either "closed" or "open", depending upon

whether or not plug flow into or out of the test section is assumed. A closed boundary condition is one in which plug flow is assumed outside the test section; open boundary conditions permit the same dispersion parameter to describe flow within and adjacent to the test section, as in the blood vessels entering and leaving the liver. Thus, the four possible conditions are completely open, completely closed, open-closed, and closed-open. Different solutions are obtained for each combination of boundary conditions.

The initial and boundary conditions for a completely open system are (Duduković, 1985):

$$C(x, 0) = 0 \quad \text{for } x > 0$$

$$C(x, 0) = C_{\text{step}} \quad \text{for } x < 0$$

$$C(x, t) = 0 \quad \text{for } x = +\infty$$

$$C(x, t) = C_{\text{step}} \quad \text{for } x = -\infty$$

The initial and boundary conditions for a completely closed system are:

$$C(x, 0) = 0 \quad \text{for } 0 < x < L$$

$$C(x, \infty) = C_{\text{step}} \quad \text{for } 0 < x < L$$

$$C(0, t) = 0$$

$$C(L, t) = 0$$

Combinations of the closed-closed and open-open boundary conditions define the boundary conditions for the open-closed and closed-open systems. The correct boundary conditions have been subject to considerable debate, and furthermore, the boundary conditions are often difficult to meet in practice. Roberts and Rowland (1985) proposed that the completely open (or Dankwerts)

boundary conditions be used to describe tracer behaviour in the liver. However, the completely open boundary conditions give an incorrect prediction of tracer behavior; that is, the tracer can appear upstream of the point of injection. Only by using the Dankwerts boundary conditions, however, can an analytical solution to Equation (1.5) be obtained. An analytical solution for the model is available for time-dependent profiles from non-eliminated tracers (Equations 1.6 and 1.7) and linearly-eliminated tracers in steady state (Equations 1.8 to 1.11); for all other cases, numerical techniques must be applied.

1) no reaction, step input of tracer:

$$C(t) = C_0 + 0.5 C_{\text{step}} \cdot (1 + \operatorname{erf} (0.5 \sqrt{(uL/\theta_L)} \left[\frac{1 - ut/L}{\sqrt{(uL/\theta_L)}} \right])) \quad (1.6)$$

2) no reaction, pulse input of tracer:

$$C(t) = \frac{C_{\text{pulse}} \cdot L}{2V_L \sqrt{\pi\theta_L t}} \exp \left[- \frac{(L - ut)^2}{4 \theta_L t} \right] \quad (1.7)$$

3) linear reaction: General form (1.8); analytical solution in steady state (1.9)

$$\theta_L \frac{\partial^2 C}{\partial x^2} - u \frac{\partial C}{\partial x} - k_R C = 0 \quad (1.8)$$

$$\frac{C}{C_{\text{in}}} = \frac{4 \alpha e^{\beta}}{(1 + \alpha)^2 e^{\alpha\beta} - (1 - \alpha)^2 e^{\alpha\beta}} \quad (1.9)$$

$$\text{where } \beta = uL/2\theta_L \quad (1.10)$$

$$\text{and } \alpha = (1 + 2k_R L/\beta u)^{0.5} \quad (1.11)$$

Estimation of the dispersion parameter is only valid theoretically for elongated systems, where the ratio of vessel length to diameter is significantly greater than one. In addition, the model only has a sound theoretical basis if the dispersion parameter is less than 0.15 (Duduković, 1985). Roberts and Rowland (1985), however, suggested that a dispersion parameter of 0.2 would accurately describe the mixing of erythrocytes within the liver. Since erythrocytes are confined to the vascular space, this value provides a minimum estimate of hepatic mixing. Values of the dispersion parameter for all other species would exceed 0.2. Hence, the model provides only an empirical method for analyzing drug elimination by the liver.

The series-compartment model (Gray and Tam, 1987), known as the tanks-in-series model in the chemical engineering literature, is a simple empirical model which is capable of describing a continuum of behavior between the extremes in mixing described by the parallel tube and well-mixed models. Its simplicity has made it the preferred model for describing complex flow and reaction (Duduković, 1985). The model discretizes the liver into a sequence of compartments connected in series. The number of compartments, N , is not indicative of liver physiology; rather, it is an arbitrary parameter used to correlate the extent of mixing in the organ. When N is equal to one, well-mixed behavior is observed, and when N is approximately 30, the plug flow behavior predicted by the parallel tube model is obtained. The model equations are algebraic, requiring the solution of a series of ordinary differential equations with known initial conditions (Equations 1.12, 1.13).

For compartment i,

$$\frac{dC_i}{dt} = \frac{Q \cdot (C_{i-1} - C_i)}{V_i} - k_R C_i \quad (1.12)$$

where $V_i = V_{tot}/N$.

For a first order reaction at steady state,

$$C_{out} = C_N = C_{in} (1 + k_R V_i / Q)^{-N} \quad (1.13)$$

A feature of the model is its ability to empirically describe efflux curves arising from indicator-dilution experiments. Solution of Equation (1.12) for a pulse in tracer concentration at the inlet of the liver gives an expression similar to the statistical Γ -distribution:

$$C(t) = \frac{\text{Dose} \cdot N^N \cdot t^{N-1}}{Q \cdot r^N \cdot \Gamma(N)} \exp(-Nt/r - Cl_{int} \cdot t / (Qr)) \quad (1.14)$$

Davenport (1983) presented a version of the model for profiles obtained from non-reacting tracers, and Gillette (1985) demonstrated the usefulness of a number of sequential compartments for describing steady state drug elimination. The model was successfully applied (Gray and Tam, 1985) to the steady state elimination of lidocaine, sulfobromophthalein, and chromium phosphate colloid. The model also accurately correlated the time-dependent profiles of red blood cells, sucrose, and galactose resulting from indicator-dilution experiments.

The series-compartment model does not explicitly include physiological phenomena such as variable transit times through sinusoids, substrate binding to liver tissues and proteins, or the effect of transport processes between the vascular and cellular

regions of the liver. The model includes these phenomena in the mixing parameter, N . If these specific processes are to be investigated, a more complex model of the liver is necessary.

Heterogeneous Models

A major deficiency of the homogeneous models is their inability to adequately account for transport processes between the vascular and cellular regions of the liver. Although the homogeneous models work well for selected substrates under specific conditions (e.g. lidocaine at steady state), they may be incapable of modelling the concentrations of species when metabolism is transport limited or if physiological and metabolic conditions are significantly altered.

To properly investigate transport processes in the liver, a heterogeneous model of the organ is required. Heterogeneous models are typically more complex than their homogeneous counterparts, and experiments must be carefully designed to obtain accurate estimates of the transport parameters in the model. Several models for heterogeneous metabolism have been developed, with varying degrees of complexity.

The classical heterogeneous model of transport in organs is Krogh's cylinder (Krogh, 1919). This model, originally formulated for the transport of oxygen from capillaries into muscle tissue, assumes a cylindrical capillary with a concentric tissue compartment surrounding the capillary. Bassingthwaite et al. (1970) developed a model which is equivalent to a combination of Krogh's cylinder with the axial dispersion model described by Roberts and Rowland (1985). In this model, described by Equations 1.15 through 1.20, the liver

was assumed to be a single, straight capillary with multiple concentrically surrounding tissue compartments.

The general equation to describe the concentration in the capillary is:

$$\frac{\partial C}{\partial t} = -u \frac{\partial C}{\partial x} - 2\pi r_c P (C - C_{t,s}) \quad (1.15)$$

To describe the concentrations in the tissue:

$$\frac{\partial C_t}{\partial t} = D_T \frac{\partial^2 C_t}{\partial x^2} + \frac{D_R}{r} \frac{\partial}{\partial r} \left(r \frac{\partial C_t}{\partial r} \right) \quad (1.16)$$

The following boundary conditions apply:

$$\text{at } r = r_c, C_t = C_{t,s} \quad (1.17)$$

$$\text{at } r = R, \frac{\partial C_t}{\partial r} = 0 \quad (1.18)$$

$$\left. \frac{\partial C_t}{\partial x} \right|_{x=0} = 0 \quad (1.19)$$

$$\left. \frac{\partial C_t}{\partial x} \right|_{x=L} = 0 \quad (1.20)$$

The original model proposed by Bassingthwaighe *et al.* (1970) allowed for diffusion in plasma. However, Bass *et al.* (1976) indicated that the rate of convective influx was nearly 50 times greater than the rate of diffusive influx. Hence, a simplified model in PDE form is presented, similar to the model of Bassingthwaighe *et al.*, but modified such that plasma diffusion was not included. The model allowed for axial and radial diffusion of materials in tissue, but neglected physiological effects such as bypassing, variable blood flow velocities in an array of sinusoids, and local changes in flow.

The model had no provision for chemical reaction, and was based upon net rates of diffusion. To estimate local capillary and tissue concentrations, the equations must be numerically integrated. Unless accurate tissue concentrations are known, estimation of the tissue diffusion coefficients (D_{TR} , D_{TX}) may be difficult. The model may be useful for estimating precise tissue levels of non-eliminated tracers if diffusion coefficients are already known. For general application, the model must be modified to account for reaction and different rates of transport into and out of the tissue.

Goresky *et al.* (1963, 1973a, 1973b, 1983, 1985) developed a heterogeneous model for multiple indicator dilution studies, and applied it to various compounds. The model combined a residence time distribution for the vascular space with transport between the vascular space, the space of Disse, and the hepatocytes. Goresky determined the mixing characteristics of the organ from a pulse injection of a tracer confined to the vascular space; concomitant injection of extravascular and extracellular markers provided information on the volume of the space of Disse and the extracellular volume. A discussion of the model equations is presented below:

Applying the principle of conservation of mass to a single sinusoid gives the following expression:

$$\frac{\partial C_{si}}{\partial t} + W_s \frac{\partial C_{si}}{\partial x} + \gamma \frac{\partial C_{vi}}{\partial t} + \theta \frac{\partial C_{ci}}{\partial t} + \frac{k_3}{K_{cr}} \theta C_{ci} = 0 \quad (1.21)$$

where x is the axial distance along the sinusoid.

The distribution in the extravascular space was considered flow limited. Hence,

$$\frac{\partial C_{vi}}{\partial t} = K_{cp} \frac{\partial C_{si}}{\partial t} \quad (1.22)$$

The intracellular concentration is described by:

$$\frac{\partial C_{ci}}{\partial t} = k_1 C_{si} - k_2 \frac{C_{ci}}{K_{cr}} - k_3 \frac{C_{ci}}{K_{cr}} \quad (1.23)$$

The boundary conditions, based on pulse experiments, are:

$$C_{si}(0, t) = \frac{M_0}{Q_s} \delta(t - \epsilon) \quad (1.24)$$

where $\delta(t - \epsilon)$ is a Dirac delta function; ϵ is a time infinitesimally greater than zero. The initial conditions are:

$$C_{si}(x, 0) = 0 \quad ; \quad C_{ci}(x, 0) = 0 \quad ; \quad \frac{\partial C_{si}}{\partial t}(x, 0) = 0$$

For the flow limited case ($k_1 = \infty$; $k_2 = \infty$; $k_1/k_2 = \text{constant}$), the effluent concentration from a single sinusoid is described by:

$$C_{si}(L, t) = \frac{M_0}{Q_s} \exp \left[\frac{k_1 k_3 \theta r}{k_2} \right] \delta \left(t - \left[1 + K_{cp} Q + \frac{k_1 \theta K_{cr}}{k_2} \right] r_s \right) \quad (1.25)$$

For the whole liver, the general equation for the overall effluent concentration at any time, t , is:

$$C_i(t) = Q^{-1} \int_{r_{s, \min}}^{r_s} \frac{M Q_s^2}{M_0 Q} C_{si}(L, t - t_0) n(r_s) d(r_s) \quad (1.26)$$

The term $n(r_s) d(r_s)$ is a discrete function describing the proportion of the sinusoids with transit times between r_s and $r_s + dr_s$, and is

obtained from the residence time distribution of a vascular tracer.

$\tau_{s,min}$ is the minimum transit time through the sinusoid.

Integration of Equation (1.26) with substitution for $C_{si}(L, t-t_0)$ and $n(\tau_s)d(\tau_s)$ is required to obtain effluent concentration-time curves. For vascular and extravascular tracers, the resulting expressions are very straightforward. However, the expression for the effluent concentration of a species undergoing linear intracellular reaction and subject to uptake and release from the cells is an integral equation. Because $n(\tau_s)d(\tau_s)$ is a discrete function that can only be obtained experimentally, Equation (1.26) must be integrated numerically. Similarly, estimation of intracellular concentrations requires numerical integration of an integral equation. The appearance and distribution of metabolites in the cells and vasculature cannot be accounted for.

Profiles from the injection of the drug of interest permitted the estimation of four species-dependent parameters: the effective cellular volume, a rate constant for cellular uptake, a rate constant for cellular release, and a rate of reaction. Effluent tracer profiles of a specific drug could then be used to analyse simple changes in steady-state elimination with subsequent changes in blood flow. Nevertheless, the transit-time-distribution model has limitations. From a practical perspective, it requires a measured, discrete residence time distribution before the model can be applied. Hence, the data requirements of the model are significant. Furthermore, like the distributed model of Bass *et al.* (1978), the transit-time-distribution model is based upon the assumption that all mixing occurs at the outlet of the liver. As discussed earlier, this

may lead to errors in the estimates of maximum reaction velocities and Michaelis constants for non-linear processes.

Forker and Luxon (1978) used a similar heterogeneous model to describe the elimination of galactose. The model is comparable to that of Goresky, except that the mass flux was related to the mass of material, rather than the concentration. Similar to Bass *et al.* (1978), the mixing characteristics of the liver were estimated using a Gaussian distribution of sinusoid transit times to approximate a vascular indicator-dilution curve, and only the special case of linear transport and metabolism were considered.

The predominant application of these microscale models has been for compounds subject to carrier-mediated transport or irreversible uptake into the cells. For these compounds, the time scale for the net interphase transport is similar to the time scale for mixing in the vasculature. If, however, the time scale for transport is significantly greater than the time scale for vascular mixing, it may be possible to use compartments and a macroscopic approach to liver modelling. The compartmental approach was first used by Kety (1951), and applied to compounds that undergo diffusive, reversible transport between the cells and the vasculature. The slower net rate of transport for these compounds permitted successful application of a compartmental model.

Tsuji *et al.* (1983) developed a three-compartment heterogeneous model for non-eliminating species (Figure 1.5a). The first compartment represented a well-mixed capillary bed; the second and third compartments were parallel to the first, and represented the space of Disse and the intracellular space, respectively. Flow of

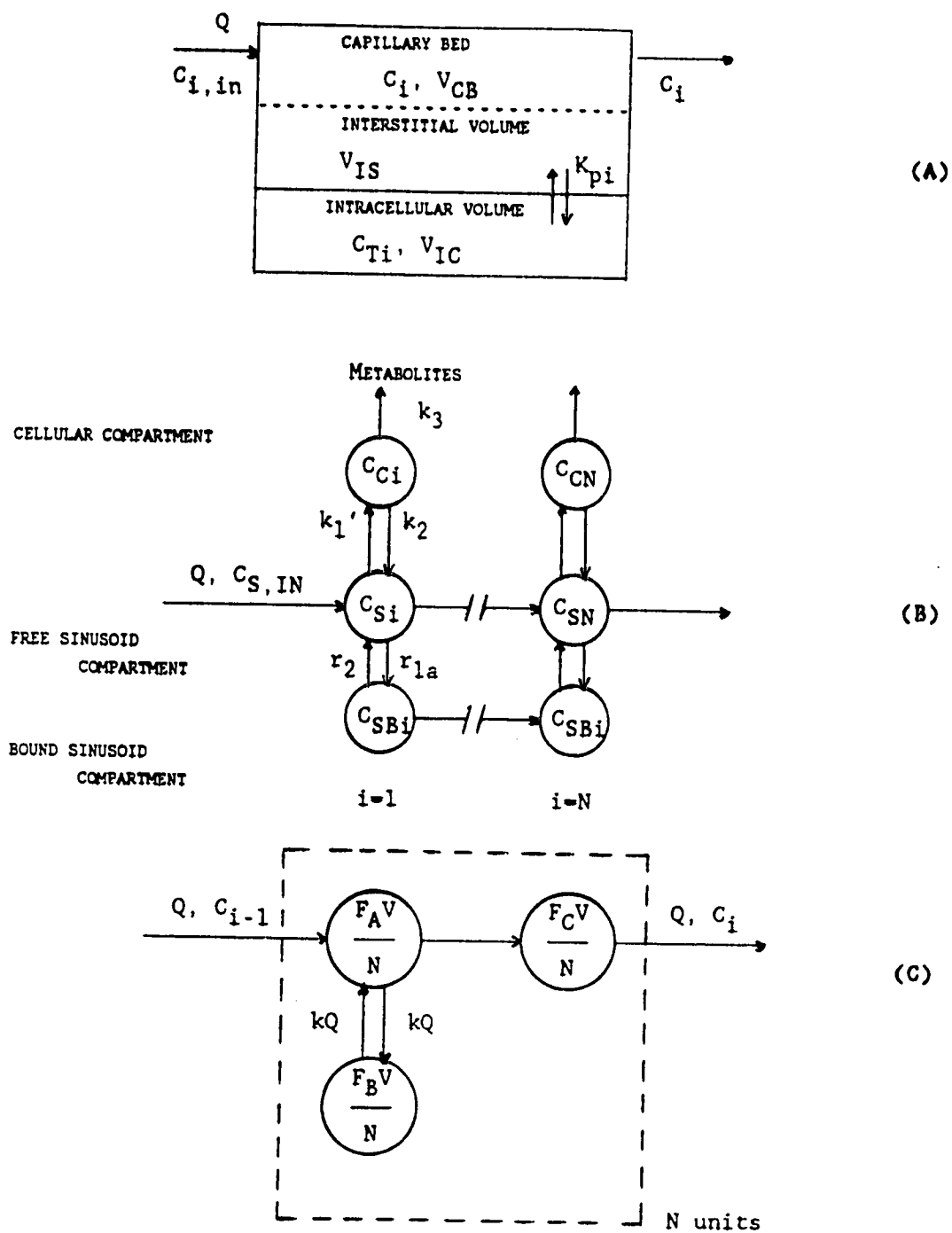


Figure 1.5 Heterogeneous models for drug elimination in the liver

(a) Model of Tsuji *et al.* (1983)

(b) Model for binding and transport proposed by Weisiger (1985).

(c) Finite stage transport model (Rogers and Gardner, 1979)

Each diagram is an adaptation of the published model.

material was restricted to the capillary bed; materials gained access to the peripheral compartments by mass transfer. It was assumed that transport processes were much faster than other processes, leading to rapid equilibration between species in the capillary bed and the tissue. Hence, transport parameters were not specifically evaluated. Instead, differences in drug levels between the capillary bed and the tissue were encompassed within a coefficient for partitioning between the compartments. The model was extended to account for drug elimination, but assumed that the reactions occurred in the capillary bed. However, by using the partition coefficient, the model was capable of accurately predicting tissue drug concentrations of several β -lactam antibiotics. The governing equation for the model is:

$$(V_{IS}+V_{SI}) \frac{dC_i}{dt} = Q \cdot (C_{i,in} - C_i) - \frac{V_m C_i}{(K_m + C_i)} \quad (1.27)$$

Equation (1.28) was used to estimate the tissue concentrations of the compounds.

$$C_{Ti} = K_{pi} C_i \quad (1.28)$$

Weisiger (1985) developed a compartmental model to describe dynamic exchange between bound and free fractions of species in plasma (Figure 1.5b). The model incorporated separate rates of uptake and release between species in the plasma and in the cells, in addition to intracellular reaction of the unbound species. The model also accounted for non-equilibrium binding to and dissociation from proteins in the plasma. The model equations are as follows:

For species in sinusoid compartment i:

$$V_{si} \frac{dC_{si}}{dt} = Q \cdot (C_{s,i-1} - C_{si}) - (k_1' + k_b A) \cdot C_{si} + k_2 C_{ci} + k_{dis} C_{sbi} \quad (1.29)$$

For bound species in sinusoid compartment i:

$$V_{si} \frac{dC_{sbi}}{dt} = Q \cdot (C_{sb,i-1} - C_{sbi}) - k_{dis} C_{sbi} + k_b A C_{si} \quad (1.30)$$

For species in cellular compartment i:

$$V_{ci} \frac{dC_{ci}}{dt} = k_1' C_{si} - (k_2 + k_3) \cdot C_{ci} \quad (1.31)$$

No effort was made to fit experimental data using the model, but a variety of limiting cases and predicted trends were discussed. Depending upon conditions, single-pass drug extraction could be limited by flow, influx, elimination, and dissociation of the compound from a bound complex. Under flow-limited conditions, 100% extraction was predicted, whereas if influx or elimination were limiting, the drug could pass through the organ virtually unchanged. A broad spectrum of conditions could be handled by the model, suggesting that the model was applicable to a variety of substrates and physiological conditions.

Models for chemical reaction and flow in multiphase systems have been presented in the chemical engineering literature. Buffham and Gibilaro (1968) discussed a model for non-eliminated species in porous media. The model consisted of a series of well-mixed vessels with exchange between each vessel and a peripheral vessel representing the stationary phase. The exchange between the flowing and stationary phases was assumed to be in equilibrium; an equivalent fraction of the material enters and leaves the stationary phase at

any given time. For practical use, the model as described must be modified to allow for substrate elimination and different rates of transport between the flowing and stationary compartments.

Rogers and Gardner (1979) used a six-parameter finite-stage transport concept to describe residence-time-distribution functions of continuous processes. The model used units of three compartments (Figure 1.5c) to describe tracer behavior. In each unit, a primary well-mixed compartment and a plug flow compartment were arranged in series; the well-mixed compartment undergoes equilibrium exchange with a peripheral well-mixed compartment. The peripheral compartment represented a dead volume in the reactor, and the plug flow compartment represented a simple time delay.

For the primary well-mixed compartment (compartment A):

$$\frac{F_A V}{N} \frac{dC_{Ai}}{dt} = Q \cdot (C_{i-1} - C_{Ai}) + kQ \cdot (C_{Bi} - C_{Ai}) \quad (1.32)$$

For the peripheral well-mixed compartment (compartment B):

$$\frac{F_B V}{N} \frac{dC_{Bi}}{dt} = kQ \cdot (C_{Ai} - C_{Bi}) \quad (1.33)$$

The time lag is accounted for by including a plug flow compartment, C. The appropriate equations are:

$$C_i(t) = C_n(t - F_C \tau) \cdot H(t - F_C \tau) \quad (1.34)$$

where $H(t - F_C \tau)$ is a step function described by:

$$H(t - F_C \tau) = 0 \text{ if } t < F_C \tau$$

$$H(t - F_C \tau) = 1 \text{ if } t \geq F_C \tau$$

$$\text{and } \tau = V_{\text{tot}}/Q$$

Similar expressions can be written for each of N compartments.

The model as stated (Equations 1.32 to 1.34) does not have any provision for chemical reaction, nor does it allow for different rates of transfer between the primary and peripheral well-mixed compartments. The model was successfully applied to tracer profiles obtained from a wet ball mill, and was deemed to be more versatile and accurate than the series compartment model.

To date, a general, physiologically accurate, mathematically simple model of liver metabolism has not been developed. Some models, such as the well-mixed and parallel tube models, require so many approximations as to limit their use to a very select number of substrates. Other homogeneous models incorporate a range of mixing phenomena, but are limited in other ways. The dispersion model is not theoretically justified, and is limited by its mathematical complexity. The series-compartment model is very general for species without transport limitations, and is mathematically simple; however, it is completely empirical in nature. There is no direct means of accounting for physiological phenomena such as transport and variable flow through the liver. The distributed model is sufficiently complex mathematically that its use is limited. The homogeneous models are not useful for investigating transport processes; for this, a heterogeneous model is required.

The heterogeneous models are more accurate physiologically, if only because they account for transport processes between species in the cells and the vasculature. The general heterogeneous models that have been tested are complex (e.g. Goresky; Forker and Luxon), but may serve as a basis for simpler models. The heterogeneous model proposed by Tsuji et al. (1983) invokes some drug-specific

assumptions, and is, therefore, not general. Further refinement could, however, lead to a useful hepatic model. Similarly, the Deans-Levich model (Buffham and Gibilaro, 1968) and the Finite Stage Transport Model (Rogers and Gardner, 1979) are promising, but require modification to include reaction and different rates of transport between adjacent compartments before they can be used to describe liver metabolism. Weisiger (1985) presented a very promising compartmental model, allowing for substrate binding, a range of flow effects, uptake and release between a vascular and cellular compartment, and the intracellular reaction of species. The model seems general, but no attempt was made to fit experimental data. Further investigation of the model is necessary before it can be accepted as a useful model of liver metabolism.

One objective of this work is to develop a physiological liver model that is mathematically simple and can be applied to a wide range of substrates. The development of the model may entail refinement of an existing model, such as the compartment model of Weisiger (1985), or, if necessary, the development of a new model.

References

- Ahmad, A.B., Bennett, P.N., and Rowland, M.: "Models of Hepatic Drug Clearance: Discrimination Between the Well-Stirred and the Parallel-Tube Models", *J. Pharm. Pharmacol.*, **35**, 219-224, (1983).
- Bass, L., Keiding, S., Winkler, K., and Tygstrup, N.: "Enzymatic Elimination of Substrates Flowing Through the Intact Liver", *J. Theor. Biol.*, **61**, 393-409, (1976).
- Bass, L., Robinson, P., and Bracken, A.J.: "Hepatic Elimination of Flowing Substrates: The Distributed Model", *J. Theor. Biol.*, **72**, 161-184, (1978).
- Bassingthwaite, J.B., Knopp, T.J., and Hazelrig, J.B.: "A Concurrent Flow Model of Capillary-Tissue Exchange", in Capillary Permeability: The Transfer of Molecules and Ions Between Capillary Blood and Tissue, C. Crone and N.A. Lassen, eds., Academic Press, (1970).
- Brauer, R.W.: "Liver Circulation and Function", *Physiol. Rev.*, **43**, 115-213, (1963).
- Buffham, B.A., and Gibilaro, L.G.: "The Analytical Solution of the Deans-Levich Model for Dispersion in Porous Media", *Chem. Eng. Sci.*, **23**, 1399-1401, (1968).

- Davenport, R.: "The Derivation of the Gamma-Variate Relationship for Tracer Dilution Curves", *J. Nucl. Med.* 24, 945-948, (1983).
- Duduković, M.P.: "Tracer Methods in Chemical Reactors: Techniques and Applications", presented at the NATO Chemical Reactor Design and Technology Symposium, London, Canada, June 2-12, 1985.
- Forker, E.L., and Luxon, B.: "Hepatic Transport Kinetics and Plasma Disappearance Curves: Distributed Modeling Versus Conventional Approach", *Am. J. Physiol.*, 235(6), E648-E660, (1978).
- Gillette, J.R.: "Pharmacokinetics of Biological Activation and Inactivation of Foreign Compounds", in Bioactivation of Foreign Compounds, M.W. Anders, ed., Academic Press, 29-70, (1985).
- Goresky, C.A.: "A Linear Method for Determining Liver Sinusoidal and Extravascular Volumes", *Am. J. Physiol.*, 204(4), 626-640, (1963).
- Goresky, C.A., Bach, G.G., and Nadeau, B.E.: "On The Uptake of Materials by the Intact Liver: The Concentrative Transport of Rubidium-86", *J. Clin. Invest.*, 52, 975-990, (1973a).
- Goresky, C.A., Bach, G.G., and Nadeau, B.E.: "On The Uptake of Materials by the Intact Liver: The Transport and Net Removal of Galactose", *J. Clin. Invest.*, 52, 991-1009, (1973b).

Goresky, C.A., Bach, G.G., and Rose, C.P.: "Effects of Saturating Metabolic Uptake on Space Profiles and Tracer Kinetics", *Am. J. Physiol.*, 244, G215-G232, (1983).

Goresky, C.A., Bach, G.G., Wolkoff, A.W., Rose, C.P., and Cousineau, D.: "Sequestered Tracer Outflow Recovery in Multiple Indicator Dilution Experiments", *Hepatology*, 5(5), 805-814, (1985).

Gray, M.R., and Tam, Y.K.: "The Series-Compartment Model For Hepatic Elimination", *Drug Metab. Disp.*, 15, 22-27, (1987).

Hill, C.G.: An Introduction to Chemical Engineering Kinetics and Reactor Design, Chapter 11, Wiley, Toronto (1977).

Kety, S.S.: "The Theory and Applications of the Exchange of Inert Gas at the Lungs and Tissues", *Pharmacol. Rev.*, 3, 1-41, (1951).

Koo, A., Liang, I.Y.S., and Cheng, K.K.: "The Terminal Hepatic Microcirculation in the Rat", *Quart. J. Exper. Physiol.*, 60, 261-266, (1975).

Krogh, A.: "The Number and Distribution of Capillaries in Muscles With Calculations of the Oxygen Pressure Head Necessary for Supplying the Tissue", *J. Physiol.*, 52, 409-415, (1919).

- Lubbers, D.W.: A Symposium on Oxygen Measurements in Blood and Tissues, J.P. Payne and D.W. Hill, eds., J. and A. Churchill Ltd., London, (1966).
- Motta, P., Muto, M., and Fujita, T.: The Liver: An Atlas of Scanning Electron Microscopy, Igaku Shoin, New York, (1978).
- Pang, K.S., and Rowland, M.: "The Hepatic Clearance of Drugs. I. Theoretical Considerations of a 'Well-Stirred' Model and a 'Parallel-Tube' Model: Influence of Hepatic Blood Flow, Plasma and Blood Cell Binding, and the Hepatocellular Enzymatic Activity on Hepatic Drug Clearance", *J. Pharmacokin. Biopharm.*, **5(6)**, 655-680, (1977).
- Rappaport, A.M.: "Hepatic Blood Flow: Morphological Effects and Physiologic Regulation", in Liver and Biliary Tract Physiology. I., N.B. Javitt, ed., University Park Press, Baltimore, (1980).
- Roberts, M.S.R., and Rowland, M.: "Hepatic Elimination: The Dispersion Model", *J. Pharm. Sci.*, **74(5)**, 585-587, (1985).
- Rogers, R.S.C., and Gardner, R.P.: "Use of a Finite Stage Transport Concept for Analyzing residence Time Distribution Functions of Continuous Processes", *Amer. Inst. Chem. Engg J.*, **25(2)**, 229-240, (1979).

Snell, R.S.: Clinical Anatomy for Medical Students , 175-262,
Littlebrown and Company, Boston, (1973).

Tsuji, A., Yoshikawa, T., Nishide, K., Minami, H., Kimura, M.,
Nakashima, E., Terasaki, T., Miyamoto, E., Nightingale, C.,
and Yamana, T.: "Physiologically Based Pharmacokinetic Model
for β -Lactam Antibiotics I.: Tissue Distribution and
Elimination in Rats", *J. Pharm. Sci.*, 72(11), 1239-1252,
(1983).

Tygstrup, N., and Winkler, K: "Kinetics of Galactose Elimination",
Acta Physiol. Scand., 32, 354-362, (1954).

Weisiger, R.A.: "Dissociation from Albumin: A Potentially
Rate-Limiting Step in the Clearance of Substrates by the
Liver", *Proc. Natl. Acad. Sci. USA*, 82, 1563-1567, (1985).

CHAPTER 2: MATERIALS AND METHODS

Lidocaine, an efficiently metabolised anti-arrythmic agent, was used as a probe of transport and metabolism in the liver. The investigations involved continuous drug or metabolite administration to the isolated rat liver under controlled conditions. Experiments with labelled lidocaine were used to investigate hepatic transport and binding to liver proteins and tissues.

Lidocaine hydrochloride and the hydrochlorides of the metabolites of lidocaine (monoethylglycinexylidide (MEGX), 3-hydroxylidocaine (3-OHLID), 3-hydroxyMEGX (3-OHMEGX), and glycinexylidide (GX)) were obtained from Astra Pharmaceuticals (Mississauga, Ontario). [^{14}C] carbonyl-labelled lidocaine was obtained from New England Nuclear (Boston, Mass.).

All experiments used rat livers isolated from male Sprague-Dawley rats (175 to 425 g) supplied by Biosciences Animal Services, University of Alberta. Surgical methods and equipment described by Miller (1973) and by Tam et al. (1987) were applied. Rats were anesthetized with diethyl-ether, and the liver was isolated by surgical cannulation of the hepatic and portal veins, and the inferior vena cava. The isolated organ was perfused with oxygenated (5:95 $\text{CO}_2:\text{O}_2$) Kreb's bicarbonate buffer at a constant flow rate. The perfusion rate was maintained at 3 to 5 ml/(min·g liver) to ensure an adequate supply of oxygen. The temperature of the perfusate was maintained at 37°C by preheating in a water bath, and the pH of the perfusate was controlled at 7.4 by an automatic titration system. During the experiment, the organ was kept moist and at a

physiological temperature within a constant temperature perfusion apparatus. The consumption of oxygen by the liver and the general physical appearance of the organ were used as guides to its viability over the course of the experiment. Furthermore, the viability of the liver was confirmed by the stability of lidocaine and metabolite levels at steady state during continuous drug infusion. Concentrated lidocaine was infused using a syringe pump. Samples of the inlet concentration were taken every 10 minutes to verify the infusion rate and ensure that a constant inlet concentration was maintained.

Frequent samples of the liver effluent were obtained; these samples were analyzed by HPLC. Separation of lidocaine and its metabolites (MEGX, 3-OHLID, 3-OHMEGX, 2-hydroxymethyl-lidocaine, GX, xylidine, 3-hydroxyxylidine, 4-hydroxyxylidine, and 3-hydroxyGX) was achieved using a Waters Novapak C₁₈ column. The mobile phase consisted of 94.83% H₂O, 5.02% acetonitrile, 0.095% H₃PO₄, and 0.047% triethylamine. Ethylmethylglycinexylidide was used as the internal standard. Although lidocaine and nine metabolites could be detected using the assay, only lidocaine and the first four metabolites listed appeared in appreciable quantities. The standard curves for all species were linear over the entire observable range of concentrations, and intrasample variation was less than 5 percent. The mathematical expressions for the standard curves are presented in Appendix A.

Radioactive samples were assayed in the following manner: 2.5 ml of scintillation fluor was added to 0.5 ml of the radioactive sample. The contents were mixed thoroughly for 10 minutes. The activity of the mixture was then determined using an LKB Redirack

liquid scintillation counter. Duplicates of each sample were prepared and analyzed; intrasample variation was less than 3 percent.

References

- Miller, L.L.: "Techniques of Isolated Rat Liver Perfusion", in
Isolated Rat Liver Perfusion and its Applications,
I. Bartosek, A. Guaitani, and L.L. Miller, eds, 11-52, Raven
Press, New York, (1973).
- Tam, Y.K., Yau, M., Berzins, R., Montgomery, P.R., and Gray, M.:
"Mechanisms of Lidocaine Kinetics in the Isolated Perfused Rat
Liver. I. Effects of Continuous Infusion", *Drug Metab. Disp.*,
15(1), 12-16, (1987).

Chapter 3

LIDOCAINE METABOLISM: GENERAL CHARACTERISTICS AND STEADY STATE MODELLING¹

Lidocaine kinetics have shown time-dependence during long term intravenous infusions in humans (Bauer *et al.*, 1982; Bax *et al.*, 1980). Time-dependent lidocaine metabolism was also observed by Lennard *et al.* (1983) and by Tam *et al.* (1987) in rats of different sex and strain, and experiments using dogs showed a significant reduction in the hepatic elimination of lidocaine during continuous infusion (Le Lorier *et al.*, 1977). Many reasons have been suggested for the observed time-dependent phenomena, including saturation of metabolism (Lalka *et al.*, 1976; von Bahr *et al.*, 1977), product inhibition (Lennard *et al.*, 1983; Suzuki *et al.*, 1984), reduction in hepatic blood flow (Lennard *et al.*, 1983), and irreversible binding of lidocaine to liver tissue (Chen *et al.*, 1980). Most of these hypotheses, however, were based on data obtained from studies in a recirculating system. In a recirculating system, the analysis of the effects of these phenomena upon metabolism are complicated by recirculation of blood through the liver, which results in a variable inlet concentration for all species. Studies with isolated, artificially sustained organs under controlled conditions can overcome difficulties with drug recirculation, and provide an effective method for assessing the phenomena affecting drug metabolism in the liver.

1. A version of this chapter has been published.
Saville, B.A., Gray, M.R., and Tam, Y.K.
Drug Metab. Disp., 15(1), 17-21. (1987).

The primary reaction pathways for the elimination of lidocaine were established by Keenaghan and Boyes (1972) and Suzuki *et al.* (1984). As shown in Figure 3.1, the reaction network consisted of parallel and sequential reactions. Reactions 1 and 5 are primarily deethylation reactions; reactions 2, 3, and 4 are primarily hydroxylation reactions. von Bahr *et al.* (1977) determined that the hydroxylation reactions were catalyzed by one fraction of the cytochrome P-450 enzyme, and the deethylation reactions were mediated by another cytochrome P-450 fraction. Kawai *et al.* (1985) established that the deethylation pathways (1 and 5) were catalyzed by at least two distinct P-450 fractions. Competition of species for common enzyme sites gave rise to competitive inhibition (Suzuki *et al.* 1984).

Material Balance Data

Chromatographic analysis of effluent samples suggested that two unknown secondary metabolites of lidocaine were formed within the liver. These species, derived from 3-OHLID and 3-OHMEGX, have not yet been identified, but their overall contribution to the material balance was small. In experiments with unlabelled lidocaine, 80 to 90 percent of the liver effluent consisted of identifiable species: either unconverted lidocaine or the nine known metabolites. As the amount of lidocaine infused was increased, the material balance improved, suggesting that the formation of the unknowns was saturable. A typical chromatogram of the species collected in the liver effluent is presented in Figure 3.2 and Table 3.1. In five

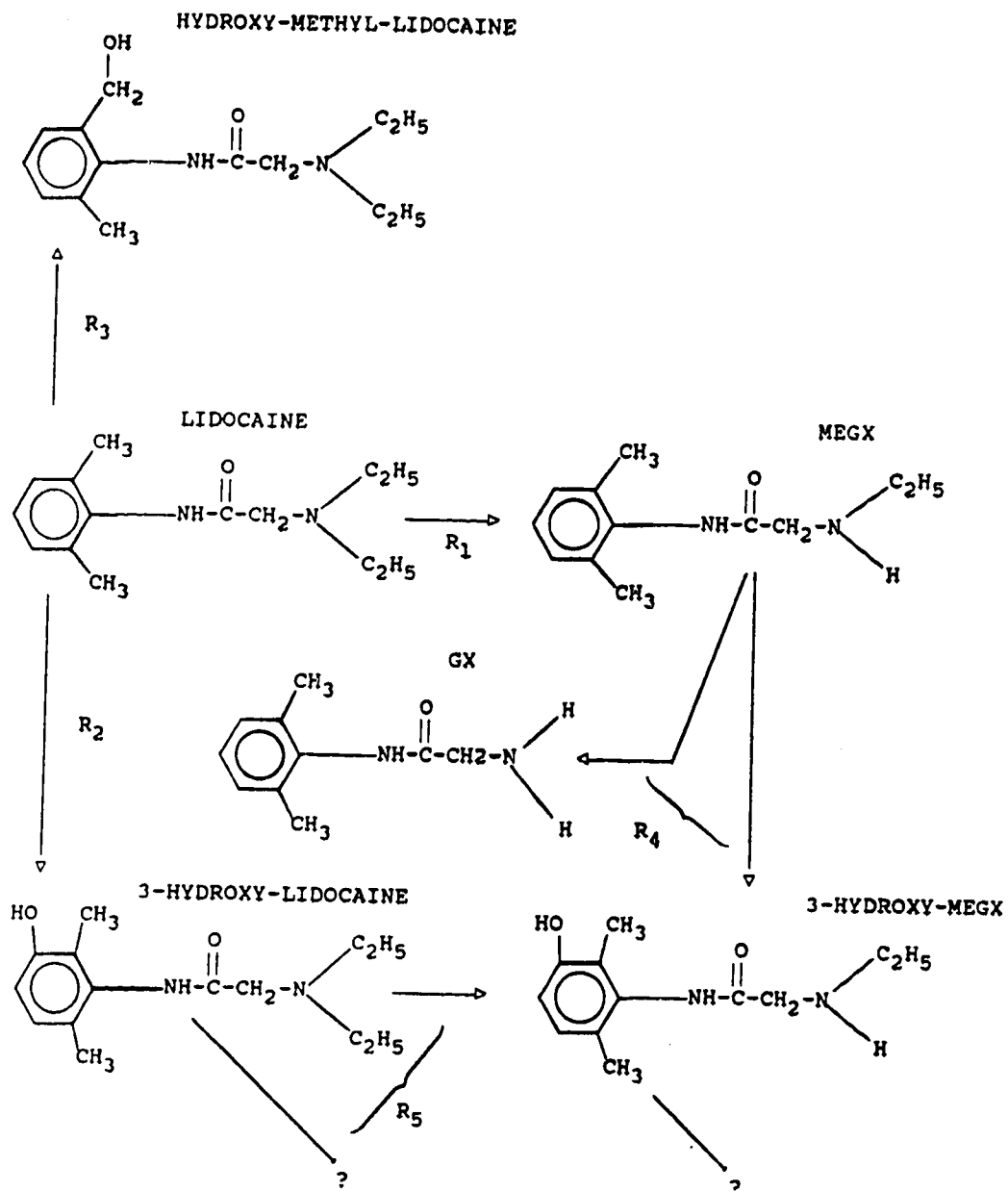


Figure 3.1 Pathways for lidocaine metabolism

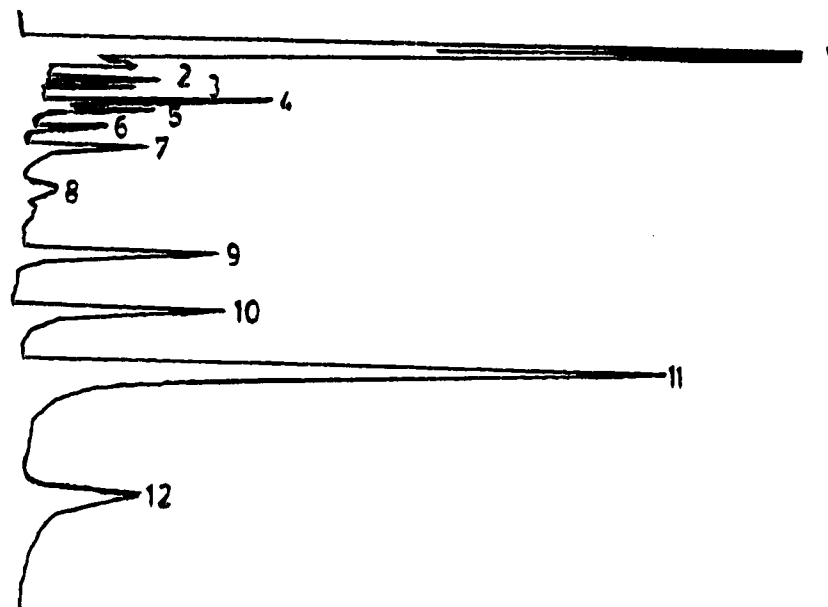


Figure 3.2 *Chromatogram of effluent sample collected during continuous infusion of lidocaine*

Chromatographic peaks identified in Table 3.1

Total time of analysis = 18 min.

experiments with ^{14}C -labelled lidocaine, 93 ± 4 percent of the infused label was recovered in the effluent. Losses through the bile duct were small, accounting for less than 1 percent of the inlet tracer.

Table 3.1: Identification of Chromatographic Peaks of Lidocaine and Metabolites

<u>Peak Number</u>	<u>Identity</u>	<u>Retention Time, min.</u>
1	solvent	1.29
2	unknown #1	1.86
3	3-OHMEGX	2.12
4	endogenous species	2.44
5	endogenous species	2.68
6	unknown #2	3.15
7	3-OHLID	3.71
8	2-hydroxymethyl-lidocaine	4.76
9	endogenous species	6.50
10	MEGX	8.05
11	EMGX	9.53
12	lidocaine	12.90

Kinetics of Steady State Elimination

The kinetics of steady-state lidocaine elimination were examined using the data of Tam *et al.* (1987). These experiments investigated the steady state elimination of lidocaine in the isolated, intact rat liver under conditions of constant perfusion.

Data from the continuous infusion of lidocaine at inlet concentrations ranging from 9.6 to 278 μM ($n=16$) were used to estimate the kinetic parameters for the formation of the primary metabolites. Kinetic parameters for secondary elimination were determined from the independent infusion of MEGX or 3-OHLID in the absence of lidocaine. Inlet concentrations of MEGX ranged from 2 to 74 μM ($n=9$), and for 3-OHLID, ranged from 5.5 to 46 μM ($n=8$). The reactions of lidocaine and its metabolites were effectively described by Michaelis-Menten kinetics, with adjustments made to account for competitive inhibition. An example is the rate expression for the hydroxylation of lidocaine (reaction 2):

$$R_2 = \frac{V_{m2} \cdot C_1}{(C_1 + [K_{m2}/K_{m4}] \cdot C_2 + K_{m2})} \quad (3.1)$$

The central term in the denominator accounted for competition between parallel reaction pathways. The rate expressions for all metabolic pathways are presented in Appendix B.

The Modified Simplex technique (Nelder and Mead, 1965) was used to calculate the optimum values of the kinetic parameters. Internally, the Simplex technique applied a method of successive substitution to predict steady state concentrations for a proposed set of kinetic parameters. The sum of squared residuals was calculated by comparing the predicted and experimental concentrations. The variance of the concentration of each species about its mean steady state value was calculated and used to weight the sum of residuals. The Simplex routine systematically adjusted the parameter values until the weighted sum of residuals was minimized.

The variance of the kinetic parameters was determined by quadratic approximation (Kemeny *et al.*, 1982).

Based on experimental data, some pathways were modified to combine reactions of minor metabolites. The kinetic parameters for the pooled elimination of exogenous MEGX and 3-OHLID were calculated first, then combined with the data from the infusion of lidocaine to determine the remaining kinetic constants. The optimal kinetic parameters are presented in Table 3.2. The values for the pathways represent averages for the population of livers. For comparison, the parameters estimated by Suzuki *et al.* (1984) are also listed in Table 3.2. Suzuki's estimates were based on data from liver microsomes (homogenized liver proteins) instead of the intact liver; therefore, the values of the reaction velocities were converted from $\mu\text{mol}/(\text{min} \cdot \text{g} \text{ microsomal protein})$ to $\mu\text{mol}/(\text{min} \cdot \text{g} \text{ liver})$, using an estimate of 30 mg microsomal protein per gram of liver tissue (Rikans and Notley, 1982).

Table 3.2: Kinetic Parameters For Steady State Lidocaine Elimination

<u>Parameter</u>	<u>Model Estimates</u>	<u>Microsomal Study</u>
k_1 , ml/(g·min)	2.62 ± 0.007	0.494
V_{m2} , $\mu\text{mol}/(\text{g} \cdot \text{min})$	0.0313 ± 0.0009	0.00894
K_{m2} , μM	2.29 ± 0.06	1.78
V_{m3} , $\mu\text{mol}/(\text{g} \cdot \text{min})$	0.0127 ± 0.0008	
K_{m3} , μM	1.99 ± 0.08	
V_{m4} , $\mu\text{mol}/(\text{g} \cdot \text{min})$	0.0723 ± 0.0116	0.0033
K_{m4} , μM	22.3 ± 6.6	20.9
V_{m5} , $\mu\text{mol}/(\text{g} \cdot \text{min})$	0.0419 ± 0.0027	0.214
K_{m5} , μM	2.35 ± 0.27	562.

In general, the maximum reaction velocities were much greater for the whole liver than the liver microsomes; estimates of the Michaelis constants were similar for the two studies. The differences in V_{m5} and K_{m5} may be attributable to the formation of an unknown species from 3-OHLID. The values of V_{m5} and K_{m5} from Suzuki *et al.* (1984) were based only on the deethylation of 3-OHLID; however, 3-OHLID undergoes both linear deethylation to form 3-OHMEGX, and forms an unknown compound via a saturable pathway. The selectivity between the parallel routes of elimination will have a significant influence upon pooled estimates for the metabolism of 3-OHLID. Furthermore, this pathway may be affected by cellular uptake. If so, different estimates for the reaction parameters would be obtained from intact cells versus the homogenated (isolated) cells, simply due to the different mass transfer characteristics in the two systems.

As shown in Figures 3.3 and 3.4, the agreement between the predicted and experimental steady state concentrations was very good. For lidocaine and MEGX, the correlation coefficients were 0.981 and 0.980, respectively. The model predictions for 3-OHLID (not shown) exhibited more deviation (correlation coefficient = 0.775) due to increased variability between the individual livers.

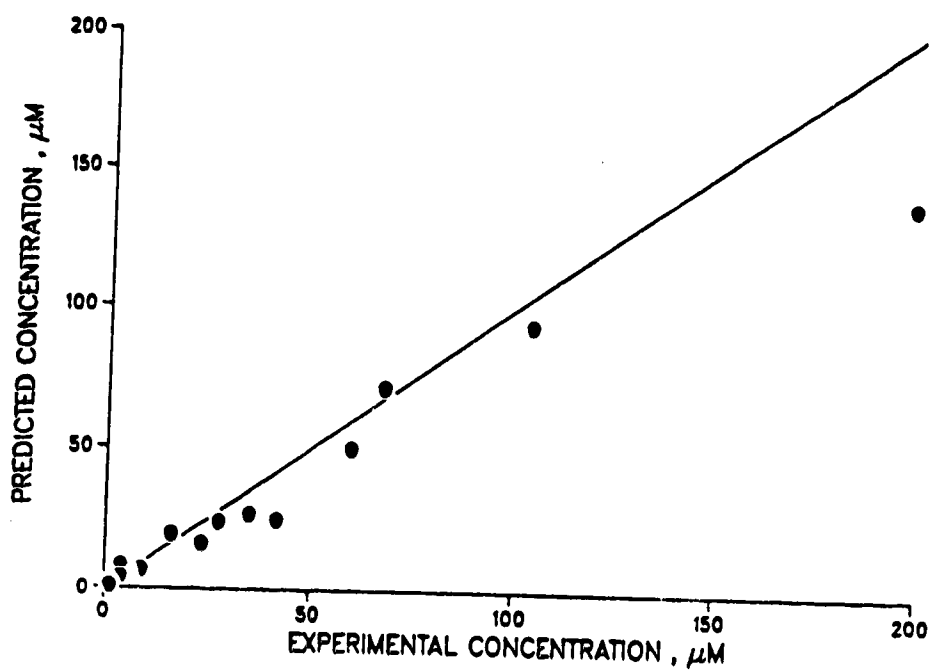


Figure 3.3 Actual vs. predicted effluent concentration of lidocaine
Predicted values obtained using parameters from Table 3.2



Figure 3.4 Actual vs. predicted effluent concentration of MEGX
Predicted values obtained using parameters from Table 3.2

The kinetic parameters (Table 3.2) and the experimental observations indicated that the metabolism of lidocaine was dominated by the linear formation of MEGX. Although the metabolites compete with lidocaine for common enzyme sites, the resulting competitive inhibition has only a minor role in lidocaine metabolism, for the following reasons:

1) MEGX will inhibit lidocaine hydroxylation, preventing the formation of 3-OHLID. However, the amount of 3-OHLID normally formed is small relative to the amount of MEGX formed from lidocaine. Hence, a decrease in 3-OHLID production will represent only a small decrease in the amount of lidocaine metabolized.

2) In principle, the formation of MEGX could be inhibited by 3-OHLID. However, because only a small amount of 3-OHLID is present, and the formation of MEGX is linear over a broad concentration range, competitive inhibition by 3-OHLID has a minor effect upon the metabolism of lidocaine.

The net result is that the metabolism of lidocaine can be approximated as a pseudo-linear process, because the competing pathways are negligible relative to the linear formation of MEGX.

References

- Bauer, L.A., Brown, T., Gibaldi, M., Hudson, L., Nelson, S., Raisys, V., and Shea, J. Paul: "Influence of Long-Term Infusion on Lidocaine Kinetics", *Clin. Pharmacol. Ther.*, **31**, 433-437 (1982).
- Bax, N.D.S., Tucker, G.T., and Woods, H.F.: "Lignocaine and Indocyanine Green Kinetics in Patients Following Myocardial Infarction", *Br. J. Clin. Pharmacol.*, **10**, 353-361 (1980).
- Chen, C.P., Vu, V.T., and Cohen, S.D.: "Lidocaine Uptake in Isolated Rat Hepatocytes and Effects of dl-propanolol", *Toxicology and Applied Pharmacology*, **55**, 162-168 (1980).
- Kawai, R., Fujita, S., and Suzuki, T.: "Simultaneous Quantitation of Lidocaine and its Four Metabolites by High Performance Liquid Chromatography: Application to Studies on In Vitro and In Vivo Metabolism of Lidocaine in Rats", *J. Pharm. Sci.*, **74**(11), 1219-1223 (1985).
- Keenaghan, J.B., and Boyes, R.N.: "The Tissue Distribution, Metabolism and Excretion of Lidocaine in Rats, Guinea Pigs, Dogs and Man", *J. Pharmacol. Exp. Ther.*, **180**, 454-463 (1972).
- Kemeny, S., Manczinger, J., Skjold-Jorgensen, S., and Toth, K: "Reduction of Thermodynamic Data by Means of the Multiresponse Maximum Likelihood Principle", *Am. Inst. Chem. Eng. J.*, **28**, 20-30, (1982).

- Lalka, D., Manion, C.V., Berlin, A., Baer, D.T., Dodd, B., and Meyer, M.B.: "Dose-Dependent Pharmacokinetics of Lidocaine in Volunteers", *Clin. Pharm. Ther.*, **19**, 110, (1976).
- Le Lorier, J., Moison, R., Gagne, J., and Caille, G.: "Effect of Duration of Infusion on the Disposition of Lidocaine in Dogs", *J. Pharmacol. Exp. Ther.*, **203**, 507-511 (1977).
- Lennard, M.S., Tucker, G.T., and Woods, H.F.: "Time-Dependent Kinetics of Lignocaine in the Isolated Perfused Rat Liver", *J. Pharmacokin. Biopharm.*, **11**, 165-182, (1983).
- Nelder, J.A., and Mead, R.: "A Simplex Method for Function Minimization", *Comput. J.*, **7**, 308-315, (1965).
- Rikans, L.E., and Notley, B.A.: "Age-Related Changes in Hepatic Microsomal Drug Metabolism are Substrate Selective", *J. Pharmacol. Exp. Ther.*, **220**, 574-578, (1982).
- Saville, B.A., Gray, M.R., and Tam, Y.K.: "Mechanisms of Lidocaine Kinetics in the Isolated Perfused Rat liver.II. Kinetics of Steady State Elimination", *Drug Metab. Disp.*, **15**(1), 17-21, (1987).
- Suzuki, T., Fujita, S., and Kawai, R.: "Precursor-Metabolite Interactions in the Metabolism of Lidocaine", *J. Pharm. Sci.*, **73**(1), 136-138 (1984).

Tam, Y.K., Yau, M., Berzins, R., Montgomery, P.R., and Gray, M.R.:
"Mechanisms of Lidocaine Kinetics in the Isolated Perfused Rat
Liver. I. Effects of Continuous Infusion", *Drug Metab. Disp.*,
15(1), 12-16 (1987).

von Bahr, C., Hedlund, I., Karlen, B., Backstrom, D., and
Grasdalen, H.: "Evidence for Two Catalytically Different
Binding Sites of Liver Microsomal Cytochrome P-450: Importance
of Species and Sex Differences in the Oxidation Pattern for
Lidocaine", *Acta Pharmacol. Toxicol.*, 41, 39-48, (1977).

CHAPTER 4: INVESTIGATION OF TIME-DEPENDENT LIDOCAINE METABOLISM:
EFFECTS OF ENZYME INACTIVATION¹

Introduction

Studies of time-dependent metabolism in the isolated rat liver with continuous single-pass perfusion of lidocaine consistently showed that drug and metabolite concentrations reached steady state within 30 to 60 minutes of the initial infusion of the drug (Tam *et al.*, 1987). The prolonged approach to steady state was, however, inconsistent with the rapid uptake of lidocaine by liver cells, which was complete within three minutes (Chen *et al.*, 1980). Profiles of lidocaine and MEGX (e.g. Figure 4.1b) showed that the concentration of the product, MEGX, reached a maximum after about 5 minutes, then declined gradually to its steady-state level. At the same time, its precursor, lidocaine, increased monotonically to steady-state. A material balance on lidocaine and its metabolites indicated that the total amount of material in the effluent was constant after 5 to 10 minutes had elapsed. Substrate binding and enzyme heterogeneity could be ruled out as possible causes for the observed overshoot behavior of lidocaine and MEGX, since these mechanisms were unable to predict a maximum in the MEGX profile (Gray *et al.*, 1987). A theoretical model incorporating partial inactivation of enzymes in the presence of lidocaine gave a consistent representation of the experimental data (Saville *et al.*, 1986) accounting for both the long approach to steady state and the decrease in MEGX production.

1. A version of this chapter has been accepted for publication. Saville, B.A., Gray, M.R., and Tam, Y.K.: "Evidence for Lidocaine-Induced Enzyme Inactivation", *J. Pharm. Sci.*, April 25, 1989.

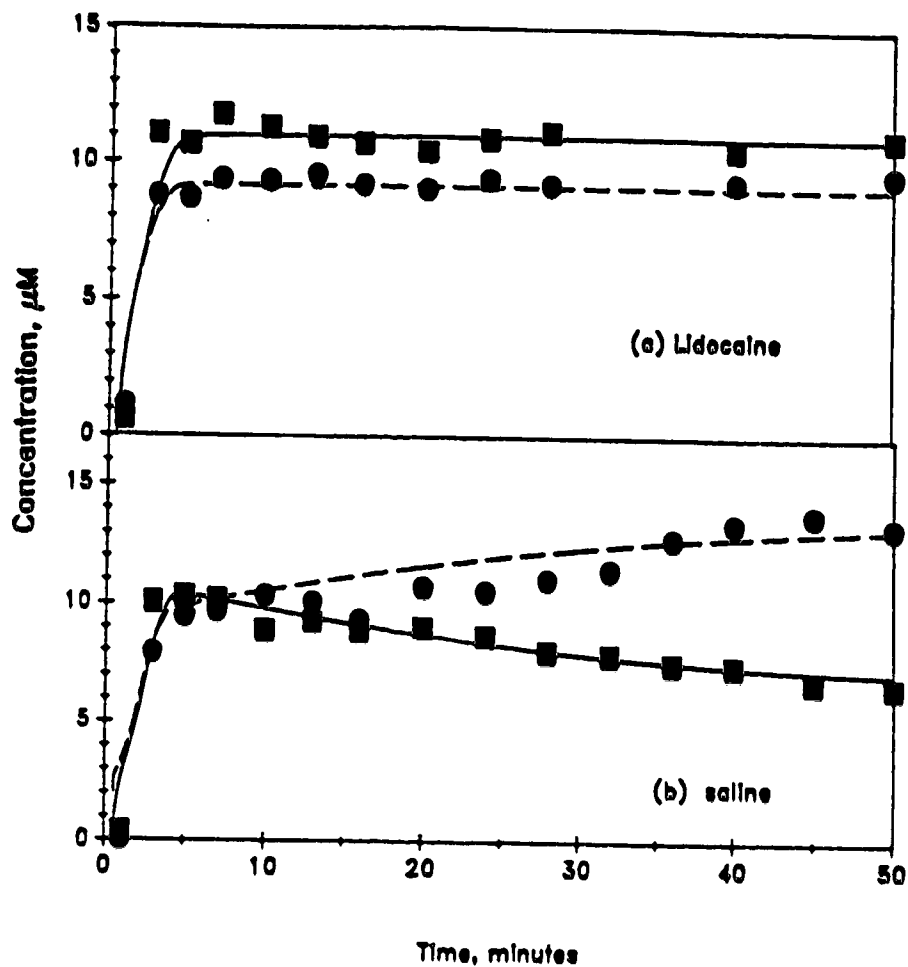


Figure 4.1. Effects of in vivo pretreatment with (a) lidocaine and (b) saline upon in vitro hepatic metabolism of lidocaine.

● lidocaine; ■ MEGX; — model MEGX; ---- model lidocaine

Model Parameters: (a) $C_{in} = 30.8 \mu\text{M}$, $k_1 = k_{1,max} = 3.05$, $k_d = 0.0$, $k_b = 200$, $S_0 = 0.05$, $V_{m2} = 0.021$, $V_{m3} = 0.012$, $V_{m4} = 0.003$, $V_{m5} = 0.025$

(b) $C_{in} = 30.9 \mu\text{M}$, $k_1 = 1.60$, $k_{1,max} = 3.60$, $k_d = 4.70$, $k_b = 250$, $S_0 = 0.075$, $V_{m2} = 0.024$, $V_{m3} = 0.005$, $V_{m4} = 0.018$, $V_{m5} = 0.013$

The objective of this study is to investigate the possible role of reduced enzyme activity as a cause for time-dependent kinetics of lidocaine. To test the validity of the hypothesis, experiments were designed to test for a reduction in lidocaine metabolism in rat livers, both *in vivo* and *in vitro*. The data from these experiments, in addition to data from the literature, were described by a mathematical model for enzyme inactivation.

Theory

Equations for Hepatic Metabolism of Lidocaine

Applying the well-mixed model to lidocaine elimination, in conjunction with a material balance on each species in the liver, gives the following equation:

$$\frac{D_i}{\rho} \frac{dC_i}{dt} = \frac{Q \cdot (C_{i,in} - C_i)}{W} + \sum_{j=1}^5 \mu_{i,j} \cdot R_j \quad (4.1)$$

$$i = 1, 2, 3$$

where C_i is the concentration of species i in the liver. The distribution coefficient for each species, D_i , was assumed to be close to unity. The model predictions were insensitive to this parameter. The detailed rate expressions, R_j , are presented in Appendix B.

To account for possible binding of lidocaine to liver proteins and tissues, an additional term in the liver model was necessary. Experimental observations (Chen *et al.*, 1980) suggested that binding was a second order process; first order in lidocaine concentration (C_1) and first order in the remaining number of binding sites (S).

The appropriate rate expression is:

$$\text{rate of lidocaine binding} = \frac{dS}{dt} = k_b \cdot S \cdot C_1 \quad (4.2)$$

In a recirculating system with the isolated rat liver (e.g. Lennard *et al.*, 1983), additional material balance equations are required to account for the reservoir and the oxygenator. The equations are based on a flow cycle of reservoir-oxygenator-liver-reservoir, as follows:

Reservoir:

$$\frac{dC_{i,R}}{dt} = \frac{Q \cdot (C_{i,L} - C_{i,R})}{V_R} \quad (4.3)$$

Oxygenator:

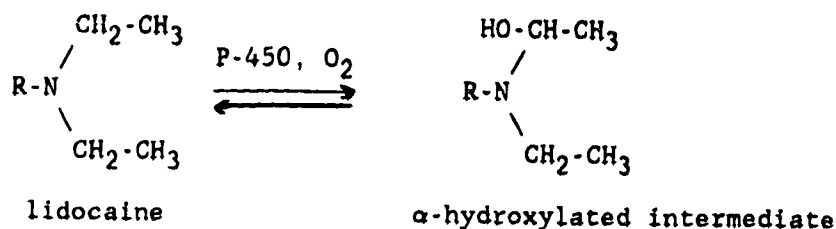
$$\frac{dC_{i,O}}{dt} = \frac{Q \cdot (C_{i,R} - C_{i,O})}{V_O} \quad (4.4)$$

For experiments using the isolated rat liver with single-pass perfusion, the inlet concentration of lidocaine, $C_{1,in}$, was constant, and for all metabolites, the inlet concentration was zero. For experiments using a recirculating system, the concentrations of all species entering the liver would be non-zero, except for the period just prior to the initial administration of lidocaine.

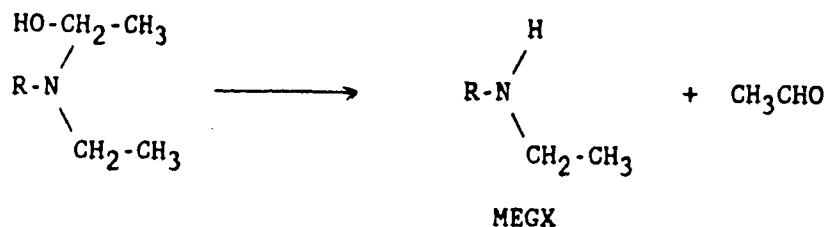
Enzyme Inactivation Model

The metabolism of lidocaine is mediated by several isozymes of cytochrome P-450. Von Bahr *et al.* (1977) determined that the hydroxylation reactions are catalyzed by one fraction of the cytochrome P-450 enzyme, and the deethylation reactions are mediated by another cytochrome P-450 fraction. Furthermore, Kawai *et al.* (1985)

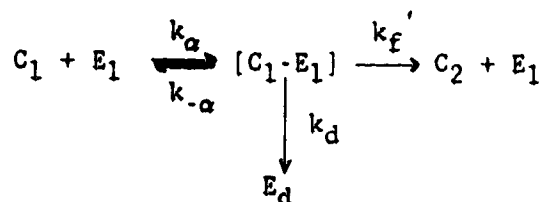
have shown that the deethylation of lidocaine is mediated by at least two cytochrome P-450 enzyme fractions. In the inactivation model presented below, the deethylation of lidocaine was assumed to be mediated by two cytochrome P-450 enzyme fractions, one of which is subject to inactivation. Hence, inactivation gradually reduces the extent of metabolism of lidocaine to a lower, non-zero level. The chemical mechanism for the deethylation of lidocaine by cytochrome P-450 is as follows:



α -hydroxylated compounds are chemically unstable, and are subject to spontaneous non-enzymatic degradation in the following manner:



Since the decomposition of the intermediate is fast, and O_2 is not a limiting substrate, a simplified kinetic mechanism, based upon Michaelis-Menten kinetics, can be used to describe the deethylation of lidocaine. To account for enzyme inactivation, a modified mechanism (shown below) was proposed which permitted degradation of the intermediate into an inactive enzyme form. The kinetic mechanism for enzyme inactivation is consistent with previous research into cytochrome P-450 degradation (Ivanetich *et al.*, 1980).



An expression for the inactivation of the deethylation fraction of the cytochrome P-450 enzyme (Equation 4.16) was developed using the assumption that the rate of inactivation is proportional to the concentration of the enzyme-substrate complex. The following derivation considers the fraction of cytochrome P-450 that is inactivated. The initial step is to apply the pseudo-steady state approximation to the enzyme-substrate complex, $[C_1-E_1]$, as follows:

$$d[C_1-E_1]/dt = k_a \cdot E_1 \cdot C_1 - (k_{-a} + k_f' + k_d) \cdot [C_1-E_1] \approx 0 \quad (4.5)$$

Applying a material balance on the active enzyme in the system at any time gives:

$$E_{1a} = E_1 + [C_1-E_1] \quad (4.6)$$

Rearranging equation (4.6) to solve for E_1 , and substituting into equation (4.5) yields:

$$k_a \cdot C_1 \cdot E_{1a} = (k_{-a} \cdot C_1 + k_{-a} + k_f' + k_d) \cdot [C_1-E_1] \quad (4.7)$$

Dividing by k_a and solving for $[C_1-E_1]$ gives the following expression:

$$[C_1-E_1] = C_1 \cdot E_{1a} / (K_{m1} + k_d/k_a + C_1) \quad (4.8)$$

$$\text{where } K_{m1} = (k_{-a} + k_f')/k_a \quad (4.9)$$

The rate of enzyme loss is given by the following equation:

$$dE_{1a}/dt = -dE_d/dt = -k_d \cdot [C_1-E_1] \quad (4.10)$$

Substituting the expression for $[C_1 \cdot E_1]$ into equation (4.10) gives the following equation:

$$dE_{1a}/dt = -k_d \cdot C_1 \cdot E_{1a} / (K_{m1} + k_d/k_a + C_1) \quad (4.11)$$

Simplifications can be made to equation (4.11) by assuming:

- 1) The rate of inactivation, k_d , is much less than the rate of formation of the enzyme complex, k_a . Thus, k_d/k_a is negligible.
- 2) The deethylation reaction is approximately linear. Hence,

$K_{m1} \gg C_1$, and (4.11) can be rewritten as:

$$dE_{1a}/dt = - (k_d/K_{m1}) \cdot C_1 \cdot E_{1a} \quad (4.12)$$

Letting $k_d' = k_d/K_{m1}$, and solving (4.12) by integrating from time zero to t gives:

$$E_{1a} = E_{10} \exp \left(-k_d' \int_0^t C_1 dt \right) \quad (4.13)$$

E_{10} is the initial amount of high activity deethylation enzyme. The overall rate of deethylation is the sum of the rate due to the inactivatable fraction (Equation 4.13) and the non-inactivatable fraction. The rate of reaction is proportional to the amount of active enzyme, and hence will have the form:

$$k_1 = k_{1ss} + r_1 \exp \left(-k_d' \int_0^t C_1 dt \right) \quad (4.14)$$

where k_{1ss} is the rate at steady state, after inactivation is completed, and r_1 is a proportionality constant for the inactivatable enzyme fraction. At time $t=0$, all of the enzyme is active and

$k_1 = k_{1\max}$. Consequently the rate at any time will be:

$$k_1 = k_{1ss} + (k_{1\max} - k_{1ss}) \exp \left(-k_d' \int_0^t C_1 dt \right) \quad (4.15)$$

Hence, the overall dealkylation activity of the enzyme is exponentially dependent upon the cumulative extent of contact of the enzyme with the drug, represented by the integral of C_1 over time. By definition, the integral of C_1 over time is the area accumulated under the concentration-time curve at time t , or $AUC(t)$. Therefore, Equation (4.15) can be rewritten as:

$$k_1 = k_{1ss} + (k_{1\max} - k_{1ss}) \exp (-k_d' \cdot AUC(t)) \quad (4.16)$$

This equation is applicable to any method of drug administration, whether continuous infusion or repeated bolus doses.

The form of Equation (4.16) indicates that enzyme activity should show an exponential dependence upon the cumulative extent of contact of the enzyme with the drug. At short times, the level of metabolism is highest; after prolonged lidocaine administration, k_1 becomes constant, and equal to k_{1ss} .

Results and Discussion

In an isolated perfused liver with constant inlet concentration of drug, a slow reduction in the metabolism of the infused drug would result in a maximum in the concentration of the product formed via the inactivated metabolic pathway. The concentration of the metabolite would rapidly rise to an initial maximum, as it is distributed within the organ, then slowly decline as the enzyme is inactivated. The peak in MEGX concentration observed when the isolated rat liver is subjected to constant infusion of lidocaine (Gray *et al.*, 1987) could, therefore, indicate inactivation of the dealkylation enzymes. Once inactivation is essentially complete, constant enzyme activity and drug levels would be observed. Any subsequent increase in the inlet concentration of lidocaine should result in a quick approach to a new steady-state, and the MEGX concentration should not exhibit a maximum. When a constant inlet concentration of drug is used in an isolated organ without attendant enzyme inactivation, a peak in the product concentration would not be observed, even if binding and inhibition occur (Gray *et al.*, 1987).

If the reduction in enzyme activity persists over a long period of time, then previous exposure to lidocaine would eliminate the characteristic time-dependent kinetics. Lidocaine would rapidly approach a steady state concentration, and the concentration of MEGX would not display a maximum. Experiments with administration of lidocaine to the rat liver both *in vivo* and *in vitro* were conducted to verify this hypothesis.

In vivo Administration Experiments

To test for inactivation of liver enzymes *in vivo*, the rats were subjected to jugular vein cannulation, and lidocaine (10 mg/kg rat) was administered via the jugular vein catheter 24 hours prior to the isolated organ study. Control experiments were performed in which a saline solution was administered, followed by infusion of lidocaine to the isolated liver 24 hours later. This protocol established the ability of lidocaine to alter enzyme activity *in vivo*, and ensured that surgical trauma did not influence the results.

The data (Figure 4.1a) indicated that pretreatment with lidocaine gave a time course consistent with constant enzyme activity. MEGX rises in a monotonic fashion to steady state, which is attained after less than 10 minutes of lidocaine infusion into the isolated liver. The time to reach steady state was statistically determined using the method described in Appendix C. Table 4.1 shows that the time to reach steady state was significantly reduced when the rat was exposed to lidocaine prior to isolating the liver.

Table 4.1

Time to Reach Steady-State Lidocaine Concentration

<u>Type of Experiment</u>	<u>n</u>	<u>Time, minutes</u>
<i>In vivo</i> lidocaine	3	7
<i>In vivo</i> saline	3	30
Stop-Infusion		
Initial infusion	3	25
Second infusion	3	9
Control		
(Infuse LID after 70 min)	3	23

The concentration-time profiles obtained from rats pretreated with saline (Figure 4.1b) showed normal time-dependent kinetics. Steady state was not achieved until after 30 minutes of drug infusion, and MEGX production decreased from an early maximum during the experiment. Hence, the primary effect of *in vivo* pretreatment with lidocaine is to qualitatively change the metabolism of lidocaine in a subsequent isolated organ study.

Due to individual metabolic variation in metabolism, quantitative comparisons of steady state metabolite/drug ratios are not possible. For example, the data from 25 isolated organ experiments indicated steady state ratios ranging from 0.16 to 1.49 μmol of MEGX per μmol of lidocaine. On an individual basis, however, the MEGX:lidocaine ratio is useful, because the ratio will be constant over time if enzyme activity is constant, but will monotonically decrease if enzyme activity decreases over time. Therefore, by qualitatively comparing the drug and metabolite time profiles in Figures 4.1a and 4.1b, it is apparent that the *in vivo* administration of lidocaine induced a change in the enzyme system of the rat which persisted over 24 hours, and which had an effect upon hepatic metabolism observed from a subsequent *in vitro* organ study.

Stop-infusion Studies

The second series of experiments tested the prediction that time-dependent kinetics would not be observed once drug levels in the isolated rat liver reached steady state. Lidocaine was infused until steady state was reached, then the drug and its metabolites were allowed to clear from the system. Ten minutes later, lidocaine was infused a second time, with the same inlet concentration. This

stop-infusion experiment was used to verify persistent alteration of metabolism in an *in vitro* organ study. The stop-infusion experiments gave drug-concentration profiles as shown in Figure 4.2a. The MEGX concentration reached a maximum soon after the initial infusion of lidocaine. During the second stage of lidocaine infusion, however, MEGX levels increased monotonically to steady state. Hypothesis tests on the slopes of the MEGX data provided statistical confirmation of the initial maximum in the MEGX profile and the absence of a peak during the second stage of lidocaine infusion.

A comparison of the time to reach steady state following the first and second infusions of lidocaine gave additional support to the inactivation hypothesis. As shown in Table 4.1, the time to reach steady state was significantly less during the second stage of lidocaine infusion than during the first. The reduction in the time to reach steady state indicated that the mechanism which caused the time-dependent kinetics was irreversibly altered over the period of the isolated liver experiment.

The results in Figures 4.1 and 4.2 also show the equivalent effects of lidocaine administration to the rat liver *in vivo* and *in vitro*. Hence, the observed time-dependent reduction in lidocaine metabolism during the *in vitro* organ studies was not simply an artifact of isolating the liver.

Although the approach to steady state was quicker when lidocaine was infused for the second time, the time to reach steady state still exceeded the time of 2 to 3 minutes indicated by the mean residence time of the perfusate in the liver (based on total liver volume and flow rate). One explanation is reversible binding of

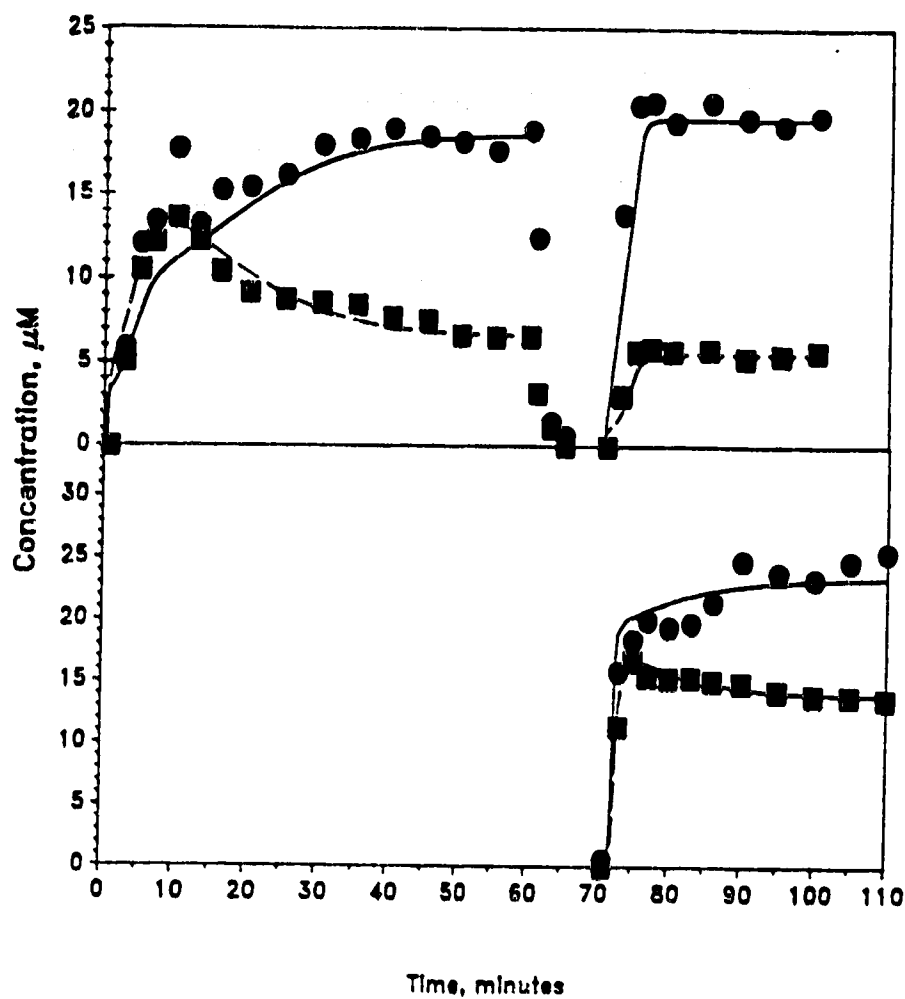


Figure 4.2. *In vitro* hepatic metabolism of lidocaine (a) following pretreatment and (b) after delaying the initial infusion of lidocaine.

● lidocaine; ■ MEGX; — model lidocaine; - - - - model MEGX

Model Parameters: (a) $C_{in} = 42.9 \mu\text{M}$, $k_1 = 1.40$, $k_{1,max} = 6.20$, $k_d = 6.5$, $k_b = 101$, $S_0 = 0.20$, $V_{m2} = 0.035$, $V_{m3} = 0.0135$, $V_{m4} = 0.04$, $V_{m5} = 0.02$

(b) $C_{in} = 47.0 \mu\text{M}$, $k_1 = 1.40$, $k_{1,max} = 2.10$, $k_d = 5.25$, $k_b = 2010$, $S_0 = 0.15$, $V_{m2} = 0.010$, $V_{m3} = 0.008$, $V_{m4} = 0.011$, $V_{m5} = 0.010$

lidocaine to liver tissue, which could increase the volume of distribution, and delay steady state by up to 5 minutes. Binding would also account for the absence of any effluent lidocaine one minute after the administration of the drug.

Control Experiments

The control experiments were designed to determine if the observed time-dependent decline in lidocaine metabolism could be related to the extended period of time that the liver was artificially sustained. Although there was no physical or metabolic evidence of a decline in liver viability over time, perfusion with a buffer solution could cause a loss of enzyme cofactors or injury to the liver cells (Schmucker and Curtis, 1974). The resulting decrease in lidocaine metabolism would resemble that from actual inactivation.

In these experiments, the isolated rat liver was perfused with oxygenated buffer for a period of 70 minutes before lidocaine infusion was started. The results from the control experiments indicated that the duration of artificial maintenance had no effect upon the time-course of lidocaine or its metabolites. The MEGX profile still revealed a maximum shortly after the initial infusion of lidocaine (Figure 4.2b), and steady state was not attained until after 23 minutes of infusion. A hypothesis test on the MEGX curve provided statistical verification of the maximum in concentration. Hence, the control experiments conclusively indicated that the decline in lidocaine metabolism could not be related to a decrease in liver viability or activity.

Estimation of Model Parameters

The data for each experiment were successfully simulated using the mathematical model described by Equations (4.1), (4.2), and (4.16). Due to the narrow range of inlet concentrations studied, independent estimates of the Michaelis constants, K_{mj} , could not be obtained. The overall accuracy of the model fit was insensitive to values for K_{mj} ; therefore, the values of K_{mj} from Table 3.2 were used. The remaining parameters were estimated using the procedure outlined in Chapter 3. The values of k_{1ss} and the maximal reaction velocities, V_{mj} , were determined for each liver experiment using steady state concentrations. Data from the time-dependent portion of the lidocaine and MEGX profiles were used to estimate the deactivation and binding parameters, k_d' , $k_{1,max}$, k_b , and S_0 . Optimal model parameters for each experiment are shown in Table 4.2. For the lidocaine pre-injection experiments and the second stage of the stop-infusion experiments, $k_{1,max}$ is equal to k_{1ss} , and k_d' is equal to zero. The large variability of the rate constants (Tables 4.2 and 4.3) is due to the wide range in the age of the rats (6 to 26 weeks). Nevertheless, the model is equally successful for young and old rats in representing time-dependent lidocaine metabolism.

Table 4.2

Parameters for Inactivation of Enzymes during Lidocaine Elimination

Experiment	Rat	k_{1ss} ml/(g·min)	$k_{1,max}$ ml/(g·min)	k_d' ml/(μmol·min)
Pre-Injection (Lidocaine)	1	2.63	2.63	0.
	2	1.80	1.80	0.
	3	3.05	3.05	0.
	avg	2.49	2.49	0.
Pre-Injection (Saline)	1	1.25	1.75	3.80
	2	1.60	3.60	4.70
	3	1.62	5.50	9.30
	avg	1.49	3.62	5.93
Stop Infusion (1st Infusion)	1	1.40	2.70	3.00
	2	1.40	6.20	6.50
	3	1.75	5.00	18.00
	avg	1.52	4.63	9.17
Stop Infusion (2nd Infusion)	1	1.15	1.15	0.
	2	1.40	1.40	0.
	3	1.40	1.40	0.
	avg	1.32	1.32	0.
Control (delayed infusion)	1	2.40	4.70	7.00
	2	1.40	2.10	5.25
	3	0.60	0.95	5.50
	avg	1.47	2.58	5.75
Lennard <i>et al.</i> (1983)		2.70	19	25

Table 4.3
Parameters for Other Pathways
(n=15)

Pathway and Model Parameter	Value [$\mu\text{mol}/(\text{g}\cdot\text{min})$]
3-hydroxylidocaine formation, V_{m2}	0.021 ± 0.009
hydroxymethyl-lidocaine formation, V_{m3}	0.006 ± 0.004
MEGX elimination, V_{m4}	0.035 ± 0.017
3-hydroxylidocaine elimination, V_{m5}	0.013 ± 0.008
Binding capacity, S_0 ($\mu\text{mol}/\text{g}$)	0.163 ± 0.095
Binding rate, k_b ($\text{ml}/(\mu\text{mol}\cdot\text{min})$)	530 ± 833

K_m values from Saville *et al.*, (1986)

The experimental data of Lennard *et al.* (1983) were used to test the model for an isolated rat liver with recirculation through a reservoir. In this study, lidocaine was injected into the reservoir in three equivalent bolus doses every fifteen minutes. Due to recirculation, the inlet concentrations of the drug and its metabolites were continuously changing with time. Hence, simulation of these data tested the model under conditions of a variable inlet concentration, and with a different sex and strain of rat.

The model gave excellent agreement with the data of Lennard *et al.* (1983) (Figure 4.3). The experimental results showed a steady, statistically significant increase in the half-life of lidocaine with each successive bolus dose. The inactivation model was able to accurately describe the data, which indicated that the increase in the half life of lidocaine was consistent with a mechanism involving enzyme inactivation. Lennard *et al.* (1983) reported data for lidocaine only. Therefore, the metabolism of lidocaine was modelled using only two metabolic pathways: the deethylation pathway to form MEGX, and a saturable pathway representing the formation of hydroxylated species. Simulation of the data of Lennard *et al.* (1983) for lidocaine elimination by the isolated rat liver required adjustment of the parameters in the inactivation model (Table 4.2). The original model parameters used data from male Sprague-Dawley rats, whereas Lennard *et al.* (1983) used female Wistar rats. The differences in metabolism exhibited between strains of rats and the metabolic variability between rats of a different sex have been widely recognized (von Bahr *et al.*, 1977; Kitagawa *et al.*, 1985); therefore, significant changes in the values

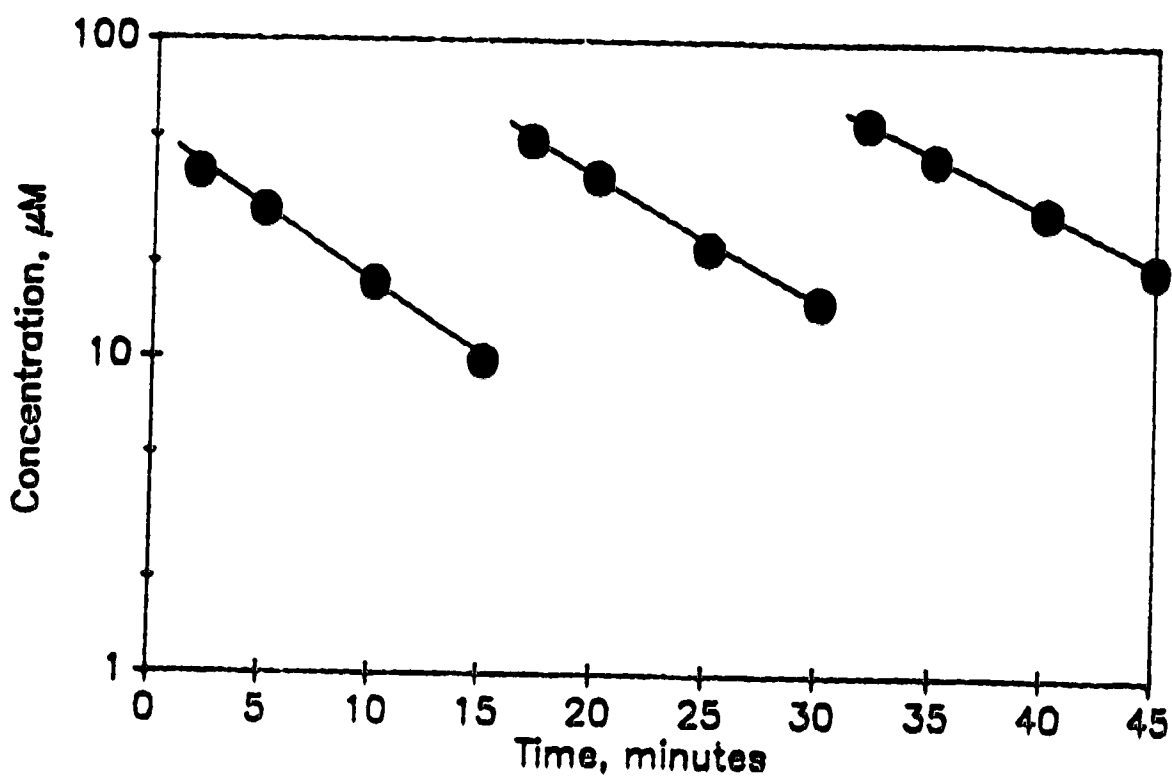


Figure 4.3. Best fit of the enzyme inactivation model to data from a recirculating system.

Experimental data for lidocaine from Lennard *et al.* (1983).

Model Parameters: $k_1 = 2.7$, $k_{1,max} = 19.$, $k_d = 25.1$, $V_{m3} = 0.020$,

$V_{m2} = V_{m4} = V_{m5} = 0$.

of the model parameters are to be expected. The success of the model in describing these data suggests that enzyme inactivation is not unique to male Sprague-Dawley rats, and the inactivation model is not limited by sex or strain differences between the animals.

Conclusions

(1) Continuous infusion of lidocaine into the isolated rat liver indicated time-dependent kinetics, typified by a maximum in the concentration of MEGX, and a slow approach to steady state (25 minutes).

(2) Pre-administration of lidocaine *in vivo* eliminated the time-dependent metabolism in a subsequent isolated organ study. Hence, the reduction in lidocaine metabolism could not be an artifact of isolating the liver. Furthermore, the reduction in activity persisted over 24 hours, consistent with inactivation of an isozyme.

(3) The second infusion of lidocaine in a stop-infusion study showed no time-dependent kinetics: the MEGX profile was monotonic, and steady state was reached within 9 minutes. Therefore, the time-dependent kinetics are due to a persistent alteration in liver activity.

(4) Delaying the infusion of lidocaine by 70 minutes did not eliminate the characteristic time-dependence, indicating that a loss of viability or the duration of artificial maintenance of the organ could not be responsible for the observed decline in lidocaine metabolism.

(5) Successful simulation of the data of Lennard *et al.* (1983) indicated that the inactivation model was not limited by sex and strain differences between rats, nor is it influenced by the dosing method.

References

- Bast, A., and Noordhoek, J.: "Spectral Interaction of Orphenadrine and its Metabolites With Oxidized and Reduced Hepatic Microsomal Cytochrome P-450 in the Rat", *Biochem. Pharmacol.*, **31**(7), 2745-2753, (1982).
- Chen, C.P., Vu, V.T., and Cohen, S.D.: "Lidocaine Uptake in Isolated Rat Hepatocytes and Effects of *dl*-propanolol", *Toxicology and Applied Pharmacology*, **55**, 162-168 (1980).
- Egan, R.W., Paxton, J., and Kuehl, F.A. Jr: "Mechanism for Irreversible Self-Deactivation of Prostaglandin Synthetase", *J. Biol. Chem.*, **251** (23), 7329-7335 (1976).
- Gray, M.R., Saville, B.A., and Tam, Y.K.: "Mechanisms of Lidocaine Kinetics in the Isolated Perfused Rat Liver. III. Evaluation of Liver Models for Time-Dependent Behavior", *Drug Metab. Disp.* **15**(1), 22-26, (1987).
- Ivanetich, K.M., Ziman, M., and Bradshaw, J.J.: "Reaction Schemes for the Degradation of Cytochrome P-450 by Allyl-isopropyl-acetamide and Fluroxene", *Biochem. Pharmacol.*, **29**, 2808-2811, (1980).

Kawai, R., Fujita, S., and Suzuki, T.: "Simultaneous Quantitation of Lidocaine and its Four Metabolites by High Performance Liquid Chromatography: Application to Studies on *In vitro* and *In vivo* Metabolism of Lidocaine in Rats", *J. Pharm. Sci.*, 74(11), 1219-1223 (1985).

Kitagawa, H., Fujita, S., Suzuki, T., and Kitani, K.: "Disappearance of Sex Difference in Rat Liver Drug Metabolism in Old Age", *Biochem. Pharmacol.*, 34(4), 579-581 (1985).

Lennard, M.S., Tucker, G.T., and Woods, H.F.: "Time-Dependent Kinetics of Lignocaine in the Isolated Perfused Rat Liver", *J. Pharmacokin. Biopharm.*, 11, 165-182, (1983).

Sadano, H., and Omura, T.: "Turnover of Different Forms of Microsomal Cytochrome P-450 in Rat Liver", in Cytochrome P-450 Biochemistry, Biophysics, and Environmental Implications, E. Heitanen *et al.*, eds., Elsevier Biomedical Press, pp. 299-306 (1982).

Saville, B.A., Gray, M.R., and Tam, Y.K.: "The Metabolism of Lidocaine in the Liver: Steady State and Dynamic Modelling", *Can. J. Chem. Eng.*, 64, 617-624, (1986).

- Saville, B.A., Gray, M.R., and Tam, Y.K.: "Mechanisms of Lidocaine Kinetics in the Isolated Perfused Rat liver. II. Kinetics of Steady State Elimination", *Drug Metab. Disp.*, 15(1), 17-21, (1987).
- Schimke, R.T.: "Control of Enzyme Levels in Mammalian Tissues", *Adv. Enzymol.*, 37, 135-187 (1973).
- Schmucker, D.L., and Curtis, J.C.: "A Correlated Study of the Fine Structure and Physiology of the Perfused Rat Liver", *Lab Investigation*, 30(2), 201-212, (1974).
- Tam, Y.K., Yau, M., Berzins, R., Montgomery, P.R., and Gray, M.R.: "Mechanisms of Lidocaine Kinetics in the Isolated Perfused Rat Liver. I. Effects of Continuous Infusion", *Drug Metab. Disp.*, 15(1), 12-16 (1987).
- von Bahr, C., Hedlund, I., Karlen, B., Backstrom, D., and Grasdalen, H.: "Evidence for Two Catalytically Different Binding Sites of Liver Microsomal Cytochrome P-450: Importance of Species and Sex Differences in the Oxidation Pattern for Lidocaine", *Acta Pharmacol. Toxicol.*, 41, 39-48, (1977).

CHAPTER 5: IMPLICATIONS OF ENZYME INACTIVATION

As described in Chapter 4, *in vivo* and *in vitro* administration of lidocaine to the rat liver caused a reduction in lidocaine metabolism which persisted over at least 24 hours. The reduction in lidocaine metabolism, attributed to enzyme inactivation, eliminated the characteristic time-dependent metabolism observed when lidocaine was continuously perfused through the isolated rat liver. Time-dependent kinetics are characterized by a slow approach to steady state (30 minutes) and a maximum in the MEGX profile (Tam *et al.*, 1987). These kinetics are consistent with partial enzyme inactivation (Chapter 4). Pre-exposure of the organ to lidocaine completes the inactivation, such that for any subsequent infusions of lidocaine, enzyme activity is constant, leading to a monotonic MEGX profile and steady state within 7 minutes (Table 4.1). The qualitative differences in the effluent profiles of lidocaine and MEGX between the two cases are useful for examining the dealkylation activity of cytochrome P-450.

Evidence exists that other drugs also cause slow enzyme inactivation. Orphenadrine, an anti-cholinergic drug, caused slow inactivation of the dealkylation fraction of cytochrome P-450 (Bast and Noordhoek, 1982). Furthermore, the metabolism of a structural analog, diphenhydramine, also showed characteristics consistent with enzyme inactivation (Bast and Noordhoek, 1982). Egan *et al.* (1976) found enzyme inactivation to be a prominent feature in the prostaglandin synthesis from arachidonic acid. Ivanetich *et al.* (1980) discovered that fluoxetine and allyl-isopropyl-acetamide induced inactivation of cytochrome P-450. Therefore, a number of

compounds appear to inhibit their own metabolism by inactivating the underlying metabolic enzymes.

Previous studies have shown that the half life for turnover of artificially-induced cytochromes in rats is approximately one to four days (Schimke, 1973; Sadano and Omura, 1982). In the previously conducted experiments (Chapter 4), no regeneration of the inactivated isozyme was observed after 24 hours. Therefore, assuming that inactivation was caused by lidocaine, the half-life for turnover of this isozyme must be greater than one day. Hence, the change in the enzyme system is prolonged, and the administration of a drug may influence the metabolism of a second drug which is administered later, simply because the first drug has altered the metabolic enzymes. Furthermore, drug interactions of this type can occur long after the first drug has cleared the system. Such a mechanism could cause a variety of previously unrecognized interactions between drugs.

The objective of this study is to determine the role of reduced enzyme activity as a cause for interactions between drugs using the same enzymatic pathway, and the time for recovery of the cytochrome P-450 deethylation fraction following inactivation. To investigate these phenomena, experiments were developed to test for a reduction in *in vivo* dealkylative metabolism in rat livers.

Methods

Potential interactions between lidocaine and other compounds were investigated in the following manner: the compound being tested was injected into the rat, followed by liver isolation 24 hours later. A continuous infusion of lidocaine into the isolated organ was used as a probe of the dealkylation activity of cytochrome P-450.

To investigate the duration of inactivation *in vivo*, the rats were subjected to jugular vein cannulation, and inactivation was induced by administering lidocaine (10 mg/kg rat) to the rat via the jugular vein. Subsequently, the liver was removed, and the isolated organ was continuously infused with lidocaine. The interval between *in vivo* lidocaine administration and the isolated organ experiment was varied from 1 to 40 days.

Results

Interaction Experiments

In control experiments, where saline was administered *in vivo*, concentration profiles of lidocaine and MEGX showed time-dependent kinetics, which indicated that the administration procedure did not affect dealkylation activity. *In vivo* injection of various N-alkylated drugs led to monotonic profiles of MEGX and lidocaine, indicating prior inactivation. A list of drugs tested is presented in Table 5.1. The existence of a peak in the MEGX profile was statistically verified using the procedure described in Appendix C. Similarly, the time to reach steady state was determined and used as a means of establishing the occurrence of prior inactivation.

Table 5.1 Interactions of Drugs with Lidocaine due to Inactivation

<u>Drug</u>	<u>dose mg/kg rat</u>	<u>Maximum in MEGX</u>	<u>Time to Steady State, min</u>	<u>Interaction</u>
Diltiazem	11.1	No	3	Yes
Diphenhydramine	14.0	No	3	Yes
3-hydroxylidocaine	19.5	No	3	Yes
Lidocaine	10.0	No	7	Yes
Orphenadrine	10.6	No	7	Yes
Verapamil	11.4	No	10	Yes
Saline (Control)	-	Yes	30	No

Enzyme Regeneration Experiments

The extent of enzyme regeneration could be estimated by monitoring the time-course of MEGX from the isolated organ study. An increase in enzyme activity would lead to a more prominent maximum in the MEGX profile, and a higher value of k_1 , the rate constant for the maximal deethylation of lidocaine. Furthermore, as the enzyme regenerates, the ratio of the maximum deethylation rate, k_1 , to the steady state deethylation rate, k_{ss} , should increase. This ratio, then, could be used to follow the degree of enzyme regeneration (Appendix D, Equation D11). Figure (5.1) indicates that the extent of enzyme regeneration is such that enzyme activity is within normal population limits after approximately 35 days. Using a population average for k_{max}/k_{ss} of 1.84, the rate of enzyme regeneration (k_{REG}) was estimated to be 0.026 d^{-1} . Because the ratio of k_1/k_{ss} for the 40 day experiment exceeded the population average, only 3 data points could be used to estimate k_{REG} . Thus, the parameter estimate may be inaccurate. Nevertheless, the model was successful in correlating the usable data. Another measure of the extent of enzyme regeneration is the time for the system to reach steady state (Appendix C). When no prior loss of enzyme activity had occurred, the time to reach steady state was 27 ± 5 minutes ($n=10$, $p=0.05$). This time was reduced to 6 ± 3 minutes ($n=3$) following complete inactivation of the dealkylation isozyme. As the isozyme regenerates, the time to reach steady state should progressively increase from 6 to 27 minutes. Figure (5.2) depicts this trend, and suggests that after about 34

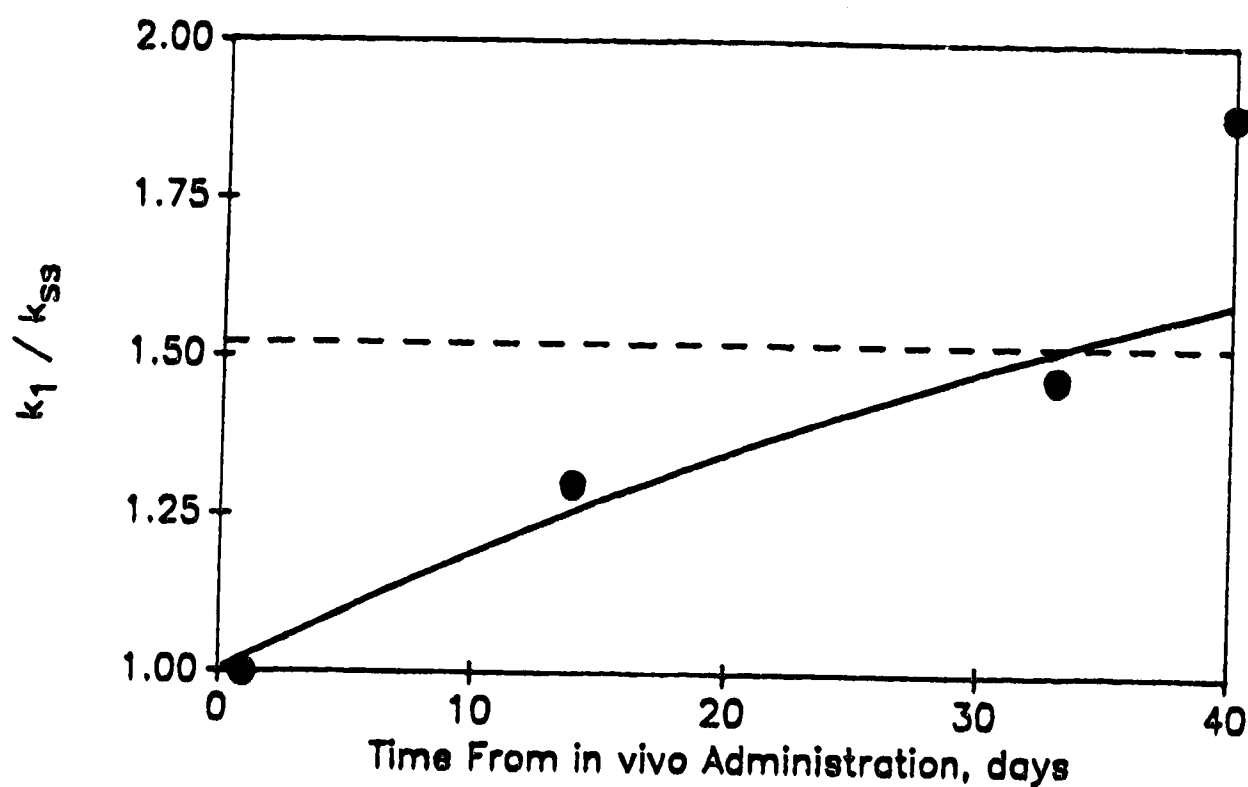


Figure 5.1 Rate of enzyme regeneration following inactivation by lidocaine based on maximal and steady state formation of MEGX

● experimental data; — model fit ($k_{REG} = 0.026d^{-1}$, $k_{max}/k_{ss} = 1.84$ for the population) ; - - - - lower population bound, based on a 95 % level of confidence for 10 individuals

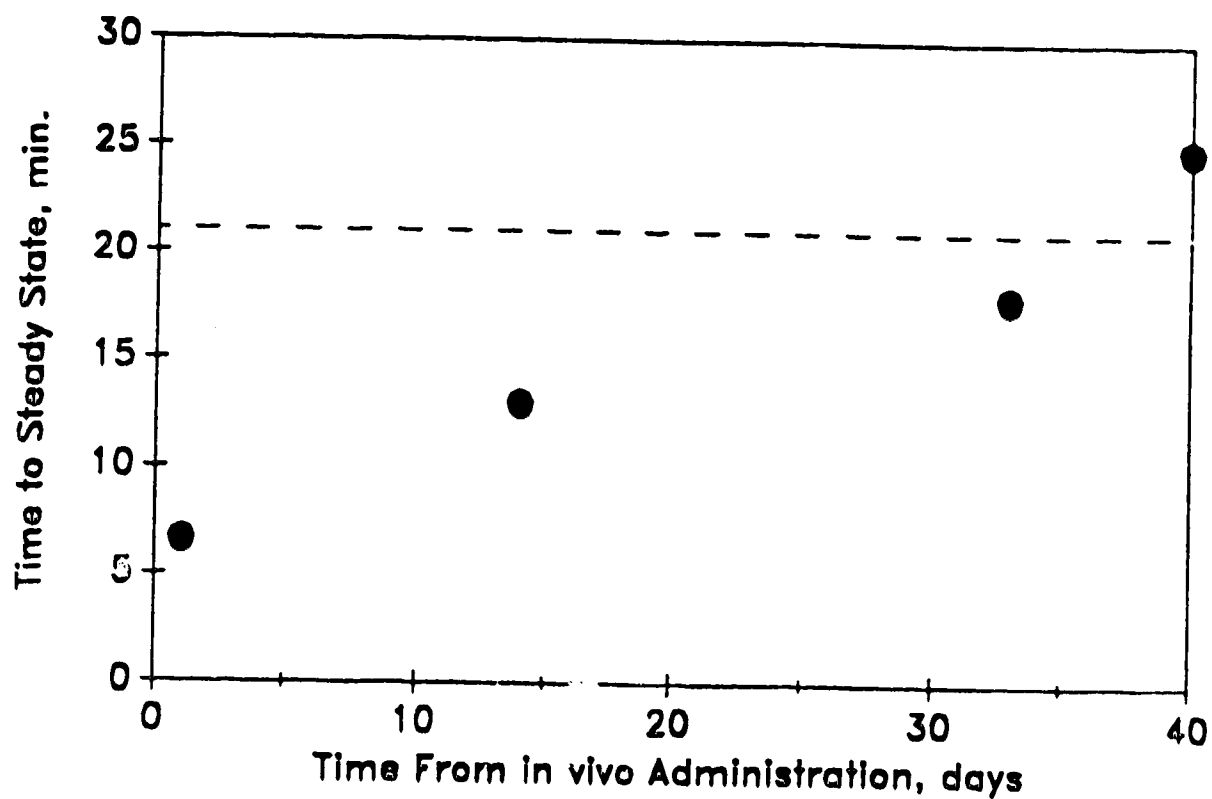


Figure 5.2 *Effect of enzyme regeneration upon the time to reach steady state concentration of lidocaine*

● experimental data; ----- lower population bound, based on a 95 % level of confidence for 10 individuals

days, the time to steady state is within the statistical bounds for the population. Hence, the two methods are consistent in their estimates of the rate of enzyme regeneration.

Discussion

This study indicated that a number of structurally similar species could influence the subsequent hepatic metabolism of lidocaine by inactivating a dealkylative isozyme of cytochrome P-450. The observations were consistent with other research. A dealkylation isozyme was inactivated by orphenadrine and a structural analog, diphenhydramine (Bast and Noordhoek, 1982; Labout *et al.*, 1982). From the results of this study, it is apparent that the same isozyme of cytochrome P-450 is inactivated by lidocaine, diphenhydramine, and orphenadrine.

The results from the enzyme regeneration experiments indicated that the metabolic function of cytochrome P-450 was impaired for about 35 days following inactivation by lidocaine. The rate of regeneration was 0.026 d^{-1} , corresponding to a half life for enzyme turnover of 25 days. This is significantly longer than the published value for the half life for turnover of cytochrome P-450 in rats of one to four days (Sadano and Omura, 1982). A possible reason for the discrepancy is that Sadano and Omura studied cytochrome P-450 that was artificially induced using phenobarbital. The effect of enzyme induction upon enzyme turnover is unknown, but the possibility exists that an induced enzyme may be subject to more rapid turnover than a normal enzyme. If so, this could account for the observed difference in the rate of enzyme turnover.

The prolonged period of reduced enzyme activity is significant, in that the administration of a drug may influence the metabolism of a second drug which is administered days or even weeks later, simply because the first drug has altered the metabolic enzymes. The implications of interactions between verapamil, diltiazem, and lidocaine are significant, since all three are commonly used cardiac agents, and it is quite possible that these drugs may be sequentially administered. Diphenhydramine is a component of non-prescription drugs such as Gravol, and could affect acute lidocaine administration, even after several days. 3-hydroxylidocaine also affects the metabolism of lidocaine by inactivating a dealkylation isozyme of cytochrome P-450. In this instance, both the precursor, lidocaine, and the product, 3-hydroxylidocaine, cause a reduction in lidocaine metabolism. Hence, interactions between species dealkylated by cytochrome P-450 are possible. Furthermore, administration of an inactivating substrate can influence the subsequent metabolism of other species administered up to 35 days later.

References

- Bast, A., and Noordhoek, J.: "Spectral Interaction of Orphenadrine and its Metabolites With Oxidized and Reduced Hepatic Microsomal Cytochrome P-450 in the Rat", *Biochem. Pharmacol.*, 31(7), 2745-2753, (1982).
- Egan, R.W., Paxton, J., and Kuehl, F.A. Jr.: "Mechanism for Irreversible Self-Deactivation of Prostaglandin Synthetase", *J. Biol. Chem.*, 251(23), 7329-7335, (1976).
- Ivanetich, K.M., Ziman, M., and Bradshaw, J.J.: "Reaction Schemes for the Degradation of Cytochrome P-450 by Allyl-isopropyl-acetamide and Fluroxene", *Biochem. Pharmacol.*, 29, 2808-2811, (1980).
- Labout, J.J.M., Thijssen, C.T., Keijser, G.G.J., and Hespe, W.: "Difference Between Single and Multiple Dose Pharmacokinetics of Orphenadrine Hydrochloride in Man", *Eur. J. Clin. Pharmacol.*, 21, 343-350 (1982).
- Sadano, H. and Omura, T.: "Turnover of Different Forms of Microsomal Cytochrome P-450 in Rat Liver", in Cytochrome P-450 Biochemistry, Biophysics, and Environmental Implications, E. Heitanen et al., eds., Elsevier Biomedical Press, 299-306, (1982).

Saville, B.A., Gray, M.R., and Tam, Y.K.: "The Metabolism of Lidocaine in the Liver: Steady State and Dynamic Modelling", *Can. J. Chem. Eng.*, 64, 617-624, (1986).

Saville, B.A., Gray, M.R., and Tam, Y.K.: "Evidence for Lidocaine-Induced Enzyme Inactivation", accepted for publication by *J. Pharm. Sci.*, April 25, 1989.

Schimke, R.T.: "Control of Enzyme Levels in Mammalian Tissues", *Adv. Enzymol.*, 37, 135-187, (1973).

Tam, Y.K., Yau, M., Berzins, R., Montgomery, P.R., and Gray, M.R.: "Mechanisms of Lidocaine Kinetics in the Isolated Perfused Rat Liver. I. Effects of Continuous Infusion", *Drug Metab. Disp.*, 15(1), 12-16 (1987).

CHAPTER 6: SHORT-TERM EFFECTS UPON LIDOCAINE METABOLISM
INFLUENCE OF PERFUSATE FLOW AND LIDOCAINE BINDING

Several processes can influence effluent concentrations of lidocaine and its metabolites, including transport between the cells and vasculature, intracellular reactions, binding to proteins in the blood and liver tissue, and the net flow of the perfusion medium through the liver. Each of these phenomena will influence unsteady state metabolism to a varying degree and for different periods of time, according to their characteristic time scales.

The mean hydraulic residence time of a compound confined to the vasculature should be only about 5 seconds. Thus, any mixing within the vasculature should be completed quickly, and would only affect unsteady-state metabolism for a short time. Chen *et al.* (1980) suggested that lidocaine could bind to liver tissue, but that the process was complete within 2 to 5 minutes, depending upon the lidocaine concentration. Enzyme inactivation, by comparison, is a relatively slow process that could be observed over 30 to 60 minutes. When enzyme activity was constant, however, the time to steady state was decreased to about 5 minutes. Hence, processes such as mixing and flow, binding, and mass transport affect lidocaine metabolism for only a few minutes, until such time as steady state is reached. Each of these phenomena must be investigated independently.

Investigation of Flow Effects

When significant conversion (> 50%) of the substrate takes place, changes in drug levels due to changes in perfusion rate can be used to characterize the extent of mixing in the liver (Gray and Tam, 1987). Since the metabolism of lidocaine is pseudo-linear until very high concentrations are reached (Chapter 3), it was possible to use Equations (1.2) and (1.4) to predict the effect of flow upon steady state effluent concentrations of the drug and its metabolites. By manipulating Equation (1.2) for the well-mixed model, the following expression for the ratio of steady state concentrations of lidocaine at different flow rates is obtained:

$$\frac{C_{L2}}{C_{L1}} = \frac{Q_2}{Q_1} \left[\frac{Q_1 + k_R V_L}{Q_2 + k_R V_L} \right] \quad (6.1)$$

If the reference conditions (C_{L1} and Q_1) are held constant, then the effect of Q_2 upon C_{L2} can be given by:

$$C_{L2} = K_{CSTR} \frac{Q_2}{Q_2 + k_R V_L} \quad (6.2)$$

where K_{CSTR} is a proportionality constant.

If the product of k_R and V_L is small, then the flow rate should not affect C_{L2} . However, if the product is significant, the effect of Q_2 upon C_{L2} may range between hyperbolic and linear.

If plug flow conditions prevail, the following expression describes the effect of flow rate upon C_{L2}/C_{L1} :

$$\frac{C_{L2}}{C_{L1}} = \frac{\exp (k_R' V_L / Q_1)}{\exp (k_R' V_L / Q_2)} \quad (6.3)$$

Again, if the same reference conditions (C_{L1} and Q_1) are used throughout, the effect of Q_2 upon C_{L2} can be described by:

$$C_{L2} = K_{PF} \exp (-k_R' V_L / Q_2) \quad (6.4)$$

where K_{PF} is a proportionality constant.

Equations (6.2) and (6.4) suggest that flow may have significantly different effects upon effluent lidocaine concentrations, depending upon the extent of mixing within the organ. Equation (6.2), developed for well-mixed conditions, suggests that, at most, C_{L2} will have a linear dependence upon flow rate. Conversely, Equation (6.4) indicates that if plug flow conditions are dominant, an exponential relationship should be observed. If the extent of mixing falls between these two extremes, an intermediate sensitivity to flow should be observed.

The linear endogenous formation of metabolites can be described by Equation (6.5). Steady-state concentrations are independent of the rate of formation; furthermore, the same basic expression applies for wellmixed and plug flow conditions.

$$C_{M2} = K_{MET} \frac{C_{L2}}{Q_2} \quad (6.5)$$

where C_{M2} is the steady state metabolite concentration at volumetric flow rate Q_2 , and K_{MET} is a proportionality constant.

Substitution for C_{L2} in Equation (6.5) using either Equation (6.2) or (6.4) permits evaluation of the dependence of the metabolite concentrations upon flow rate.

Pang and Rowland (1977) investigated the influence of flow upon lidocaine metabolism. However, the experiments were conducted using a relatively low inlet concentration of lidocaine, and virtually 100%

conversion of lidocaine was observed. Given that lidocaine is affected by inactivation of enzymes, and the time to complete inactivation increases as the inlet concentration decreases, it is possible that inactivation was not complete in these experiments. Hence, it is uncertain whether a true steady state existed during the experiments, or if the observed concentrations resulted from a pseudo-steady-state condition. In addition, high extraction ratios lead to low effluent concentrations of lidocaine, which may be very close to the minimum detectable concentration. Thus, the assayed concentrations may be erroneous. Furthermore, Pang and Rowland did not investigate the influence of flow upon metabolite concentrations. Thus, it was necessary to check the results of their experiment by performing a similar experiment at a higher inlet concentration and with less conversion of lidocaine. Additional information would be obtained by monitoring the effect of flow upon metabolite levels. To prevent time-dependence due to enzyme inactivation, inactivation was completed by *in vivo* pretreatment of the rat with lidocaine. To investigate flow-induced changes in metabolism, Krebs' buffer, containing lidocaine, was continuously perfused through the isolated liver for 120 minutes. This procedure permitted changing the flow rate while maintaining a constant inlet concentration of lidocaine. The perfusion rate was changed every 15 minutes, and multiple samples of the liver effluent were collected during each 15 minute interval. The initial perfusion rate through the organ was 39 ml/min. For subsequent intervals, the following perfusion rates were used: 36 ml/min, 29 ml/min, 22 ml/min, 39 ml/min, 31 ml/min, 22 ml/min, and 39 ml/min. Repeating the flow rate in subsequent intervals ensured

that the steady state concentration was not affected by time-dependent phenomena.

The ratio of the steady state level at a particular flow rate to the base concentration at 22 ml/min was used to assess the extent of mixing within the organ. The dependence of this ratio upon flow rate is presented in Figure 6-1. The experimental data were successfully simulated using the well-mixed model with linear reaction (Equations 6.2 and 6.5). The model described drug and metabolite concentrations with equal success. The dependence of the steady state concentrations of lidocaine and its metabolites upon flow rate was consistent with the well-mixed model. In addition, the results agreed with the findings of Pang and Rowland (1977), who performed a similar experiment at lower lidocaine concentrations and perfusate flow rates.

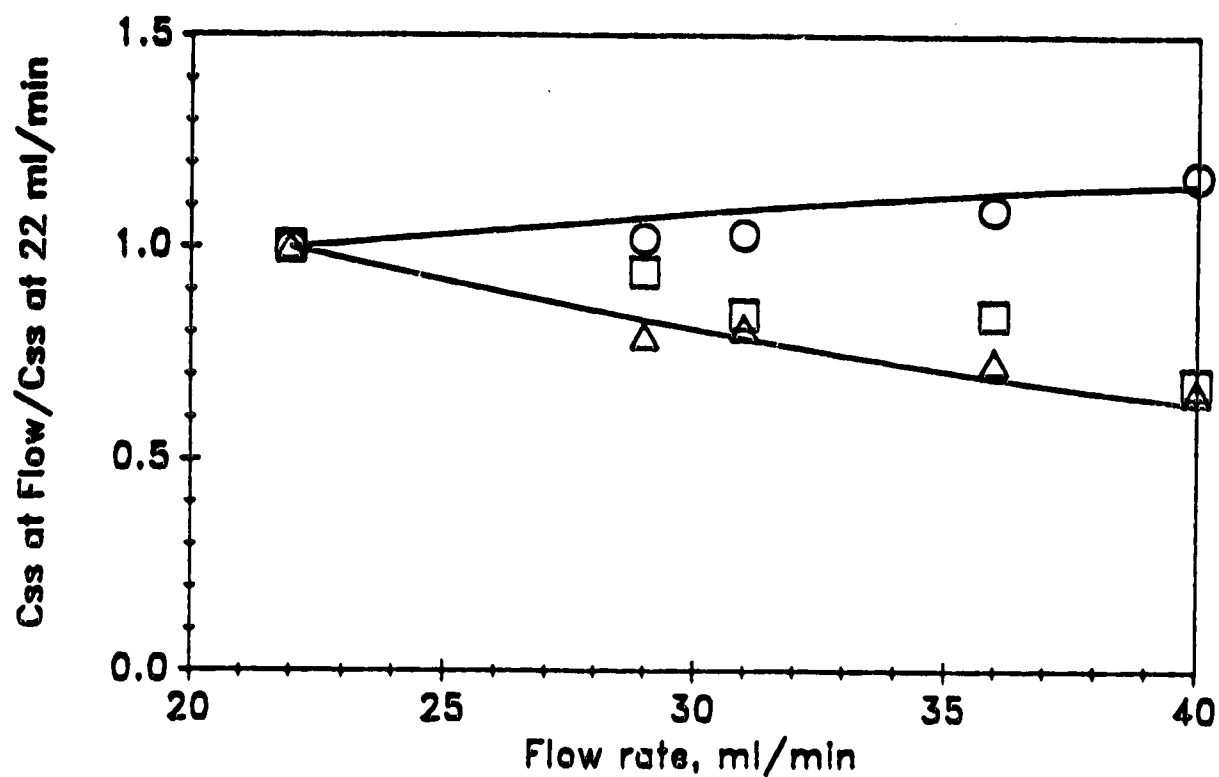


Figure 6.1 Effect of perfusate flow rate upon steady state drug and metabolite concentrations

○ lidocaine; □ MEGX; △ 3-OHLID; — predicted concentrations based on the well-mixed model ($k_1 = 9.06 \text{ min}^{-1}$; $C_{in} = 29.6 \text{ } \mu\text{M}$)

Binding Effects

Substrate binding can occur in many forms. Substrates can reversibly bind to enzymes, where they are transformed and released as products. Furthermore, substrates will commonly bind to proteins in the blood, reducing the amount of free substrate in the system, and decreasing the fraction of the administered drug that is metabolized. Lipid-soluble drugs can be highly bound to blood proteins, but are less likely to bind to tissues. Conversely, many basic drugs are preferentially bound to extravascular tissues (Gibaldi and Perrier, 1982). The term "binding", therefore, includes a variety of solubility, adsorption, and reversible dissociation phenomena. In the context of the investigations described in this chapter, irreversible binding accounts for the material retained within the liver after a suitable period for clearing the organ has elapsed. In these experiments, following the administration of the labelled and unlabelled drug, the organ was washed out by perfusion with Krebs' buffer for 25 to 30 minutes. Any material remaining in the liver after the washout process, then, was deemed irreversibly bound.

Chen *et al.* (1980) suggested that lidocaine could irreversibly bind to components in the liver. They performed 30 minute batch experiments in which ^{14}C -labelled lidocaine was added to a 5 ml suspension of liver microsomes. The experiments were performed with a wide range of lidocaine concentrations, but even at the highest concentration, the total amount of lidocaine in the system was quite small, due to the small volume of buffer used in the cell suspension. Hence, the binding capacity of the system may not have been fully

investigated. Nevertheless, their data did indicate that lidocaine would bind to cell debris, but that binding to cellular proteins was unlikely.

To verify the findings of Chen *et al.* (1980), experiments were designed to determine the full extent of lidocaine binding to liver proteins and tissues, and the fraction of material lost to irreversible binding.

Methods

Unlabelled and labelled lidocaine were coadministered and continuously perfused through the isolated liver (Sprague-Dawley rats 63 to 114 days old, 310 to 500 g, liver weight of 13.3 to 18.7 g) until steady state was reached (25 to 30 minutes). The amounts of labelled and unlabelled lidocaine infused were $0.093 \pm 0.009 \mu\text{mol}$ and $24.9 \pm 6.2 \mu\text{mol}$, respectively. Ratios of unlabelled to labelled drug ranged between 190 and 340. In order to permit the elution of metabolites slowly released by the liver, the organ was then washed out by perfusing Krebs' buffer for an additional 25 to 30 minutes. While lidocaine was infused, frequent samples from the hepatic vein were obtained and analyzed. While the organ was being washed out, periodic samples were collected. The radioactivity of samples from the inferior vena cava was also determined, and the bile duct was cannulated and the radioactivity of the biliary effluent was evaluated. Upon completion of perfusion, the organ was homogenized, and the volume of the homogenate recorded. Multiple samples of the homogenate were analyzed by liquid scintillation counting. These samples contained liver tissue, proteins, and cell debris. Additional samples of the homogenate were subject to protein precipitation with

0.05M trichloroacetic acid. The protein precipitate was separated from the homogenate by centrifugation. The precipitate was resuspended in buffer, and the precipitation procedure was repeated twice. The radioactivity of the protein sample and the supernatant was determined after each stage of the extraction procedure.

Results and Discussion

In the 5 binding experiments conducted, between 90 and 98 percent of the infused labelled lidocaine was recovered in the effluent from the hepatic vein. The results from the experiments suggested that very little material was irreversibly retained by liver tissues and proteins. Of the labelled lidocaine infused into the organ, only $0.40 \pm 0.15\%$ was irreversibly retained by components in the liver. The total amount of labelled lidocaine bound to liver components was 0.37 ± 0.13 nmol; for unlabelled lidocaine, 106 ± 58 nmol was bound. Chen *et al.* (1980), using significantly lower total doses of label, observed that 0.45 nmol of a labelled dose of 1.5 nmol was irreversibly held within the liver. Hence, the total capacity for binding was similar, even though the percentage of drug bound differed between the two experiments. In addition, the amount of labelled lidocaine bound was 0.024 ± 0.008 nmol per gram of liver tissue, consistent with Chen *et al.* (1980), who observed between 0.020 and 0.022 nmol of ^{14}C bound per gram of liver tissue.

To determine the amount of material bound to liver proteins, the homogenate was subjected to a non-specific protein extraction procedure. The extraction process was performed three times to ensure that all cell debris was removed; the ^{14}C content of the purified precipitate was determined. The analysis indicated that of the total

material bound, only 2.9 ± 0.9 percent was bound to liver proteins. This corresponds to 2.6 ± 0.8 nmol of hepatic protein bound to labelled and unlabelled lidocaine. For comparison, a typical rat liver contains about 100 nmol of cytochrome P-450, and each of the constitutive isozymes of cytochrome P-450 contributes between 8 and 16 nmol to the total cytochrome P-450 content. Since the extraction procedure was non-specific, it was impossible to know which protein lidocaine was bound to, i.e. to cytochrome P-450 or to some other protein in the liver. If lidocaine was bound to cytochrome P-450, only 2.6 percent of the total enzyme or up to 40 percent of the least common isozyme could be involved.

Analysis of the samples from the bile duct and the inferior vena cava indicated that losses of labelled drug via these routes were minimal. Of the total lidocaine infused, 0.005% appeared in the bile, and 0.3% was excreted through the inferior vena cava. Furthermore, the amount of drug in the hepatic vein was, on average, about 1450 times the amount of drug in the bile duct. Therefore, losses by these pathways were negligible.

Conclusions

The results from investigations on flow and binding indicated that the effects of these phenomena upon lidocaine metabolism were small. The effect of fluid flow upon steady state levels of lidocaine and its metabolites was consistent with a system that is well-mixed. Losses of lidocaine due to irreversible binding were minimal; less than 0.5% of the infused tracer was bound. Of the material that was bound, 97% was to tissues and cell debris; the remaining 3 percent was bound to proteins in the liver. The amount of lidocaine irreversibly bound to proteins was small relative to the amount of cytochrome P-450 and P-450 isozymes in the liver, indicating that it is unlikely that lidocaine is bound to cytochrome P-450 by any specific mechanism. Losses of material through the bile duct and the inferior vena cava were insignificant.

References

- Chen, C.P., Vu, V.T., and Cohen, S.D.: "Lidocaine Uptake in Isolated Rat Hepatocytes and Effects of *dl*-Propanolol", *Toxicology and Applied Pharmacology*, 55, 162-168, (1980).
- Gibaldi, M., and Perrier, D.: Pharmacokinetics, 199-219, Dekker, New York, (1982).
- Gray, M.R., and Tam, Y.K.: "The Series-Compartment Model For Hepatic Elimination", *Drug. Metab. Disp.*, 15, 22-27, (1987).
- Pang, K.S., and Rowland, M.: "The Hepatic Clearance of Drugs. I. Theoretical Considerations of a "Well-Stirred" Model and a "Parallel-Tube" Model. Influence of Hepatic Blood Flow, Plasma and Blood Cell Binding, and Hepatocellular Enzymatic Activity on Hepatic Drug Clearance", *J. Pharmacokin. Biopharm.*, 5(6), 655-680, (1977).

CHAPTER 7: SHORT-TERM EFFECTS UPON LIDOCAINE METABOLISM

APPLICATION OF A HETEROGENEOUS MODEL

Although enzyme inactivation can affect the elimination of lidocaine for 30 to 60 minutes during continuous infusion of the drug, it cannot account for all of the time-dependent metabolism of the drug. In experiments where enzyme activity was constant, the time to steady state was reduced to between 5 and 7 minutes (Chapter 4). The mean hydraulic residence time of a compound with full access to all regions of the liver is only about 20 to 30 seconds (using the total liver volume and assuming no transport limitations). This suggests that mixing processes, in the absence of mass transfer limitations, should cause unsteady state conditions for only 2 or 3 minutes. The effect of irreversible binding to liver proteins and tissues is negligible, with less than 0.5% of the infused drug being lost in this manner. Hence, neither mixing nor binding can account for the extended time to steady state. Some other process, therefore, must affect the metabolism of lidocaine during the first 5 minutes of drug infusion. Preliminary observations of drug metabolism following cessation of drug infusion indicated detectable effluent levels of lidocaine and its metabolites for up to 7 minutes after drug infusion was stopped. By comparison, the time scale for mixing within the organ indicated that the organ should be free of drug within 2 to 3 minutes. Hence, lidocaine and its metabolites were subject to retention within the liver, suggesting that a heterogeneous model may be necessary to fully describe the time-dependent metabolism of lidocaine.

Development of a Heterogeneous Model

To properly describe drug metabolism using a heterogeneous model, it is necessary to devise experiments that facilitate estimation of the vascular and cellular volumes, in addition to the rates of transport between the cells and vasculature, and the rate of reaction within the cells. Unsteady-state data provide the best means for estimating rates of transport, since concentrations in the cells and the vasculature are not in equilibrium. Three methods exist for obtaining unsteady-state data: pulse experiments, step increases in tracer concentration, and washout experiments.

Pulse experiments, such as those used by Goresky *et al.* (1973), have many disadvantages for investigating transport processes between phases. An impulse of tracer rarely exposes the entire organ to an equivalent concentration of tracer. If diffusional barriers exist between the cells and the vasculature, very little material may gain access to the cells, and the capacity of the cells will never be reached. Slow release of species from the cells, therefore, cannot be fully investigated, since the amount of tracer initially in the cells will be very minute. This is advantageous if the objective is to study vascular processes only. However, if the objective is to investigate transport processes between phases or to assess slow, transport-limited phenomena, the usefulness of pulse experiments is limited.

Step changes in the inlet concentration of a tracer are significantly more effective for investigating transport phenomena. For a step increase in tracer, the cells will eventually be filled to capacity, and equilibrium between the cells and the vasculature will

be observed. The primary drawback of a step increase in tracer is the inherent difficulty in maintaining a constant inlet concentration. Fluctuations lead to errors in the final steady state concentration, which, in turn, lead to imprecision as the unsteady state levels approach steady state. Since most information on transport is obtained from the tail of the tracer curve (Dudoković, 1985), these errors in steady state levels significantly limit the effectiveness of a step increase in tracer concentration as a means of investigating transport phenomena.

Conversely, it is very easy to control the inlet concentration during a washout experiment, since it is identically equal to zero. There are, therefore, no errors in the final steady state level, which permits accurate quantitation of the tail portion of the tracer curve. Before the washout period begins, the cells are filled to capacity, and concentrations in the cells and the vascular network will be in equilibrium. During the washout experiment, any slow, non-equilibrium processes can be clearly observed. Hence, washout experiments provide the maximum amount of information from tracer curves, and are the most effective method for examining mass-transport limitations and reaction.

Theory

Equations for Transport and Intracellular Reaction

The heterogeneous model follows the form of the series-compartment model (Gray and Tam, 1987), but has been modified to include peripheral compartments representing the liver cells. The model is similar to that proposed by Weisiger (1985), and is

essentially a discrete form of the model of Goresky *et al.* except that the RTD behavior is based on mixing compartments rather than a measured exit age distribution. If appropriate simplifications are made to the model, the Deans-Levich model for interphase transport (Buffham and Gibilaro, 1968) is obtained.

In the heterogeneous model presented herein, the number of cellular compartments, N_c , was assumed to be equal to the number of vascular compartments, N_v . The following section presents the theoretical development of the heterogeneous model illustrated in Figure 7.1.

$$N = N_v = N_c \quad (7.1)$$

$$V_c = V_{tot} - V_v \quad (7.2)$$

$$V_{tot} = \frac{W_L}{\rho_L} \quad (7.3)$$

The volume of each vascular compartment, V_{1j} , is calculated from Equation (7.4).

$$V_{1j} = \frac{V_v}{N} \quad (7.4)$$

The volume of each cellular compartment, V_{2j} , can be determined using Equation (7.5).

$$V_{2j} = \frac{V_c}{N} \quad (7.5)$$

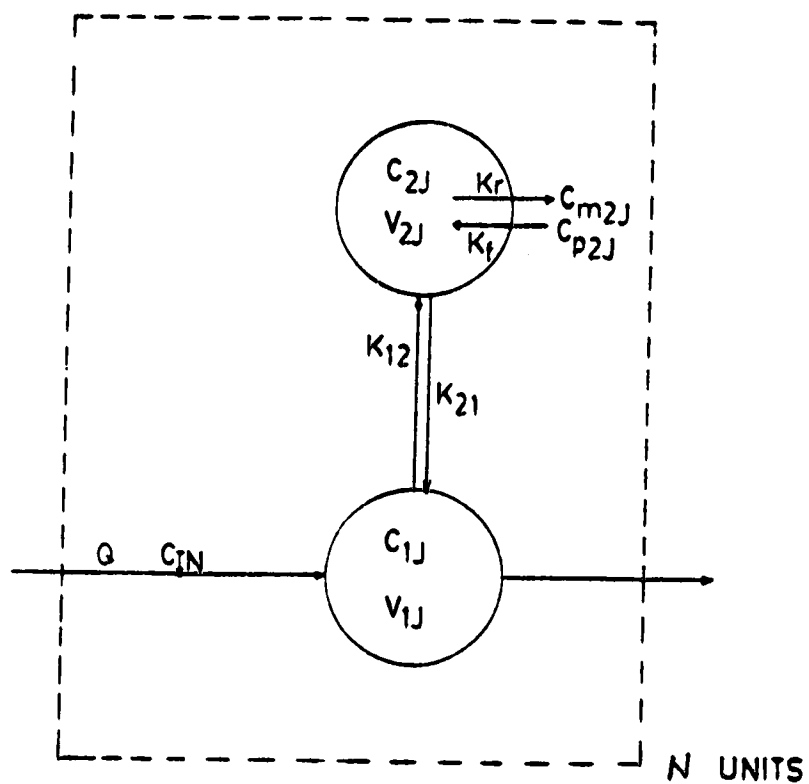


Figure 7.1 *Basic Heterogeneous Model*

Compartment 1 represents the vascular and interstitial spaces;
compartment 2 represents the cellular space

Differential equations can be written for the cellular and vascular compartments in each unit, j . The following equations can be applied to both drug and metabolites.

For the vascular compartment:

$$V_{1j} \frac{dC_{1j}}{dt} = Q \cdot (C_{1,j-1} - C_{1j}) - k_{12}C_{1j} + k_{21}C_{2j} \quad (7.6)$$

For the cellular compartment:

$$V_{2j} \frac{dC_{2j}}{dt} = k_{12}C_{1j} - k_{21}C_{2j} - V_{2j}k_rC_{2j} + V_{2j}k_fC_{p2j} \quad (7.7)$$

C_{p2j} represents the concentration of the precursor which reacts to form the species of interest. In the case of lidocaine, $C_{p2j} = 0$. For MEGX and 3-OHLID, both of which are formed from lidocaine, C_{p2j} would be the concentration of lidocaine in the cellular compartment of unit j . The expressions as presented assume linear kinetics; however, extension to non-linear kinetics is straightforward. If transport into the tissue is insignificant ($k_{12} = 0$), the model reduces to the tanks-in-series model for tracer concentrations. If transport is very fast ($k_{12} \gg Q$), then the model gives the tanks-in-series model with reaction. The model can also be solved analytically for the case of linear elimination and one set of compartments ($N = 1$). The solution in this case is a biexponential equation. At short times, the concentration in the effluent is dominated by clearance of the sinusoid compartment; at longer times, transport and elimination from the tissue compartment is dominant.

Equations to Describe Flow and Mixing in the Catheters and Vasculature

A residence time distribution analysis can be applied to determine the extent of mixing in the catheters and in the vascular network of the liver. The mean residence time in the system, \bar{t} , and the variance, σ^2 , of the exit age distribution profile, E_t , can be used to relate experimental observations to models that describe mixing behavior. Previous work with vascular tracers indicated that concentration-time curves followed a Gamma distribution (Davenport, 1983). The tanks-in-series model gives a Gamma distribution (Gray and Tam, 1987; also see Equation 1.14), and is the recommended model for describing complex flow in a homogeneous system (Dudoković, 1985). Since albumin is confined to the vascular and interstitial spaces of the liver and is not subject to transport into the hepatocytes, the tanks-in-series model, then, is an appropriate descriptor of mixing within the vasculature. The subsequent section, based upon the work of Levenspiel (1984), describes the equations used to develop an E_t curve from experimental data, and how the characteristics of the E_t curve can be related to the mixing parameter, N , of the tanks-in-series model.

The absorbance of albumin at any time during a washout experiment, ABS_t , can be related to a residence time distribution function, F_t , according to Equation (7.8).

$$F_t = \frac{ABS_t - ABS_0}{ABS_f - ABS_0} \quad (7.8)$$

ABS_0 and ABS_f are the initial and final steady state levels, respectively. Clearly, the F_t curve should monotonically increase

from zero to one over the course of a washout experiment. For continuous data, the mean residence time can be related to the F_t curve by Equation (7.9):

$$\bar{t} = \int_0^1 t \cdot dF_t \quad (7.9)$$

The exit age distribution function, E_t , is related to F_t in the following manner:

$$E_t = \frac{dF_t}{dt} \quad (7.10)$$

For discrete data, Equation (7.9) is replaced by Equation (7.11).

$$\bar{t} = \sum_{k=1}^n t_k \cdot (F_k - F_{k-1}) \quad (7.11)$$

Hence, the mean residence time can be estimated from discrete experimental data. To determine the extent of mixing, the variance of the exit age distribution function must be evaluated. The second moment of the distribution must be calculated, using either Equation (7.12) or (7.13).

$$M_2 = \int_0^1 t^2 \cdot dF_t \quad (7.12)$$

For discrete data:

$$M_2 = \sum_{k=1}^n t_k^2 \cdot (F_k - F_{k-1}) \quad (7.13)$$

The variance, σ^2 , is determined from Equation (7.14):

$$\sigma^2 = M_2 - \bar{t}^2 \quad (7.14)$$

These data can be related to the tanks-in-series model to estimate

the number of tanks, N .

$$N = \frac{\bar{t}^2}{\sigma^2} \quad (7.15)$$

Values for N , \bar{t} , and σ were first determined for the catheters alone; after subtracting the effect of the catheters from the total system, N , \bar{t} , and σ were determined for the vascular space of the liver.

The volume of the system was calculated from Equation (7.16):

$$V = \bar{t} \cdot Q \quad (7.16)$$

where Q is the volumetric flow rate through the system. Hence, the volume of fluid in the catheters, V_{cat} , and the volume of the vascular and interstitial spaces, V_v , can be determined from the mean residence times of the albumin in the catheters and in the liver, respectively.

Methods

Albumin, which is restricted to the vascular and interstitial spaces of the liver, was used to investigate the flow characteristics of the vasculature. Washout experiments were performed both with and without the liver in the system to determine time delays in the catheters. Effluent samples were collected every 6 seconds by a fraction collector, and analyzed using a spectrophotometer.

Ideally, a non-reacting analog of lidocaine or its metabolites would be used to investigate transport between the vasculature and the cells; however, non-reacting analogs of lidocaine or its metabolites do not exist. The drug and its metabolites, therefore, were used as a probe of both transport and intracellular reaction. In the mass transfer experiments, lidocaine was infused until steady

state was reached. Drug infusion was then stopped, and the organ was perfused with Krebs' buffer to wash out any drug remaining in the cells and the vasculature. Data from the steady state elimination of lidocaine and the washout of the drug and metabolites were used to analyze transport and intracellular reaction.

Three types of experiments were performed to investigate transport and intracellular reaction. Washout experiments with unlabelled lidocaine were used to obtain rates of release from the cells. Effluent samples were collected every 6 seconds, and analyzed using HPLC.

Washout experiments with ^{14}C -labelled lidocaine were used to assess the possibility of non-linear transport and metabolism. The use of a labelled compound superimposed upon an unlabelled compound guarantees a linear response with respect to the labelled material (Goresky, 1973). A linear response occurs because administration of the labelled compound represents only an incremental increase in the total drug concentration. Thus, the characteristics of the system will be controlled by the unlabelled compound. If non-linear transport and kinetics are occurring, then the characteristics of the tracer washout curve will change as the concentration of the unlabelled compound changes. In the event of non-linear processes, the slope of the tracer washout curve, when plotted on log-linear coordinates, should decrease as the concentration of the unlabelled drug increases. A decrease in slope with an increase in the concentration of the unlabelled drug indicates a transition from a

first order to a second order process. By monitoring the curves from the washout experiments, the existence of non-linear phenomena can be determined.

The following procedure for experiments with labelled lidocaine was used: Unlabelled lidocaine was administered throughout. Once steady state was reached, labelled lidocaine was coinjected with the unlabelled drug for 5 minutes. Infusion of the labelled drug was then stopped, and the elution of the labelled compound was monitored for 5 minutes. The ratio between the concentration of the unlabelled and labelled drug ranged from 15 to 180. Effluent samples were analyzed for total radioactivity by scintillation counting. The samples were also analyzed using HPLC, and the radioactivity of the HPLC fractions was determined.

Washout experiments with unlabelled metabolites were performed to obtain information on metabolite transport and reaction. Exogenous administration of a metabolite gave a more accurate estimate of transport and reaction rate constants, since analysis was not complicated by formation of the metabolite from a parent compound. Furthermore, metabolite levels during exogenous administration were typically higher than those observed from endogenous formation; therefore, more data were available over a broader concentration range. Accurate information on mass transfer and reaction of the metabolites permitted more accurate estimation of the true intrinsic rates of lidocaine uptake and release. Effluent samples from these washout experiments were collected every 6 seconds and analyzed using HPLC.

Methods for Parameter Estimation

The development of a heterogeneous model for lidocaine metabolism must follow three stages. First, time lags in the catheters must be assessed. Second, the influence of mixing in the liver vasculature must be investigated by subtracting the effect of catheter time delays from washout profiles obtained with the liver in place. Albumin was used to investigate time lags in the catheters and the extent of mixing in the vasculature. The data from albumin experiments permit estimation of two key parameters of a heterogeneous model: the vascular volume, V_v , and the number of compartments, N_v , required to describe the extent of mixing in the vasculature. The vascular mixing data must then be combined with mass transfer and kinetic data obtained from lidocaine and its metabolites to give a fully functional model which combines vascular mixing with hepatic transport and intracellular reaction.

Estimation of parameters for transport and reaction were based upon data obtained from the washout of lidocaine and its metabolites. Using the Simplex algorithm (Nelder and Mead, 1965), the rate of cellular release, k_{21} , and the rate of intracellular reaction, k_r , were estimated. Steady state data and the steady-state solutions to Equations (7.6) and (7.7) were then used to calculate k_{12} and the steady state concentration of the compound in the cellular compartment. Within the Simplex routine, a Runge-Kutta-Fehlberg method was used to numerically integrate the differential equations for the heterogeneous model (Equations 7.6 and 7.7); parameters were adjusted until the objective function was minimized. The objective

function was the sum of squared residuals between estimated and experimentally observed effluent concentrations.

The parameters for transport (k_{12} , k_{21}) and reaction (k_r) were first determined for the metabolites using data from experiments where the individual metabolites were infused. These parameters were then used as initial estimates for determining the rates of metabolite transport and reaction when lidocaine was infused. Once the metabolite profiles were correlated, rates of lidocaine transport and elimination could be estimated.

Results and Discussion

Flow and Mixing in the Catheters and Vasculature

Albumin was used to investigate time delays in the experimental apparatus and catheters leading to the liver. Analysis of the washout profiles from these experiments indicated that the catheter volume from the point of injection to the point of collection was 15 ± 1 ml. The mixing parameter, N , was estimated to be 24, suggesting conditions approaching plug flow behavior.

Albumin washout experiments with the liver as part of the experimental apparatus were used to investigate flow characteristics in the vasculature. To properly analyze the data, the effect of the catheters was subtracted. The "adjusted" data then represented the characteristics of the liver. The mean residence time in the vascular and interstitial regions of the liver was between 3.5 and 5.6 seconds, depending upon the volumetric flow rate of the perfusate through the organ. The vasculature was found to occupy between 14 and 20 percent of the total liver volume, consistent with previous

research by Goresky (1963) and Brauer (1963). The number of compartments required to describe the albumin profiles was 2.05 ± 0.13 . For comparison, two albumin profiles obtained by Goresky (1963) were analyzed. These data indicated that the mean residence time of the perfusate in the vasculature was between 3.5 and 6.2 seconds. The number of compartments necessary to describe Goresky's albumin profiles was 1.74 and 2.07. Therefore, the results obtained from our experiments with rats were consistent with other literature data for the dog. Combining data from both sources suggested that the volume of the vascular and interstitial spaces was approximately 15 percent of the total liver volume. The number of vascular compartments, N_v , was approximately 2, suggesting that the vasculature was reasonably well mixed. The mean time for passage through the vascular network was about 4.7 ± 1.2 seconds. This result indicated that the time scale for mixing in the vasculature was very short, and that vascular mixing should contribute to unsteady state metabolism for less than 20 or 30 seconds. By comparison, the observed unsteady-state metabolism lasted for nearly 5 minutes. Hence, the time scale for vascular mixing was very short relative to the probable time scale for equilibration between the cells and the vasculature. Thus, effects due to incomplete mixing may be virtually unobservable, simply because the process is quickly completed. Furthermore, this result suggests that the value of N is unlikely to influence the effectiveness of a heterogeneous model in representing washout profiles of lidocaine and its metabolites, since the time to complete cellular uptake and release is significantly longer than the

time required to clear the vascular network. For simplicity, therefore, a single well-mixed compartment was used to represent the vascular and interstitial regions of the liver.

Investigation of Mass Transfer Using Labelled Lidocaine

Previous discussion indicated that the utility of experiments with labelled lidocaine is their ability to discern between linear and non-linear transport and reaction. In these experiments, the animals were administered unlabelled lidocaine *in vivo* to complete enzyme inactivation. The liver was removed 24 hours later, and unlabelled lidocaine mixed with Krebs's buffer was infused into the organ until steady state was reached. Labelled lidocaine was then co-infused with unlabelled lidocaine for 5 minutes, followed by a complete washout of the labelled drug. Following cessation of infusion of labelled drug, the total radioactivity of the effluent exhibited a first order decline. The data, when plotted on log-linear coordinates, exhibited a linear decline ($r^2 = 0.960$ to 0.996) with time. After analyzing the samples using HPLC, the separated compounds were checked for radioactivity. The radioactivity of lidocaine samples was well above levels of background radiation; these data also showed a log-linear decline ($r^2 = 0.965$ to 0.980). Because the transient profile from the washout of labelled lidocaine is controlled by the unlabelled compound, it is guaranteed to act as a tracer (Goresky, 1973). Since the transient profiles from labelled lidocaine were consistent with those arising from experiments with unlabelled lidocaine, it was apparent that the response of the cells was unaffected by lidocaine administration. The linearity of these

profiles indicated that transport processes between the cells and the vasculature were linear.

The radioactivity of the metabolite samples was too close to background levels to accurately quantify the concentrations. However, because there was significant conversion of lidocaine during the experiment, the profile of the total effluent may serve as an indicator of the overall linearity of the system. Lidocaine, which was subject to linear transport, comprised 65 percent of the total effluent. The primary metabolites, then, accounted for 35 percent of the effluent. Thus, their levels were high enough to influence the total effluent curve, and if the metabolites were subject to non-linear transport, the curve representing the total effluent would have been affected. Since the washout profile of the total effluent showed a first order decline, it is apparent that linear transport also prevailed for the metabolites.

Investigation of Mass Transfer Using Unlabelled Compounds

Experiments with unlabelled compounds were used to investigate hepatic transport and metabolism. MEGX and 3-OHLID were infused independent of lidocaine to obtain estimates of the transport and reaction parameters for the metabolites. Inlet concentrations of 3-OHLID ranged from 26 to 55 μM , and for MEGX, from 45 to 60 μM . Data from the continuous infusion of lidocaine were used to obtain estimates of the transport parameters for lidocaine and the kinetic parameters for the formation of the primary metabolites. Inlet concentrations of lidocaine were between 31 and 65 μM . Experiments with labelled lidocaine suggested that the drug and metabolites were subject to linear transport and metabolism. Profiles from washout

experiments with unlabelled species also displayed a first order decline (Figures 7.2 and 7.3), supporting the conclusion that transport and elimination kinetics were linear.

Parameters for transport and reaction were estimated using the procedure outlined previously. The population-average values of k_{12} , k_{21} , and k_r for lidocaine, MEGX, and 3-OHLID are presented in Table 7.1. The values of k_{12} and k_{21} were normalized relative to the volumes of the vascular and cellular regions, respectively. The tabulated values represent the mean parameter values and their variations based on a 95% level of confidence. The parameter estimates revealed that rates of transport were significantly higher than the rate of reaction; intracellular reaction was clearly the rate-limiting step.

**Table 7.1: Average Parameters For Transport and Reaction
of Lidocaine and its Metabolites**

Compound	k_{12}/V_1 s^{-1}	k_{21}/V_2 s^{-1}	k_r s^{-1}	k_{12}/k_{21}
lidocaine (n=4)	1206 \pm 830	46 \pm 39	0.49 \pm 0.15	5.5 \pm 1.2
MEGX (n=7)	60 \pm 25	3.1 \pm 0.5	0.24 \pm 0.13	3.9 \pm 1.6
3-OHLID (n=8)	275 \pm 120	7.9 \pm 2.3	0.35 \pm 0.13	6.2 \pm 2.4

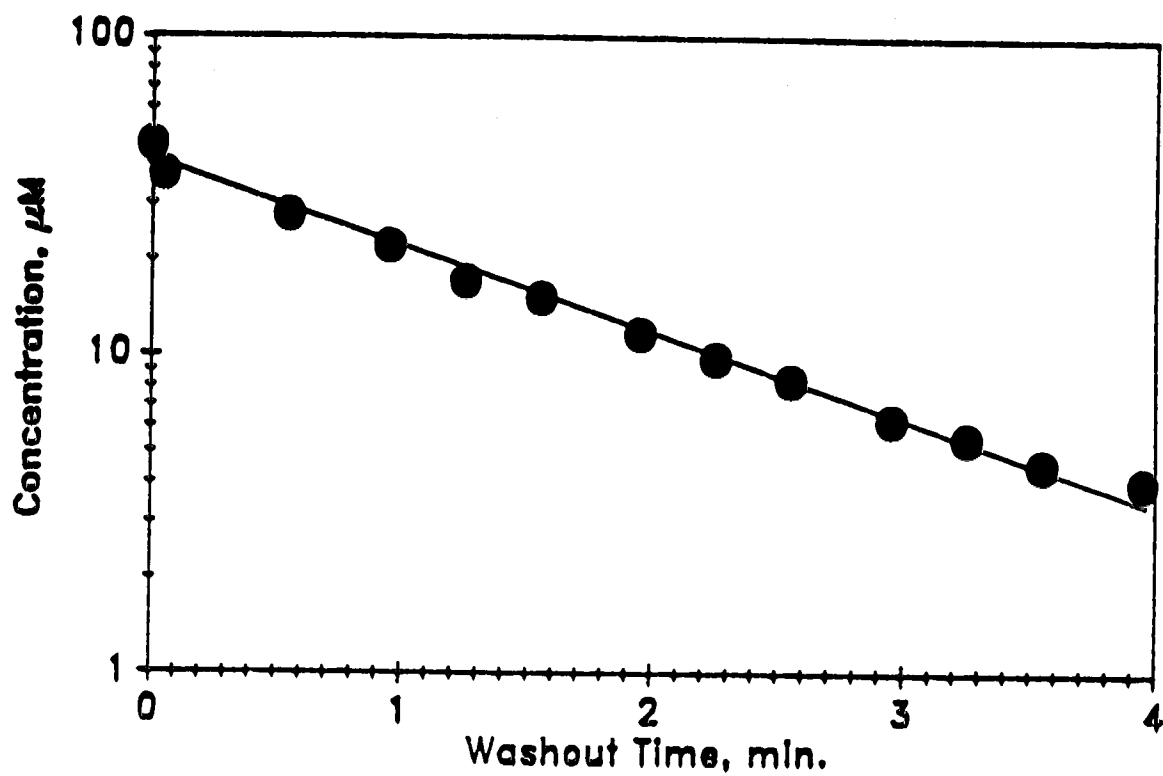


Figure 7.2 Concentration of MEGX in liver effluent during washout experiment following MEGX administration

$C_{in} = 60.4 \mu\text{M}$; ● experimental data; — heterogeneous model

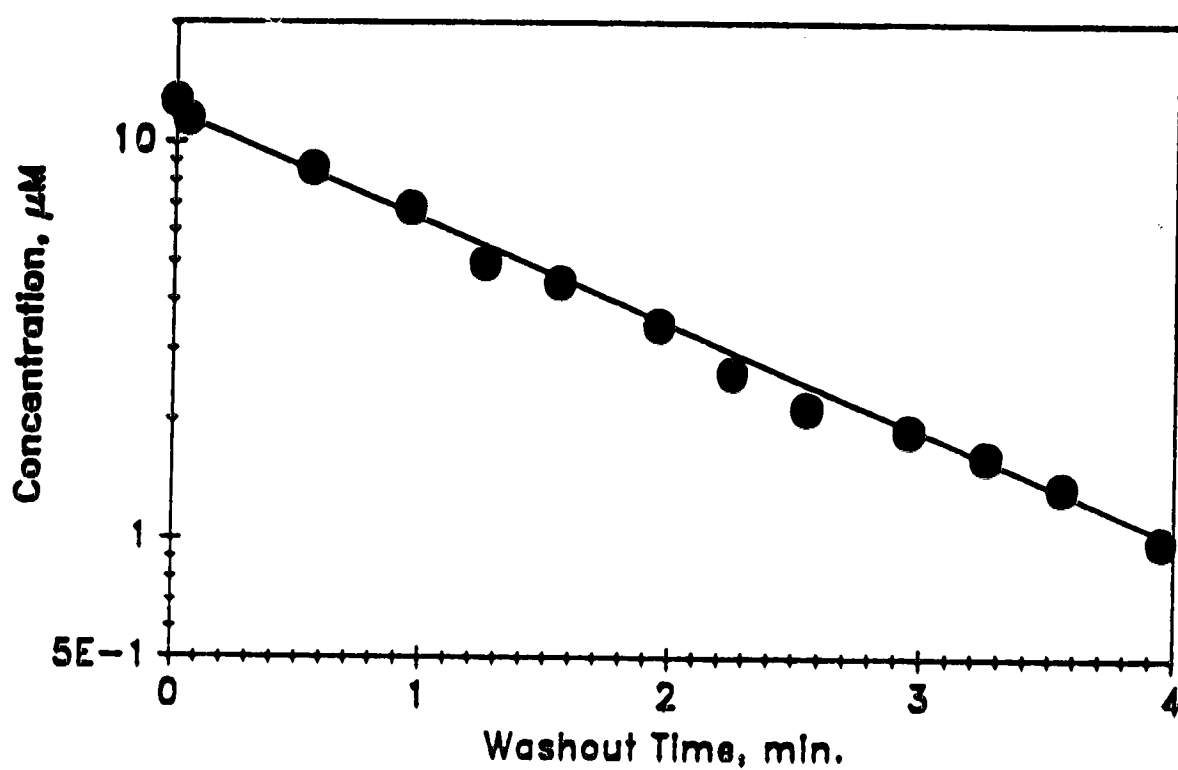


Figure 7.3 Concentration of 3-OHLID in liver effluent during washout experiment following 3-OHLID administration

$C_{in} = 26.3 \mu\text{M}$; ● experimental data; — heterogeneous model

Although the rate of uptake was very fast, there was no evidence of facilitated transport, for the following reasons:

1) Facilitated transport is structurally selective. Lidocaine, however, is structurally different from compounds known to undergo active transport, such as glucose and amino acids.

2) The rate of uptake for galactose, which is subject to active transport, is approximately 50 times higher than that predicted for lidocaine.

3) Chen *et al.* (1980) demonstrated that lidocaine uptake was not influenced by structurally similar compounds. If active transport is occurring, inhibition by structural analogs is generally observed.

4) Facilitated transport is usually influenced by temperature. Chen *et al.* (1980) showed that temperature had no effect upon lidocaine uptake.

For all 3 species, the rate of uptake was consistently higher than the rate of release from the cells, suggesting that each compound had an affinity for the cellular region of the liver. The rate of uptake was significantly different for each species, lowest for MEGX and highest for lidocaine. Similarly, the rate of release from the cells differed for each species, again lowest for MEGX and highest for lidocaine. Despite these variations in the rates of cellular uptake and release, the ratio of the two rates was statistically the same for all three compounds. The average ratio of uptake to release was 5.0 ± 1.3 ($n=19$, $p=0.05$). The data suggest that transport is very sensitive to structure, but the extent of binding of the compounds to tissues within the organ is much less sensitive to structure. The ability of the model to describe washout

profiles arising from the infusion of MEGX and 3-OHLID is depicted in Figures 7.2 and 7.3, respectively. Figure 7.4 shows that when the model is applied to both drug and metabolites, washout profiles of all three species can be accurately represented.

To determine if any cross-correlation existed between the reaction and transport parameters, regressions of k_r vs k_{12}/V_1 and k_r vs k_{21}/V_2 were performed for all three species. In each case, a hypothesis test upon the slope of the regression line indicated that the slope was statistically equal to zero. Hence, the rate of reaction was independent of the rates of cellular uptake and release. A typical correlation plot is presented in Figure 7.5.

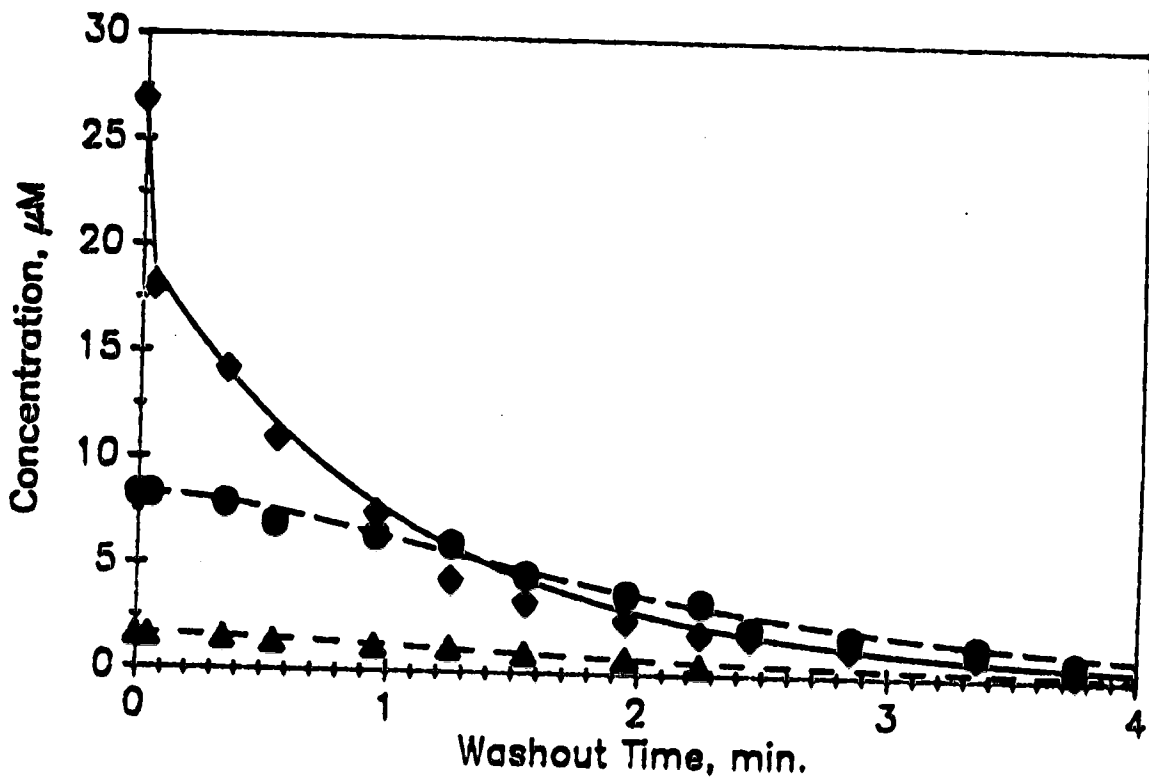


Figure 7.4 Concentrations of lidocaine, MEGX, and 3-OHLID in liver effluent following lidocaine administration

♦ lidocaine; ● MEGX; ▲ 3-OHLID; — model lidocaine;

- - - model MEGX; ---- model 3-OHLID; $C_{in} = 45.2 \mu\text{M}$

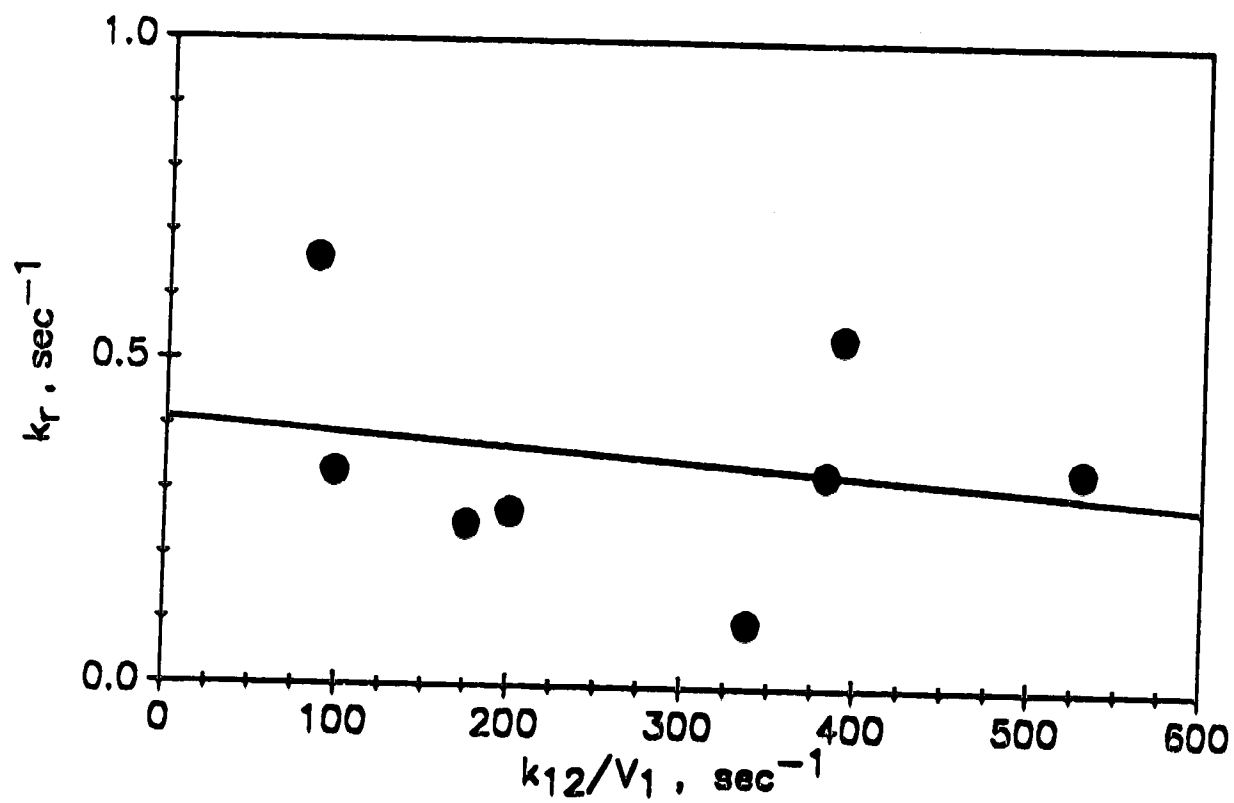


Figure 7.5 Cross-correlation between rate of reaction and rate of uptake

Data based on washout of 3-OHLID (n=8); — regression line;

$r^2 = 0.037$

Model Verification

Clearly, a heterogeneous model can account for the slow elution of drug and metabolites during a washout experiment. The parameter estimates suggest, however, that transport processes are fast, indicating that the slow washout was not due to transport limitations. Rather, the model suggests that the experimental observations may be due to a partitioning effect. As noted previously, the average ratio of the rate of cellular uptake to the rate of cellular release was 5.0. Because reaction rates are small relative to rates of transport, this ratio is approximately equal to an equilibrium constant between tissue and vascular concentrations. Hence, tissue concentrations of lidocaine, MEGX, and 3-OHLID are approximately 5 times higher than their respective vascular concentrations. Furthermore, the volume of the cellular region is nearly 6 times that of the vascular region. Therefore, under steady-state conditions, there is close to 30 times more material in the tissue than in the vasculature, suggesting that the tissue can act as a large reservoir for the drug and metabolites. Upon initial administration of the drug, it can take a long time to fill this reservoir. Similarly, emptying the cellular reservoir during a washout experiment would take some time. Hence, distribution of the drug into the tissue can delay the onset of steady state, and account for the experimental observations.

Distribution effects are commonly accounted for by applying a homogeneous model in conjunction with a coefficient for distribution into tissues (e.g. Tsuji et al., 1983). Such a model, however, is not

sufficient to describe these data, for the following reasons:

1) The washout experiments showed a two-phase decline in drug and metabolite concentration, characterized by a rapid drop in concentration within 3 to 10 seconds due to clearing of the vascular space, followed by a linear decline due to emptying of the cells. A homogeneous model, either with or without a distribution coefficient, cannot account for a two-phase decline in drug concentration. In the washout experiments depicted in Figures 7.2, 7.3, and 7.4, two-phase declines are clearly observed.

2) The rates of release from the cells differed for all three species. As shown in Figure 7.4, the concentration of the metabolite, MEGX, could cross over with the concentration of its precursor, lidocaine. In this instance, steady state data indicated that only 46 percent of the lidocaine was metabolized, with MEGX accounting for 60 percent of the metabolites formed. Thus, the initial level of MEGX was lower than that of lidocaine. However, after only 75 seconds of washout, the concentration of MEGX exceeded that of lidocaine, which clearly indicated that the two species were subject to different rates of release from the cells. A homogeneous model can account for crossover of drug and metabolite profiles by assuming different coefficients of distribution for each species; however, the heterogeneous model indicates that the relative distribution between the cells and the vascular network is statistically the same for all three compounds. Thus, using a homogeneous model and different distribution coefficients for each compound is not justified.

Additional tests of the model were performed. An experiment was conducted in which a step decrease in drug concentration was followed

by a step increase in concentration. By applying the model parameters determined from the washout experiment, the model was capable of describing uptake profiles arising from the step increase in 3-OHLID concentration. When the model was coupled with an expression for enzyme inactivation (Equation 4.16), it successfully combined the effects of cellular uptake and distribution, enzyme inactivation, and cellular release to describe effluent concentrations of lidocaine, MEGX, and 3-OHLID (Figure 7.6). The model was equally successful in accounting for enzyme inactivation when 3-OHLID was exogenously administered to the liver. Thus, it is apparent that a heterogeneous model with enzyme inactivation can account for the observed characteristics of lidocaine metabolism.

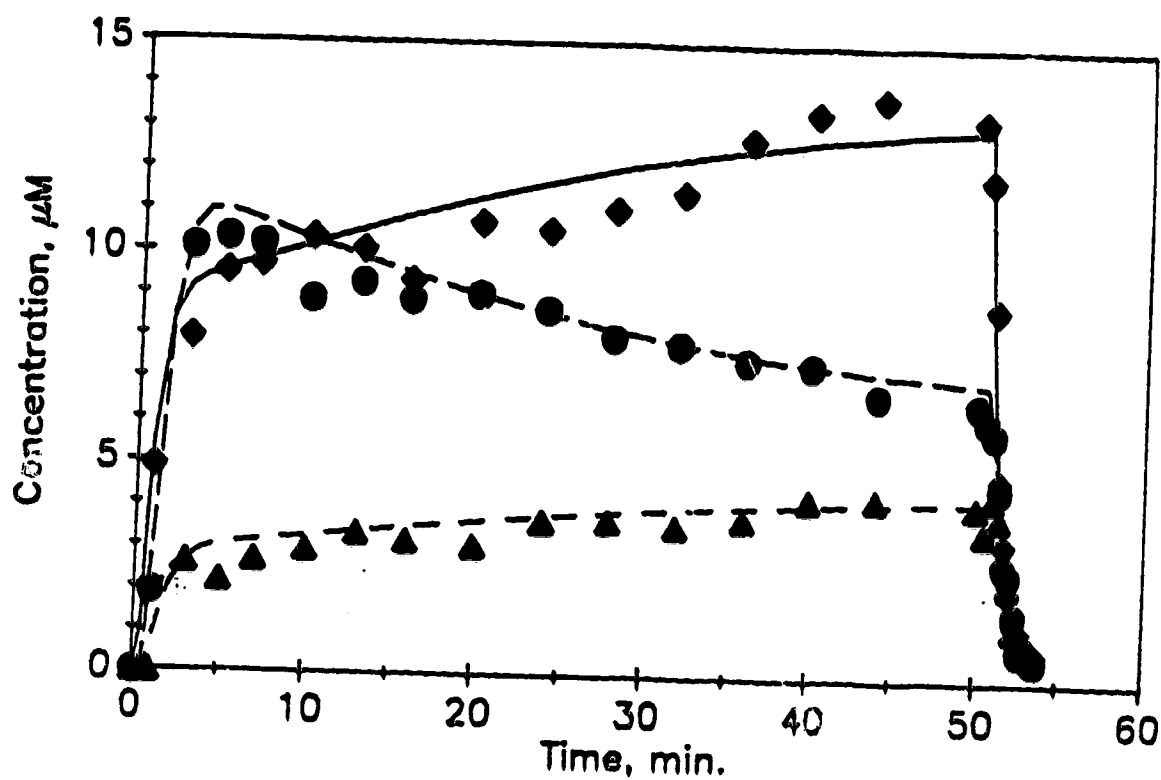


Figure 7.6 Best fit of heterogeneous model with enzyme inactivation to composite drug and metabolite concentration data

♦ lidocaine; ● MEGX; ▲ 3-OHLID; — model lidocaine;
 --- model MEGX; ---- model 3-OHLID; $C_{in} = 30.9 \mu\text{M}$

Conclusions

The heterogeneous model presented herein (Equations 7.6 and 7.7) is appropriate for describing drug metabolism. It combines the effects of cellular uptake, flow, intracellular reaction, and cellular release into a single model. Data from washout experiments with albumin clearly indicated that vascular mixing had a negligible effect upon unsteady state metabolism; the liver vasculature can simply be represented by a single, well mixed compartment. Although liver physiology is such that flow is intermittent and complex, such complexity is not required in a heterogeneous model, because the time scale for vascular mixing is very short relative to the time for distribution of drug into the liver tissue. Therefore, using distributions of sinusoidal transit times (e.g. Bass *et al.*, 1978; Goresky, 1963, 1973, 1983) is clearly unnecessary.

The heterogeneous model meets the criteria for an effective liver model that were outlined in Chapter 1. It accounts for the vascular and cellular regions of the organ; the long distribution time of lidocaine indicated that additional detail to account for frequently occurring physiological phenomena such as local pressure gradients and flow reversals would not be justified. The model is mathematically simple. It consists of two ordinary differential equations for each species to be described. The model has a minimal number of parameters, and the parameters can be easily used for predicting drug and metabolite levels. The model can be applied to both the parent drug and its metabolites, and should be applicable for a wide variety of substrates. Because the organ was perfused with

buffer, binding of lidocaine to plasma proteins was not included in the model. However, such phenomena can be accounted for, as demonstrated by Weisiger (1985).

The heterogeneous model, when combined with an expression for enzyme inactivation, is capable of describing all of the observed characteristics of hepatic lidocaine metabolism. It can account for time-dependent phenomena, including distribution into the cells, reactions within the cells mediated by various stable and unstable isozymes of cytochrome P-450, and slow release of drug and metabolites from the cells. It clearly demonstrated that the rate of intracellular reaction was significantly less than rates of transport. Rates of transport varied between compounds, but the ratio of the rate of uptake to the rate of release was the same for all three species. Each species had an affinity for the cellular region of the liver, which indicated a significant distribution effect, whereby the cells could act as large reservoirs of drug and metabolites. The time to empty and fill the cellular reservoir could delay the onset of steady state by up to 5 minutes.

References

- Bass, L., Robinson, P., and Bracken, A.J.: "Hepatic Elimination of Flowing Substrates: The Distributed Model", *J. Theor. Biol.*, 72, 161-184, (1978).
- Brauer, R.W.: "Liver Circulation and Function", *Physiol. Rev.*, 43, 115-213, (1963).
- Buffham, B.A., and Gibilaro, L.G.: "The Analytical Solution of the Deans-Levich Model for Dispersion in Porous Media", *Chem. Eng. Sci.*, 23, 1399-1401, (1968).
- Chen, C.P., Vu, V.T., and Cohen, S.D.: "Lidocaine Uptake in Isolated Rat Hepatocytes and Effects of *dl*-propranolol", *Toxicol. Appl. Pharmacol.*, 55, 162-168, (1980).
- Davenport, R.: "The Derivation of the Gamma-Variate Relationship for Tracer Dilution Curves", *J. Nucl. Med.*, 24, 945-948, (1983).
- Duduković, M.P.: "Tracer Methods in Chemical Reactors: Techniques and Applications", presented at the NATO Chemical Reactor Design and Technology Symposium, London, Canada, June 2-12, 1985.
- Goresky, C.A.: "A Linear Method for Determining Liver Sinusoidal and Extravascular Volumes", *Am. J. Physiol.*, 204(4), 626-640, (1963).

- Goresky, C.A., Bach, G.G., and Nadeau, B.E.: "On the Uptake of Materials by the Intact Liver: The Transport and Net Removal of Galactose", *J. Clin. Invest.*, 52, 991-1009, (1973).
- Goresky, C.A., Bach, G.G., and Rose, C.P.: "Effects of Saturating Metabolic Uptake on Space Profiles and Tracer Kinetics", *Am J. Physiol.*, 244, G215-G232, (1983).
- Gray, M.R., and Tam, Y.K.: "The Series-Compartment Model for Hepatic Elimination", *Drug. Metab. Disp.*, 15, 22-27, (1987).
- Levenspiel, O.: The Chemical Reactor Omnibook, Chapter 61, OSU Book Stores, Corvallis, Oregon, (1984).
- Nelder, J.A., and Mead, R.: "A Simplex Method Function Minimization", *Comput. J.*, 7, 308-315, (1965).
- Saville, B.A., Gray, M.R., and Tam, Y.K.: "The Metabolism of Lidocaine in the Liver: Steady State and Dynamic Modelling", *Can. J. Chem. Eng.*, 64, 617-624, (1986).
- Saville, B.A., Gray, M.R., and Tam, Y.K.: "Mechanisms of Lidocaine Kinetics in the Isolated Perfused Rat Liver: Kinetics of Steady State Elimination", *Drug Metab. Disp.*, 15(1), 17-21, (1987).

Suzuki, T., Fujita, S., and Kawai, R.: "Precursor-Metabolite Interactions in the Metabolism of Lidocaine", *J. Pharm. Sci.*, 73(1), 136-138, (1984).

Tsuji, A., Yoshikawa, T., Nishide, K., Minami, H., Kimura, M., Nakashima, E., Terasaki, T., Niyamoto, E., Nightingale, C., and Yamana, T.: "Physiologically Based Pharmacokinetic Model for β -Lactam Antibiotics I. Tissue Distribution and Elimination in Rats", *J. Pharm. Sci.*, 72(11), 1239-1252, (1983).

Weisiger, R.A.: "Dissociation From Albumin: A Potentially Rate-Limiting Step in the Clearance of Substrates by the Liver", *Proc. Natl. Acad. Sci. USA*, 82, 1563-1567, (1985).

CHAPTER 8: SUMMARY AND RECOMMENDATIONS

The heterogeneous model suggests that drug concentrations will be higher in the tissue than in the vasculature. For lidocaine, which inhibits its own metabolism by inactivating an isozyme of cytochrome P-450, this may have significant implications. The inactivation mechanism indicates that enzyme activity will exponentially depend upon the cumulative exposure of the enzyme to lidocaine. The enzymes, of course, are exposed to the drug in some portion of the cells, rather than in the vasculature. Thus, when modelling enzyme inactivation, it is the local concentration that must be used. If the vascular concentration is used, the rate of inactivation, k_d' , may be significantly overestimated. Therefore, for species which cause enzyme inactivation, knowledge of the local concentration is important. The local concentration of lidocaine will depend upon the location of the active site of cytochrome P-450 within the cells. If the active site is exposed to the cytosol (the fluid portion of the cytoplasm), the local concentration should be fairly close to the concentration in the vasculature. If, however, the active site of P-450 is a component of the membrane of the endoplasmic reticulum, and lidocaine has an affinity for the tissue membrane, then the concentration of lidocaine adjacent to the active site may be 5 times higher than the vascular concentration. Thus, unequal concentrations in the tissue and vasculature may have a significant influence upon substrate-induced enzyme inactivation.

The elimination of many compounds are governed by Michaelis-Menten kinetics; however, estimation of the Michaelis

constant for saturation, K_m , is usually based upon vascular data, or upon data obtained from isolated enzyme studies. The true level of saturation may be much different, since it depends upon the local concentration. As outlined above, the location of the enzyme active sites in the cells and substrate affinity for the tissue or liquid phase of the cells can have a significant impact upon local concentrations. In isolated enzyme studies, such effects cannot be accounted for, and therefore, estimates of K_m may not be indicative of the level of saturation that would be observed in an intact organ. Similarly, if the local drug concentration is significantly different from the vascular concentration, estimation of K_m based upon vascular data is likely to be erroneous. Independent experiments with lidocaine and lidocaine metabolites were conducted in intact organs (Chapter 3) and using isolated enzymes (Suzuki *et al.*, 1984). Estimates of K_m based on the two studies were generally comparable (Table 3.2), suggesting that for most of the metabolic pathways of lidocaine, the active sites of the isozymes were exposed to the cytosol.

The use of non-linear reactions with a homogeneous model (Chapter 3) and linear reactions with a heterogeneous model (Chapter 7) is justifiable, for the following reasons:

- 1) The parameters from the heterogeneous model indicated very rapid rates of transport, tissue concentrations that were significantly higher than the vascular concentration, and a substantial reservoir for compounds in the tissue. During a washout experiment, effluent concentrations are controlled by release from the tissue, because any material released will be rapidly transported

from the tissue into the vasculature and out of the organ. Due to the large tissue reservoir, however, the excreted material is quickly replaced by more material released from the tissue. Conversion of lidocaine within the cells is much slower than the rate of transport, and the amount of lidocaine converted to metabolites is significantly less than the amount of lidocaine freed from the tissue. Thus, any non-linear kinetics affecting the conversion process will be unobservable relative to the transport-dominated release of drug from the tissue reservoir. Since the observed washout profiles of lidocaine and its metabolites exhibited a first-order decline, the elimination could, therefore, be approximated as a linear process.

2) In steady state, elimination dominates the effluent concentrations, and therefore, changes in drug levels are solely due to changes in the rate of drug elimination. Thus, by observing the change in elimination rate with effluent concentration, it is possible to investigate non-linear elimination kinetics. The experiments outlined in Chapter 3 provided steady state data over a wide range of concentrations, which successfully permitted the estimation of parameters for non-linear elimination.

Implications Upon Pharmacokinetic Modelling and Analysis

The traditional technique for pharmacokinetic analysis of drug metabolism in the body is to apply an all-encompassing one, two, or three compartment model that unites processes such as drug transport, hepatic elimination, intestinal absorption, urinary excretion, and blood flow. The models do not permit specific evaluation of these processes, and the justification for using a specific number of compartments is generally based upon whether or not an additional

compartment is required to fit the data. The compartments, therefore, have no physiological meaning. An additional compartment may be necessary due to the influence of any one of a number of physiological processes. However, determining which process is affecting metabolism is usually based upon speculation alone. A major deficiency of these compartmental models is that the models are often applied blindly. The approximations of physical processes inherent within the models are generally not checked to determine their validity. The net result is conclusions and postulations of physiological phenomena that are based only upon an empirical model. A second deficiency of these models is that it is possible to hide unknown phenomena within the model. One such example is enzyme inactivation, which has significant implications upon drug metabolism and drug administration, and is involved in the metabolism of some common pharmacological agents, yet has received negligible discussion in the pharmacokinetic literature. For lidocaine, the time-dependent metabolism caused by enzyme inactivation has been attributed to six different processes, none of which was related to long term modification of enzyme activity. Again, unguided use of a whole-body model prevented assessment of the physiological processes affecting drug metabolism.

Implications Upon Models for Hepatic Elimination

The heterogeneous model suggests that transport and reaction within the liver dominate over any effects within the sinusoids. Thus, the well-stirred homogeneous model has a reasonably good basis in physiology, provided partitioning between the tissue and the vasculature is accounted for. Furthermore, because vascular processes

are completed very quickly relative to intracellular processes, models that include additional complexity to describe physiological effects within the sinusoids cannot be justified.

The heterogeneous model indicated that the vascular region of the liver could be represented by a single, well-mixed compartment. Similarly, the cellular region of the organ could be represented as a single homogeneous compartment. Despite the existence of enzyme heterogeneity between the lobes of the liver, the average activity in the entire organ was sufficient to describe the experimental data. Thus, models that are based upon different enzyme activity (or content) in different liver compartments appear to be unnecessary.

This work has thoroughly investigated and verified the existence of enzyme inactivation caused by lidocaine; initial information suggests that enzyme inactivation may have significant implications upon drug metabolism, and may lead to several previously unrecognized interactions between drugs. In addition, this work has assessed the phenomena which affect drug metabolism in the liver, and has united the dominant processes into an effective heterogeneous model for hepatic metabolism. The model accounts for the two distinct regions of the organ, has a minimum of parameters, and is broadly applicable.

References

- Saville, B.A., Gray, M.R., and Tam, Y.K.: "The Metabolism of Lidocaine in the Liver. Steady State and Dynamic Modelling", *Can J. Chem. Eng.*, 64, 617-624, (1986).
- Saville, B.A., Gray, M.R., and Tam, Y.K.: "Mechanisms of Lidocaine Kinetics in the Isolated Perfused Rat Liver: Kinetics of Steady State Elimination", *Drug Metab. Disp.*, 15(1), 17-21, (1987).
- Suzuki, T., Fujita, S., and Kawai, R.: "Precursor-Metabolite Interactions in the Metabolism of Lidocaine", *J. Pharm. Sci.*, 73(1), 136-138, (1984).

Appendix A: HPLC Data

Table A.1: Mathematical Expressions for HPLC Calibration Curves

lidocaine:	Concentration = $14.04 * \text{Area Ratio}$; $r^2 = 0.989$
MEGX:	Concentration = $12.23 * \text{Area Ratio}$; $r^2 = 0.996$
3-OHLID:	Concentration = $10.98 * \text{Area Ratio}$; $r^2 = 0.996$
3-OHMEGX:	Concentration = $10.00 * \text{Area Ratio}$; $r^2 = 0.994$
MeOHLID:	Concentration = $58.90 * \text{Area Ratio}$; $r^2 = 0.950$
GX:	Concentration = $13.77 * \text{Area Ratio}$; $r^2 = 0.985$
xylidine:	Concentration = $4.99 * \text{Area Ratio}$; $r^2 = 0.979$
3-OH GX:	Concentration = $3.43 * \text{Area Ratio}$; $r^2 = 0.975$
(3-OH)-xylidine:	Concentration = $2.52 * \text{Area Ratio}$; $r^2 = 0.978$
(4-OH)-xylidine:	Concentration = $6.46 * \text{Area Ratio}$; $r^2 = 0.621$

All concentrations are in $\mu\text{g/ml}$.

Table A.2: Sensitivity of Lidocaine Assay

<u>Species</u>	<u>Minimum Detectable Concentration, $\mu\text{g/ml}$</u>
lidocaine	0.64
MEGX	0.44
3-OHLID	0.34
3-OHMEGX	0.09
MeOHLID	0.91
GX	0.08
xylidine	0.17
3-OHGX	0.40
(3-OH)-xylidine	0.05
(4-OH)-xylidine	0.25

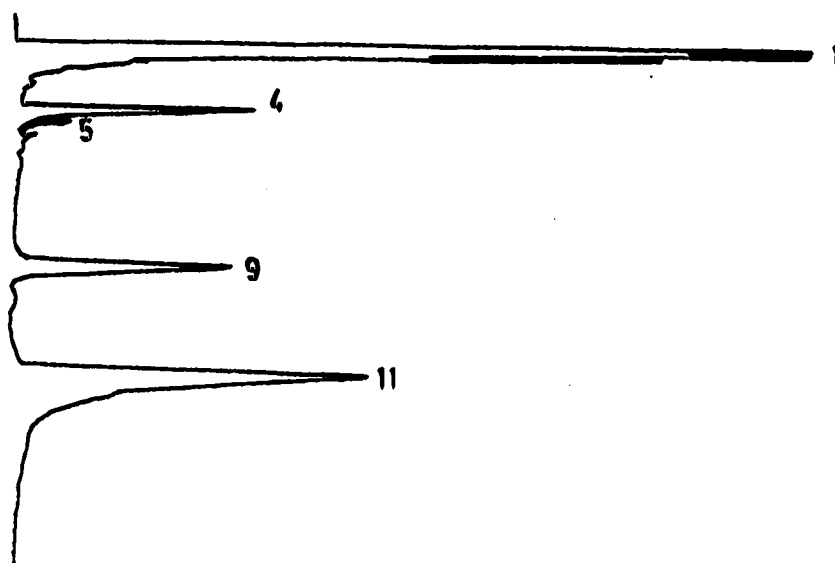


Figure A.1 Chromatogram of liver effluent collected prior to drug administration

Chromatographic peaks identified in Table 3.1

Total time of analysis = 18 min.

Appendix B: Detailed Rate Expressions for Lidocaine Metabolism

Reaction 1: Deethylation of Lidocaine

$$R_1 = k_1 \cdot C_1 \quad (\text{linear reaction, } K_{m1} \gg V_{m1}) \quad (B1)$$

Reaction 2: Hydroxylation of Lidocaine

$$R_2 = V_{m2} \cdot C_1 / (C_1 + (K_{m2}/K_{m4}) \cdot C_2 + K_{m2}) \quad (B2)$$

Reaction 3: Pooled elimination of lidocaine to minor metabolites

$$R_3 = V_{m3} \cdot C_1 / (C_1 + K_{m3}) \quad (B3)$$

Reaction 4: Pooled elimination of MEGX

$$R_4 = V_{m4} \cdot C_2 / (C_2 + K_{m4}) \quad (B4)$$

The elimination of MEGX is dominated by hydroxylation to give 3-OH MEGX (Suzuki *et al.*, 1984).

Reaction 5: Pooled elimination of 3-hydroxylidocaine

$$R_5 = V_{m5} \cdot C_3 / (C_3 + K_{m5}) \quad (B5)$$

Appendix C: Statistical Derivations

I) Statistical Determination of Time to Reach Steady-State

The data were analyzed starting with the last measured data point for lidocaine (C_1) which was at steady state. At each previous sample, C_N , the following values were determined:

- 1) $C_{AVG,N}$, the average lidocaine concentration for the last N values
- 2) S_N^2 , the sample variance
- 3) $t_{0.025,N-1}$, the t-statistic corresponding to a 95 percent confidence interval with N-1 degrees of freedom.

The absolute error of the average lidocaine concentration at each sample point can be estimated as follows:

$$Err_N = \frac{t_{0.025,N-1} \cdot S_N}{\sqrt{N}} \quad (C1)$$

The confidence interval for the lidocaine concentration of each sample is given by:

$$C_{1,R} = C_{AVG,N} \pm Err_N \quad (C2)$$

where $C_{1,R}$ describes the statistical range encompassing $C_{1,AVG}$.

To determine the time at which steady-state was reached, the previous data point, C_{N+1} , was tested to determine if it fell within the bounds described by equation (C2). If C_{N+1} met this criterion, it was deemed to be at steady state. If it failed the test, it was deemed to be in a transient state if and only if all preceding points also failed the comparison described by Equation (C2). The time to reach steady state corresponds to the last data point which meets the criterion described by Equation (C2) (working backward in time).

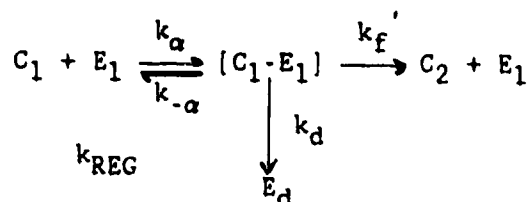
II) Tests For Maxima in MEGX Concentration-Time Profile

The slope of the pre-steady-state concentration-time profile of MEGX was used to test for the existence of a maximum in concentration. A slope that is zero, or positive, indicates that the MEGX profile is monotonic. A negative slope indicates that there must be a decline in the MEGX profile, and therefore, a maximum. The slope was determined by linear regression, using all MEGX data from the highest recorded MEGX concentration to the first MEGX data point at steady state (time to steady state determined from lidocaine). A hypothesis test was performed on the slope, using a 95% level of significance. Acceptance of the null hypothesis indicated that the regression slope was not statistically different from zero, and therefore, the MEGX profile was monotonic. Acceptance of the alternate hypothesis indicated a negative slope, which implied a maximum in the concentration of MEGX.

Appendix D

Derivation of Model for Regeneration of Hepatic Enzymes

The following mechanism was used for enzyme inactivation and regeneration:



where:

- C_1 : lidocaine
- C_2 : MEGX
- E_{1a} : active enzyme for deethylation
- E_1 : unstable isozyme for deethylation
- E_d : inactivated deethylation isozyme
- E_{max} : maximum amount of total deethylation enzyme
- E_{ss} : steady state amount of deethylation enzyme
- k_d : rate of enzyme inactivation
- k_{REG} : rate of enzyme regeneration

The total deethylation enzyme, E_a , consists of at least two fractions: the stable isozyme(s), represented by E_{ss} , and the inactivatable form(s), denoted by E_1 . The conversion of lidocaine into MEGX is mediated by all of these fractions. Once inactivation is complete, all of the labile isozyme has been converted into an inactive form, E_d . At this point, E_1 is equal to zero. As time progresses, some of the inactive form is replaced by new isozyme,

increasing E_1 until normal levels are restored or until such time as another dose of substrate causes further inactivation.

The following material balance applies for the total active enzyme:

$$E_A = E_{ss} + E_1 \quad (D1)$$

By differentiating Equation (D1) at any time after exposure to lidocaine is complete:

$$\frac{dE_A}{dt} = \frac{dE_1}{dt} = k_{REG} E_d \quad (D2)$$

A material balance on the total deethylation enzyme at any time gives:

$$E_d = E_{max} - E_{ss} - E_1 \quad (D3)$$

Combining Equations (D1) and (D3) yields:

$$E_d = E_{max} - E_A \quad (D4)$$

Substituting for E_d in Equation (D2) and integrating gives:

$$E_A = (E_{ss} - E_{max}) e^{-k_{REG}t} + C \quad (D5)$$

The following boundary conditions can be applied to evaluate C:

$$\text{At } t = 0, E_A = E_{ss}$$

$$\text{At } t = \infty, E_A = E_{max}$$

$$\text{Hence, } C = E_{max} \quad (D6)$$

Combining Equations (D5) and (D6) yields:

$$E_A = E_{max} - (E_{max} - E_{ss}) e^{-k_{REG}t} \quad (D7)$$

The rate constant for dealkylation, k_1 , is directly proportional to the total amount of active enzyme, E_A . Similarly, k_{ss} and k_{max} are

proportional to E_{ss} and E_{max} , respectively. Therefore, Equation (D7) can be given in an equivalent form as follows:

$$k_1 = k_{max} - (k_{max} - k_{ss}) e^{-k_{REG}t} \quad (D8)$$

Rearranging Equation (D8) gives:

$$\frac{(k_{max} - k_1)}{(k_{max} - k_{ss})} = e^{-k_{REG}t} \quad (D9)$$

Taking the natural logarithm of each side of Equation (D9) gives:

$$\ln \frac{(k_{max} - k_1)}{(k_{max} - k_{ss})} = -k_{REG}t \quad (D10)$$

For an individual experiment where regeneration is not complete, k_{max} is not known. Only k_1 and k_{ss} can be estimated. Hence, Equation (D10) must be recast such that an estimate of regeneration can be obtained.

Division by k_{ss} yields:

$$\ln \frac{(k_{max}/k_{ss} - k_1/k_{ss})}{(k_{max}/k_{ss} - 1)} = -k_{REG}t \quad (D11)$$

To apply Equation (D11), (k_{max}/k_{ss}) for the population must be used. From individual experiments on enzyme regeneration, the value of (k_1/k_{ss}) at various times, t , can be evaluated. Hence, Equation (D11) can be used to estimate the rate of regeneration, k_{REG} .